The Islamic University–Gaza

Research and Postgraduate Affairs

Faculty of Engineering

Master of Computer Engineering

الجـامعــــــــة الإســــــلاميـة ــ غـزة

شئون البحث العلمي والدراسات العليا

كليــــة الهندســـــــــــــــــــة

ماجستير هندسة الحاســـــــــــوب

Modern Multiresolution Techniques for Fingerprint Recognition

تقنيات حديثة متعددة الحلول لنظام التعرف على بصمات الأصبع

Waleed A. Abudalal

Supervised by

Dr.Mohammed Alhanjouri

Associate Prof. of Artificial Intelligence and Digital Signal Processing

A thesis submitted in partial fulfilment
of the requirements for the degree of
Master of Computer Engineering

August 2016

<div dir="rtl">

إقــــــرار

أنا الموقع أدناه مقدم الرسالة التي تحمل العنوان:

</div>

Modern Multiresolution Techniques for Fingerprint Recognition

<div dir="rtl">

تقنيات حديثة متعددة الحلول لنظام التعرف على بصمات الأصبع

أقر بأن ما اشتملت عليه هذه الرسالة إنما هو نتاج جهدي الخاص، باستثناء ما تمت الإشارة إليه حيثما ورد، وأن

هذه الرسالة ككل أو أي جزء منها لم يقدم من قبل الاخرين لنيل درجة أو لقب علمي أو بحثي لدى أي مؤسسة

تعليمية أو بحثية أخرى.

</div>

Declaration

I understand the nature of plagiarism, and I am aware of the University's policy on this.

The work provided in this thesis, unless otherwise referenced, is the researcher's own work, and has not been submitted by others elsewhere for any other degree or qualification.

<div dir="rtl">

Student's name:	وليد عبد المالك أبودلال	اسم الطالب:
Signature:		التوقيع:
Date:	20/8/2016	التاريخ:

</div>

Abstract

Using biometrics in recognition of persons has received more and more attention in the last years, due to the necessity to improve the information security and access restrictions of authentication systems. Fingerprint is considered the most practical biometrics due to some specific features which make them widely accepted.

Reliable feature extraction from poor quality fingerprint images is still the most challenging problem in fingerprint recognition system. So it needs a lot of pre-processing steps to improve the quality of fingerprint images, then it needs a reliable feature extractors to extract some distinctive features. Recently, multiresolution transforms techniques have been widely used as a feature extractor in the field of biometric recognition. These features can be used as an identification marks in fingerprint recognition. The goal of this thesis is to develop a complete and an efficient fingerprint recognition system that can deal with poor quality fingerprint images. To deal with poor quality fingerprint image with various challenging, a reliable pre-processing stage and an efficient feature extraction are needed. Segmentation is one of the most important pre-processing steps in fingerprint identification followed by image alignment, and enhancement. We improve a common enhancement technique based on STFT analysis by replacing the used segmentation technique which based on thresholding the energy map, with another one based on morphological operation. We use modern multiresolution techniques; Curvelet, Wave Atoms, Shearlet transforms in extracting distinctive features from the enhanced fingerprint images in a new methodology. The selected features are matched through multiple classifier techniques. We use the Minimum Distance Classifier, K-Nearest Neighbour, Self-Organizing Map and Support Vector Machine. We compare between all these classifiers with respect to the various feature extraction techniques. We test our methodology in 114 subjects selected from a very challenges database; CASIA-FingerprintV5; and we achieve a high recognition rate of about 99.5%.

Keywords: Fingerprint Recognition, Multiresolution Feature Extraction, Wave Atoms, Shearlet, Curvelet, Real Noisy Database, Fingerprint Image Enhancement, CASIA-FingerprintV5.

الملخص

استخدام القياسات الحيوية في التعرف على الأشخاص لاقى الكثير من الاهتمام في السنوات الأخيرة, ويرجع ذلك الى ضرورة تطوير أمن المعلومات والقيود الأمنية على أنظمة التحقق من الهوية. تعتبر بصمة الأصبع الأكثر عمليا من ضمن جميع القياسات الحيوية لما لها من مميزات محددة جعلتها مقبولة على نطاق واسع. ان استخراج السمات الفارقة من صور بصمات الأصابع ذات الجودة السيئة هي المشكلة الأكبر تحديا في نظام التعرف على بصمة الأصبع, لذلك فهي تحتاج الكثير من خطوات المعالجة لتحسين جودة الصورة, ومن ثم بحاجة الى تقنية فعالة لاستخراج بعض السمات المميزة في الصورة. لقد تم استخدام تقنيات التحليل المتعددة الحلول في الآونة الأخيرة على نطاق واسع في استخراج السمات المميزة في أنظمة التعرف الحيوية, حيث من الممكن استخدام هذه السمات كعلامات فارقة لتحديد الهوية في التعرف على بصمات الأصابع. ان الهدف من هذه الرسالة هو تطوير نظام فعال ومتكامل للتعرف على بصمة الأصبع يستطيع التعامل مع الجودة المنخفضة لصور بصمات الأصابع وحتى يستطيع التعامل مع الجودة الرديئة لصور بصمات الاصبع والمليئة بالعديد من التحديات, لا بد من توفر نظام معالجة قوي ونظام فعال لاستخداج السمات الفارقة. يحتوي نظام المعالجة على العديد من العمليات الضرورية مثل : تعديل ازاحة الصورة, فصل أجزاء الصورة, وتحسين جودة الصورة. لقد قمنا بتطوير تقنية مشهورة لتحسين جودة الصورة, حيث قمنا باستبدال عملية فصل أجزاء الصورة والمعتمدة على خريطة الطاقة بتقنية أخرى جديدة تعتمد على عمليات الشكليات, أيضا لقد قمنا باستخدام تقنيات التحليل المتعددة الحلول مثل: تحويل المنحنى المصغر(Curvelet) ,تحويل موجة الذرة (Wave Atoms), وتحويل القص المصغر (Shearlet) لاستخراج سمات مميزة للصورة بطريقة جديدة, حيث يتم تصنيف هذه السمات باستخدام تقنيات التصنيفات. والتي قد استخدمنا منها: تصنيف الحد الأدنى للمسافات (Minimum Distance Classifier) , وتصنيف العدد الأقرب للجيران (K-Nearest Neighbour), وتصنيف خريطة التنظيم الذاتي (Self-Organizing Map), وتصنيف دعم آلة المتجهات (Support Vector Machine). ولقد قمنا بالمقارنة بين تقنيات التصنيفات المستخدمة وبين تقنيات استخراج السمات. و قمنا بفحص طريقتنا على 114 شخص والذين تم اختيارهم من قاعدة بيانات لصور بصمات الأصابع مليئة بالتحديات وتسمى (CASIA- FingerprintV5), وقمنا بتحقيق معدل التعرف بنسبة 99.5%

كلمات مفتاحية: التعرف على بصمات الأصبع, تقنيات التحليل المتعدد, استخراج السمات الفارقة, وتحويل القص المصغر, تحويل المنحنى المصغر , تحويل موجة الذرة, قاعدة بيانات سيئة لبصمات الأصبع, تحسين جودة الصورة.

﴿إِنَّ الَّذِينَ كَفَرُوا يُنفِقُونَ أَمْوَالَهُمْ لِيَصُدُّوا عَن سَبِيلِ اللَّهِ ۚ فَسَيُنفِقُونَهَا ثُمَّ تَكُونُ عَلَيْهِمْ حَسْرَةً ثُمَّ يُغْلَبُونَ ۗ وَالَّذِينَ كَفَرُوا إِلَىٰ جَهَنَّمَ يُحْشَرُونَ(36) لِيَمِيزَ اللَّهُ الْخَبِيثَ مِنَ الطَّيِّبِ وَيَجْعَلَ الْخَبِيثَ بَعْضَهُ عَلَىٰ بَعْضٍ فَيَرْكُمَهُ جَمِيعًا فَيَجْعَلَهُ فِي جَهَنَّمَ ۚ أُولَٰئِكَ هُمُ الْخَاسِرُونَ﴾

[الأنفال: 36-37]

V

Dedication

This thesis work is dedicated to the spirit of my dear Father, I ask God Almighty to reward him richly rewarded, and to my dear Mother, who has been a constant source of support and encouragement during the challenges of graduate school and life. I am truly thankful for having you in my life. This work is also dedicated to my wife, who have always loved me unconditionally and whose good examples have taught me to work hard for the things that I aspire to achieve. Dedication is connected also to my children who ask God to their benefit Islam and Muslims.

Acknowledgment

- First, I would like to thank ALLAH for his great support to me in accomplishing this work.

- I would like to express my deepest gratitude to Dr. Mohammed Alhanjouri for suggesting of the point of research, and his great efforts revising the thesis. I cannot express my thanks to him for his care and guidance that started long time ago during my Master of Computer Engineering degree.

- I would like also to thank the person who encourage me to join the master degree Dr. Wesam Ashour, and his great efforts during the master study.

- I would like also to express my deepest gratitude for my dear mother for her patience, great support and encouragement during the most critical stages of the thesis. I thank her for taking responsibility of my daughter and my son providing me with full means of comfort to concentrate well in my work.

- Last but not least, I would like to thank my lovely wife for her care, patience, and encouragement during the thesis development. In fact, I do not find the words that would fairly express my thankfulness and gratitude to her

Table of Content

List of Tables

List of Figures

List of Abbreviations

2DPCA	Two-Dimensional principal components analysis
AFIS	Automatic Fingerprint Identification Systems
ANSI-NIST	The American National Standards Institute- National Institute of Standard and Technology
ATM	Automated Teller Machine
BPNN	Back Propagation Neural Network
BMP	Bitmap Images
B2DPCA	Bidirectional Two-Dimensional Principal Component Analysis
CASIA	Chinese Academy of Sciences' Institute of Automation
CLAHE	Contrast Limited Adaptive Histogram Equalization
DWT	Discrete Wavelet Transform
DCT	Discrete Cosine Transform
ERR	Equal Error Rate
ELM	Extreme Learning Machine
EBFNN	Ellipsoidal Basis Function Neural Network
FAR	False Acceptance Rate
FFT	Fast Fourier Transform
FRR	False Rejection Rate
FVC	Fingerprint Verification Competition
GGD	Generalized Gaussian density
KNN	K-Nearest Neighbour
HMM	Hidden Markov Model
LL	Left Loop fingerprint class
MI	Mutual Information
MLP	Multilayer Perceptron
NIST	National Institute of Standards and Technology
PA	Plain Arch fingerprint class
PCA	Principle Component Analysis
PPI	Pixel Per Inch
PSO	Particle Swarm Optimization
PZM	Pseudo-Zernike Moments
ROI	Region Of Interest
RL	Right Loop fingerprint class
RBFN	Radial Basis Function Network
STFT	Short Time Fourier Transform
SVM	Support Vector Machine
SVD	Singular Value Decomposition
TA	Tented Arch fingerprint class
TFCP	True Fingerprint Centre Point

Chapter 1

Introduction

Chapter 1
Introduction

As our everyday life is getting more and more computerized, the authentication systems are getting more and more important. Authentication is the determination of the identity or the role that someone has. This determination can be done in a number of different ways, but it is usually based on a combination of something the person has (like a smart card), something the person knows (like a password), or something the person is (like a human with a fingerprint). The current user's authentication models are divided into three categories: knowledge-based authentication, token-based authentication, and the biometric authentication. The knowledge-based authentication can be a text-based password or a graphical password, which both depends on something the user knows (i.e. PIN, or password), so it suffers from many problems, such as it can be forgotten or stolen or guessed. The token-based authentication may be a physical device that an authorized user of the computer services is given to make the authentication easier. An example of the token is the bank cash card. Tokens can be easily stolen and used for malicious purposes. The biometric authentication includes behavioural biometrics such as the keystroke latency or signature dynamics, and physiological characteristics that study physical characteristics such as the fingerprint, voice or vein pattern. The biometrics cannot be easily changed and they are easy to manage (Hamad & Abudalal, 2016).

A biometrics system is a pattern recognition system that establishes the authenticity of a specific physiological or behavioural characteristic possessed by a user (Eriksson, 2001). However, each biometric has its strengths and weakness, and the choice depends on the used application. No single biometric is expected to meet the requirement of all applications. The various biometrics are compared in many researches, and the fingerprint recognition has a very good balance of all the desirable properties (Jalutharia, 2010).

Recently, using biometrics in recognition of persons is an emerging phenomenon in modern society, due to the wide need of security in many applications.

1.1 Background and Context

Scientific studies in the mid-1800's proved two critical characteristics of fingerprint: the uniqueness and the persistence. The uniqueness means that every fingerprint from different fingers has its own ridge pattern. The persistence means that the fingerprint ridge patterns do not change throughout the life. These studies led to the use of fingerprints for criminal identification, and with the development of technology, an Automatic Fingerprint Identification Systems (AFIS) are deployed widely throughout the world, and used for many applications.

Fingerprint has several advantages over the other biometrics, such as: high university, high distinctiveness, high performance, easy collectability, high permanence, and wide acceptability (Jalutharia, 2010). The popularity of fingerprint recognition system is due to the low price of fingerprint sensors, simplicity to use, and good performance. Today, fingerprint identification system is included in Apple's latest iPhone, which is an important step in bringing biometrics to the mainstream (Lewis, 2014).

1.1.1 Fingerprint Representation

There are three levels of information which can be collected from fingerprint, which are categorised as: level 1, Level 2, and Level 3 (Rawat, 2009). Level 1 is the global level, and exhibits the regions where the ridge lines make distinctive ridge shapes, such as: singular points which contain arch, loop, and whorl structures, ridge orientation map which is the local direction of the ridge-valley structure, and ridge frequency map which is the inter-ridge distance. The information or the features gathered from this type cannot be used to identify the fingerprints, but it can be useful for fingerprint classification. The second level is named the local level or Galton characteristics or minutiae, which are the ridge endings and the ridge bifurcations, as shown in Figure 1.1. The ridge endings is the points where a ridge ends, and the ridge bifurcations is the points where a ridge forks or diverges into branch ridges. Minutiae are the most prominent features that can be used to uniquely identify the fingerprints, but the location and direction of minutiae alone are not sufficient to achieve high recognition rate, because of the variations caused by the flexibility and the elasticity of fingerprint skin, furthermore the minutiae is sensitive to rotation and translation of

fingerprint (Wu., 2007). The third level is the fine intra ridge details level, which are the sweat pores and the ridge contour. The features gathered from this level are highly distinctive, but they rarely used since extracting this information requires very high resolutions, and good quality fingerprint images, but they rarely used since extracting this information requires very high resolutions, and good quality fingerprint images.
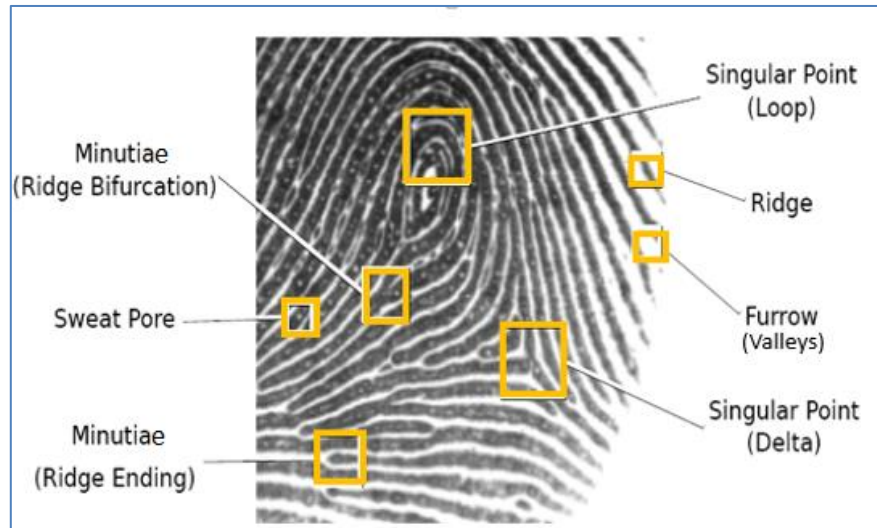
Figure (1.1): Overview over different features detectable in a fingerprint image. Quoted from **(Pober, 2010)**

Depending on the application context, a fingerprint recognition system may be called either a verification system or an identification system (Amira, 2011):

1. A verification system authenticates a person's identity by comparing the captured fingerprints with his own pre-stored biometric templates in the system. It conducts one-to-one comparison to determine whether the identity claimed by the individual is true.

2. An identification system recognizes an individual by searching the entire template database for a match. It conducts one-to-many comparisons to establish the identity of the individual.

In this thesis, we will deal with the identification problem using fingerprint. The identification process contains two modules; the first one is the enrolment module, in which the fingerprint image is captured, processed, some features will be extracted, and finally these features are stored in the database. The second one is the authentication module, in which the fingerprint image is captured, processed, some

features will be extracted, and finally the features are compared with all features in the database to match or mismatch.

1.1.2 The Identification Processes

The identification process contains several stages, which are common in construction and organization as all biometric systems. After collecting the data, the fingerprint images, the process of identification can be divided into the following stages as shown in Figure 1.2:

1.1.2.1 Pre-processing Stage

Fingerprint image quality is an important factor in the performance of AFIS. Extracting reliable features from poor quality fingerprint images is not an easy task. Major causes for degradation of fingerprint image quality include the physiological condition of fingers friction skin, performance of the capture devices (device reliability, consistency, degradation of sensing elements, image resolution, signal-to-noise ratio, etc.), acquisition environment (external light, temperature and humidity weather conditions), user/device interaction, cleanliness of device surface, acquisition pressure, and contact area of the finger with the scanner. Thus, current fingerprint recognition technologies are vulnerable to poor quality images (Wu., 2007).

In most cases this stage contains the alignment and the enhancement processes. The alignment process deals with the problems of image transition, image orientation, and image scale. The enhancement process contains several processes to enhance the clarity and the structure of the fingerprint image, and eliminate the noise. This stage will be explained in Chapter 3. In this thesis we will deal with a very poor, and a very challenges fingerprint database.

1.1.2.2 Feature Extraction Stage

In this stage, we need to use a sufficient feature extractor algorithm to give distinctive features. There are over 150 known local ridge characteristics in fingerprint, which can be used for identification process. The most popular characteristics are called minutiae points which are the ridge endings, and the ridge bifurcations. A good quality fingerprint typically contains somewhere in between 40 and 100 minutiae

4

(Eriksson, 2001). Forensic experts use this representation which has now become part of several standard for exchanging information between different systems across the world, such as the American National Standards Institute- National Institute of Standard and Technology (ANSI-NIST) slandered (Jea, 2005). For the past 100 years, the fingerprint features and matching techniques have been based on minutiae points, but this technique is not useful when we cannot extract enough and reliable minutiae points due to poor quality fingerprint images, or the fingerprint image does not have a sufficient number of points (Severance, 2015). For this reason, a lot of research have been done in extracting distinctive features from fingerprint images. Recently, researchers attempt to use the multiresolution transform techniques such as: Wavelet transform, Curvelet transform, Bandlet transform, Contourlet transform, Shearlet transform, and Wave Atoms transform as feature extractors in many biometric recognition such as face recognition, palm recognition, fingerprint recognition, and etc. In this thesis, we use the Wave Atoms transform, Curvelet transform, and Shearlet transform as feature extractors in fingerprint recognition system. These multiresolution transforms will be explained in Chapter 4.
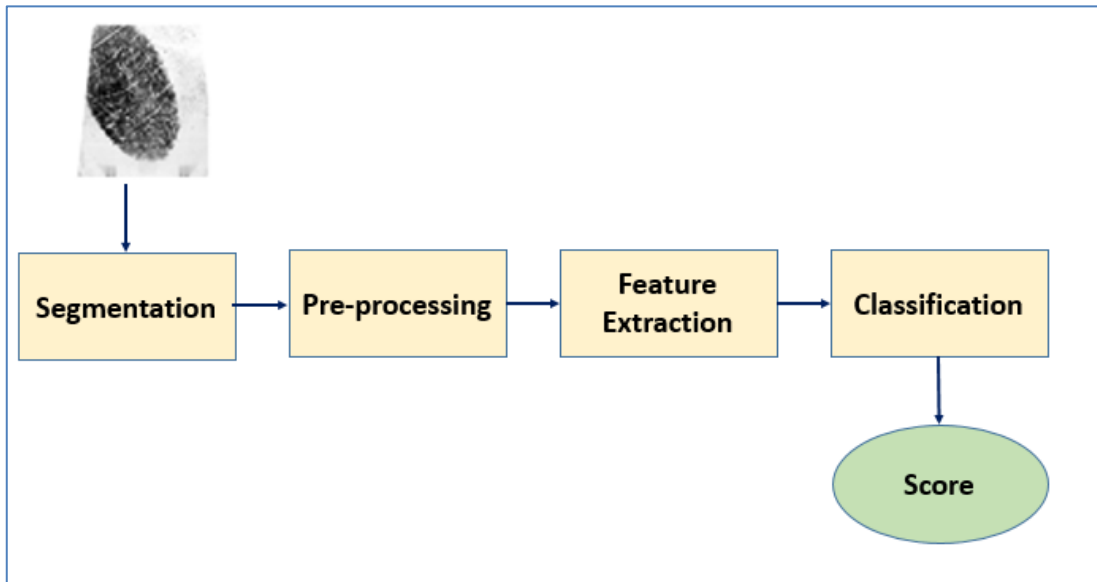
Figure (1.2): Main modules of a fingerprint identification system**.**

1.1.2.3 Classification Stage

Once a set of features is extracted from the fingerprint image, the final goal is to recognise the identity of a person whose fingerprint has been previously enrolled into

the system. The matching mechanism is the responsible to provide a likeliness score between two fingerprints. Fingerprint matching is a crucial step in both verification and identification problems. Roughly, a fingerprint matching algorithm compares two fingerprints and returns either a degree of similarity or a hard output (matched or non-matched). Two fingerprints are called genuine if they represent the same finger, and impostor when they are different.

In this thesis we will use several types of classifiers: the Minimum Distance Classifier (MD), K-Nearest Neighbour (KNN), Self-Organization Map (SOM), and Support Vector Machine Classifier (SVM). These techniques will be explained in Chapter 5.

1.2 Scope and Objectives

Fingerprint recognition is a complex pattern recognition problem. It is difficult to design a complete and robust fingerprint recognition system especially when dealing with poor quality fingerprint images. Fingerprint recognition is still a challenging and important recognition problem, due to the following challenges:

1. The high displacement and rotation which make an overlap between the query and the template fingerprint image.
2. Different pressure of fingertips
3. Different skin conditions of fingertips
4. Non-linear distortion caused by finger plasticity
5. Wounds and cutting in fingertips caused by hard worker people.

The aim of this research is to make more robust and reliable fingerprint recognition system by using an efficient feature extraction and matching techniques. In this research we will achieve the following contributions:

- Most researchers tested their approaches on clear fingerprint database, almost noisy database, or artificial one. Furthermore, researchers who used the multiresolution techniques, tested their approaches on small databases (10-30 subjects), and they suggested to increase the number of their databases. We test our approach on a large real noisy database (Test Biometrics Ideal, 2010). We choose a very challenge database to be our

work environment, which is the CASIA-FingerprintV5 Fingerprint database (Li, Busch , & Yang, 2014). We increase the size of our selected database to 114 subjects which contain 570 fingerprint images. We face an unexpected issues in many fields:

- o The number of samples is limited to 5 samples per individual; 3 samples for learning and 2 samples for testing; which is not enough for machine learning.
- o The very bad quality of fingerprint images database, which contains all types of challenges.
- o The high displacements of fingerprint images, in which 80% from our selected database is out of image borders, it feels like we work in partial fingerprint images.
- o The high and different image rotations, in which the rotation angle ranges from 0-360 degrees.

- Recently, there are a series of researches that had used the multiresolution feature extraction techniques in Fingerprint Recognition System, which began with Wavelet, followed by Contourlet and Curvelet. We continue with these researches, and use the Shearlet and Wave Atoms transforms in extracting features from fingerprint images. We use the Shearlet transform as the first time as a feature extraction technique in fingerprint recognition. We compare between Curvelet, Shearlet, and Wave Atoms, and we achieve a high recognition rate of 99.5%.

- We improve the performance of fingerprint recognition system by modifying a common enhancement technique based on Short Time Fourier Transform (STFT) analysis by replacing the segmentation technique based on energy map and optimal automatic threshold with a segmentation technique based on morphological operation and an adaptive threshold. In the same manner, we replace the segmentation process based on grey level variance which used in an alignment algorithm by replacing with the same one that based on morphological

operation which enhance the alignment process because of smoothing the segmentation contour.

1.3 Signification

A wide variety of applications require reliable authentication system to confirm the identity of individuals ,and to keep their personal information more secured from impostor users, and let only the genuine users to access their services more secure. Examples of such applications include secure access to buildings, computer systems, laptops, cellular phones and ATMs. Security systems based on biometrics have an advantage characteristics over the other. Fingerprint have been a precious tool for low enforcement, forensics and recently in commercial use for over a century. Using fingerprints in security purposes is proved to be reliable and efficient due to the high uniqueness and persistence properties, but building an efficient automatic fingerprint recognition system depends on the quality of input fingerprint image, and the feature extraction algorithm. Recognition of the fingerprint becomes a complex computer problem while dealing with noisy and low quality images.

In this thesis we are going to improve an automatic fingerprint recognition system of noisy and low quality images, and introduce the use of modern multiresolution techniques as a feature extractors, which will be helpful for improving the performance of recognition system

1.4 Limitations

This thesis is limited to the extent that only 570 fingerprint images are only considered. Furthermore, we eliminate the fingerprint images which do not have a reference point (Arch). In addition, we eliminate the fingerprint image which needs a rotation angle more than 90 degree.

1.5 Benchmarks

To test our new methodology of an automatic fingerprint recognition system on a very challenges fingerprint database, we select CASIA Fingerprint Image Database Version 5.0 (or CASIA-FingerprintV5). The volunteers of CASIA-FingerprintV5 include graduate students, workers, waiters, etc. Each volunteer

contributed 40 fingerprint images of his eight fingers (left and right thumb/second/third/fourth finger), i.e. 5 images per finger. The fingerprint images of CASIA-FingerprintV5 were captured using URU4000 fingerprint sensor in one session. The volunteers were asked to rotate their fingers with various levels of pressure to generate significant intra-class variations. All fingerprint images are 8 bit grey-level BMP files and the image resolution is 328*356 (Test Biometrics Ideal, 2010).

1.6 Overview of Thesis

This thesis is presented in seven chapters, and organized as follows:

- Chapter 1 introduces the needs of biometrics in our life, and the advantages of using biometrics in authentication process, also give a brief introduction about the fingerprint recognition systems, and the presentation of fingerprint.

- Chapter 2 presents the literature review on the fingerprint recognition systems. The first section presents the research done in image pre-processing stage, which includes: the orientation map estimation, filtering, alignment, and core point detection. The second section presents the research done in feature extraction techniques, and the last section presents the research done in classification techniques.

- Chapter 3 explains our used methodology in fingerprint pre-processing stage, which includes fingerprint alignment technique, fingerprint enhancement based on STFT analysis, and our slight modification in segmentation process, and finally it presents the core point detection technique of fingerprint images.

- Chapter 4 explains the feature extraction techniques, which are used in this thesis, and namely: Curvelet, Wave Atoms, and Shearlet multiresolution techniques.

- Chapter 5 explains a brief introduction about the matching or the classification techniques, which are used in this thesis, and namely: MD, KNN, SOM, and SVM.

- Chapter 6 shows the obtained results of our methodology, and discuses some related points

- Chapter 7 presents the conclusions and the future work.

Chapter 2

Literature Review

Chapter 2
Literature Review

The first stage of fingerprint identification is the pre-processing stage which contains image alignment and image enhancement processes and both are based on reliable segmentation process, will directly affects the result of fingerprint identification.

There are dozens of techniques which are proposed in fingerprint enhancement and matching. Most of them have no difficulty in matching good quality fingerprint, but matching low quality fingerprint remains a challenging problem (Chaudhari & Patil, 2013).

Good quality fingerprint image has high contrast and well defined ridges and valleys, while poor quality fingerprint is marked by low contrast and ill-defined boundaries between the ridges and valleys. There are some factors of the uneven force and collection environment that degrade the quality of fingerprint image (Chikkerur, Cartwright, & Govindaraju, 2007; Hong, Wang, & Jain, 1998; Khan, Khan, & Muhammad, 2010):

- Presence of creases, bruises or wounds may cause ridge discontinuities.
- A dry skin can cause inconsistent contact of finger ridges with scanner surface causing broken ridges and low contrast ridges.
- Oily or wet skin make the valleys tends to fill up.
- Moister can cause the valleys to appear dark similar to ridge structure
- Sweat on fingerprints leads to smudge marks and connects parallel ridges.
- Variations in impression conditions, ridge configuration.

These factors lead to poor quality fingerprint images, in which the ridge structures are not always defined and detected. In order to facilitate the extraction of the fingerprint feature points, an effective pre-processing step for fingerprint images is essential. The pre-processing steps usually include: fingerprint image normalization, segmentation, ridge orientation estimation, ridge frequency estimation, filtering techniques, binarization, thinning (Hong, Wang, & Jain, 1998; Jia, 2012), and alignment. These processes are often employed to reduce the noise and enhance the

contrast between ridges and valleys and even get better matching score by incorporating enhancement prior to feature extraction. A combination between these steps may lead to image enhancement.

We divide this chapter into three main parts: the first part summarizes the research done in the pre-processing stage, while the second part describes the feature extraction techniques, and the final one presents the classification techniques.

2.1 Pre-processing Techniques for Fingerprint Image Recognition System

This section summarizes the works done in image pre-processing stage of fingerprint image recognition, which includes different steps. According to our research, we divide this stage into 3 parts: the first part is the enhancement part, which contains a series of steps to achieve its goal. The second part is the alignment step, and the last one is the core point detection step.

2.1.1 Fingerprint Image Enhancement

Fingerprint image enhancement can be conducted on either a binary ridge image or a grey level image (Hong, Wang, & Jain, 1998). A binary ridge image is an image where all the ridge pixels are assigned a value of 1 and the non-ridge pixels are assigned a value of zero. Binarization before enhancement often generates more spurious minutiae structures and lose some true ridge structure, therefore enhancement of binary ridge image has its inherent limitations, and therefore most enhancement algorithms are performed on grey images directly (Baghelani, Eshkaftaki, & Ebrahimi, 2010).

Binarization method contains several processes such as: histogram equalization, Wiener filtering, binarization and thinning. The aim of using histogram equalization is to uniform the intensity distribution of grey level image, but the use of histogram equalization in fingerprint enhancement dose not give the required enhancement, and does not suitable for extracting minutiae from enhanced image (Rajinikannan, Kumar, & Muthuraj, 2010). A comparison study between three enhancement techniques was proposed in (Namburu & Praveen, 2007). They compared between the histogram equalization, FFT enhancement, and Gabor filter. The results showed that enhancement using Gabor filtering is more reliable and efficient than the others.

Similarly the use of contrast limited adaptive histogram equalization (CLAHE) (Kumar & Verma, 2012) gave a poor recognition rate of 70-75%. Some researchers attempted to use the optimization algorithms to maximize the information content of the enhanced image with intensity transformation function in order to enhance the contrast and minutiae detail in a fingerprint image such as using the Particle Swarm Optimization (PSO) (Stephen, Reddy, & Vasavi, 2013), and Bat algorithm (Bouaziz, Draa, & Chikhi, 2015).

There are many techniques are proposed to enhance the grey level image. One of the most common approach for fingerprint image enhancement and still used today is the algorithm of Hong et al. (Hong, Wang, & Jain, 1998). The main steps of their algorithm were the following processes: normalization, local orientation estimation which based on gradient method, local frequency estimation, region mask estimation, and filtering with a bank of symmetric Gabor filters, which was designed according to image orientation and frequency. The algorithm was tested on 50 poor quality fingerprint images, and they achieved an improvement results.

Researchers tried to improve Hong's et al. algorithm by improving one or more of their main processes with various ideas. These improvements concentrated on local orientation estimation and filtering.

Estimating the ridge orientation map is an important step in enhancement process. The local ridge orientation can be estimated either on a square grid block or less reliable on every pixel position in fingerprint image. There were much work done in improving ridge orientation estimation. An approach is based on Median filter-Mehtre method (Wang, Zhag, Liu, & Yu, 2011) which depended on dividing the fingerprint direction into 8 directions, computing the median grey of all directions at each pixel, then estimating the minimum grayscale variation along all 8 ridge directions.

The orientation map was estimated in each pixel in (Chakraborty & Rao., 2012) by centring a window of size (32x32) at the point where the orientation was to be estimated, the window was rotated to 16 different orientations, and at each orientation a projection along the y-axis of the window was formed, so the projection with greatest

variation correspond to the local ridge orientation in this window. The drawback of this solution is it cannot deal with noisy regions.

Recently, a new approach based on Wave Atom decomposition is proposed by (Boutella & Serir, 2013) to estimate the orientation image. They compared their results with the gradient based algorithm by human vision.

Filtering is an important step in fingerprint enhancement process. After ridge orientation have been estimated, filtering has to be applied to image to correct false estimation. Although the Gabor filters have an important properties from a signal processing perspective, the Gabor filter based approach has some errors in orientation estimation, and propagate to ridge frequency estimation leading to imperfect reconstruction (Chikkerur, Cartwright, & Govindaraju, 2007; Hu, Jing, Zhan, & Zhu, 2010), this is due to bandwidth limitation of Gabor filter (Wang, Li, Huang, & Feng, 2008).

Instead of having used Gabor filter in spatial domain, the proposed algorithm in (Namburu & Praveen, 2007), used the Gabor filter in Wavelet domain. Their idea was that the fingerprint approximation of subimage contained fewer noises than in spatial domain, and hence computing the orientation image is more reliable.

Some researchers tried to solve the limitations of traditional Gabor filtering, such as using log-Gabor filtering instead of Gabor filter (Wang, Li, Huang, & Feng, 2008), using a modified Gabor filtering with adaptive parameters (Yang, Liu, Jiang, & Fan, 2003), using fast Gabor filtering (Wang & Sun, 2010), using the anisotropic filter instead of Gabor (Greenberg, Aladjem, Kogan, & Dimitrov, 2000), using a series of notch filter high-pass filter and Gabor filter (Khan & Zakirullah, 2010), and using directional morphological filter (Wang, Zhag, Liu, & Yu, 2011).

However 2D convolution of an image using Gabor filter, or Log-Gabor filter contributes to high computational complexity due to the filter components used in designing the filter (Dyre & Sumathi, 2014).

One of the most popular fingerprint image enhancement techniques is based on Short Time Fourier Transform (STFT) analysis and contextual filtering in the Fourier domain was proposed in (Chikkerur, Cartwright, & Govindaraju, 2007; Chikkerur, Wu, & Govindaraju, 2004). The algorithm had several advantages that the ridge

orientation, ridge frequency, and region mask (segmentation) were estimated simultaneously from STFT analysis. This would prevent errors in ridge orientation estimation from propagating to other stages. Furthermore, the estimation was probabilistic and therefore was more robust. The results showed that the proposed algorithm had better than Hong in recognition rate of over a set of 800 images in FVC2002 DB3 database. This algorithm is explained in Chapter 3.

An enhancement algorithm based on combination of STFT technique and Gabor filter was proposed in (Hu, Jing, Zhan, & Zhu, 2010). The algorithm used the main concept of (Chikkerur, Cartwright, & Govindaraju, 2007) to estimate the orientation and frequency map of fingerprint image, but they changed the type of window, the size of blocks, and the overlapping parameters. They did not depend on contextual filtering, and instead they used Gabor filtering. They compared their results with Hong (Hong, Wang, & Jain, 1998) algorithm, and got better results. They admitted that their enhancement fingerprint image did not seem to be better than the enhancement algorithm of (Chikkerur, Cartwright, & Govindaraju, 2007).

Several enhancement algorithms based on Wavelet transform are performed. The proposed technique in (Saeed, Tariq, & Jawaid, 2011) included the following steps: image segmentation, normalization, image sharpening, Gabor Wavelet filtering to enhance the feature of sharpened image, binarization, and thinning. Experimental results of their selected fingerprint images form FVC2004 database, showed a good accuracy in enhancing the fingerprint image quality, but they did not refer to how they estimated the quality of their enhancement. Another Wavelet based technique was proposed in (Hsieh, Lai, & Wang, 2003). The main steps of their algorithm are: segmentation, normalization, Wavelet decomposition, global texture filtering, local directional compensation, and Wavelet deconstruction.

An enhancement algorithm that combined filtering in both spatial and frequency domains was proposed in (Dyre & Sumathi, 2014). Fingerprint enhancement models in (Babatunde, Charles, Kayode, & Olatubosun, 2012) included segmentation, normalization, ridge orientation estimation, ridge frequency estimation, Gabor filtering, binarization and thinning. They tested their solution on synthetic and real

fingerprint images. The results showed that with free or minimal noise level, the algorithm performs well.

In (Rajinikannan, Kumar, & Muthuraj, 2010), the performance of three models of image enhancement techniques was evaluated, and their impact in minutiae detection were compared. These minutiae detection techniques were: a) The Histogram Based Image Enhancement, b) The FFT filter Based Fingerprint Image Enhancement, and c) The Gabor filter Based Fingerprint Image Enhancement. These techniques were particularly very much different in the way of enhancing the input image for minutiae detection. They compared the performance of image enhancement algorithms using the number of minutiae in all the three cases with the values of a human observer. Among the three evaluated fingerprint image enhancement algorithms, the Gabor filter based algorithm performed very well. It was performed 5 to 6 times better than the other two algorithms

Similarly, a comparative study between six different enhancement techniques was proposed in (Malwade, Raut, & Thakare, 2015). The first one was based on Histogram Equalization. The second one was based on 2D Fourier transform and Butterworth filter. The third one was based on Gabor filters. The forth one was based on Gabor filters combined with Wavelet transforms. The fifth one was based on directional filters. The last one was based on Laplacian-based pyramidal decomposition (LPD). They computed the peak signal-to-noise ratio, and Equal Error Rate (EER) for all the testing algorithms. The result showed that the LPD method and Wavelet based enhancement have been given a slight better results.

Another comparative study between three different enhancing algorithms was proposed in (Yusharyahya, Nugroho, Purnama, & Galinium, 2014) to evaluate the effectiveness of fingerprint image enhancement. These algorithms included the use of FFT, smoothing on the spatial domain, and contextual filtering using Gabor filters. The result showed an improvements in enhancing poor quality fingerprint images in frequency domain. Although the FFT produced the best result in enhancing fingerprint images, it also introduced noise outside of the fingerprint image as a side effect of the frequency domain process, which can be solved by using a better segmentation algorithm. The enhancement based on Gabor filters worked well in good and

recoverable region of fingerprint image, but it leaved empty blocks in unrecoverable regions. Algorithms based on only the spatial domain could not enhance minutiae details in the fingerprint image.

A three-stage enhancement algorithm was proposed in (Kabir, Ahmad, & Swamy, 2013) to enhance the quality of fingerprint images. The first-stage performed diffusion filter on the computed orientation field to connect broken ridges. Although it connected the broken ridges, it reduced the contrast of the image and failed to separate the falsely conglutinated ridges. In the second stage, filtering was applied to the enhanced image to remove the smears and scars, to separate the falsely ridges, and to improve the contrast of the image. Although the second stage overcomes the limitations of the first-stage, it produced black borders and created false minutiae in the enhanced image. In the third-stage, an angular filter was applied to overcome the shortcomings of the second-stage, and this enhanced the low-quality fingerprint images to a large extent. The drawback of this solution is the complexity of its procedures, which needs to compute several pre-processing techniques in addition to their main process, such as normalization, orientation field estimation.

2.1.2 Fingerprint Image Alignment

In order to achieve high recognition rate when comparing fingerprint images or even the features extracted from the fingerprint images, these images or features of both the reference sample and the test one have to be aligned. There are three major challenges involved in capturing fingerprint images: translation, rotation and scaling (Li, Busch, & Yang, 2014). Fingerprint translation refers to the position of a captured fingerprint with respect to the fingerprint image background, and for optimum functionality of AFRS, the fingerprint should be positioned in the central area of the fingerprint image background. Fingerprint rotation refers to the alignment of a captured fingerprint image when measured against the image background, and for optimum functionality of AFRS, the captured image should sit at an angle of approximately 0 degrees (more or less upright) relative to the vertical axis (Msiza, Leke-Betechuoh, & Malumedzha, 2011). The most effort of research of addressing these challenges is focused on translation and rotation issues, because capturing

fingerprint images does not lead to scaling problem since most fingerprint images could be scaled as per the dpi specification of the sensors.

Various techniques are proposed to solve the rotation problem, and each of them has its advantages and disadvantages. One of them (Wegstein, 1982) depended on finding both a core point and a delta point in the fingerprint image to estimate the re-alignment angle. In particular the translation invariance is accomplished by locating the reference point. The drawback of this solution in addition to the difficulty of finding delta point, is that it will fail when dealing with Plain Arch (PA) fingerprint class, which does not contain a core or delta point. Another instance where this algorithm may fail, is when dealing with Tented Arch (TA) fingerprint class, which has a single core and a single delta, with the core located almost directly above the delta. Many singular point detection techniques, however, find it relatively difficult to detect this delta point. Another instance where this method is likely to fail is when dealing with the Left Loop (LL) and the Right Loop (RL) fingerprint classes. Although these classes of fingerprint have both the core point and the delta point, in most cases the delta point is not captured.

Because of the problem of finding a reference point in the Plain Arch fingerprint class, researchers attempted to solve this issue by different techniques (Lam, et al., 2009), (Li, Busch, & Yang, 2014). The only problem with this recent development is that this technique is dedicated only to those fingerprints that belong to the PA class. This is a problem, because this solution requires to classify the fingerprint classes, then to use the appropriate reference point detection method before re-aligning the fingerprint.

An independent and efficient approach was proposed in (Msiza, Leke-Betechuoh, & Malumedzha, 2011). Their approach did not depend on a particular fingerprint class, and so it can be used for all types of fingerprint classes. They used a new reference point named as True Fingerprint Centre Point (TFCP), which determined after segmentation process, and it lied on the centre of Region of Interest (ROI) area. From this point, they determined the rotation angle and direction of rotation. This algorithm is explained in Chapter 3.

The rotation problem was handled in (Jain, Prabhakar, Hong, & Pankanti, 2000) by cyclic rotation the extracted feature values in the matching stage. Similarly, in (Guesmi, Trichili, Alimi, & Solaiman, 2012) the feature vector of each fingerprint template is rotated with 5 angles; -20, -10, 0, 10, 20; and when matching, the test image is compared for all templates.

The other solution of translation and rotation issues is what is called the registration. Registration means that you have to choose a base image, then you have to translate the test image to lie exactly on the base image in order to achieve the maximum response between the two images. Registration is a common concept in image process which can achieve the translation and rotation invariant. An approach based on fingerprint registration was proposed in (Liu, Jiang, Yang, & Zhu, 2006), in which the best alignment of two fingerprint images, template and input, is achieved by maximization of Mutual Information (MI) between the extracted features from their orientation fields, i.e., maximization of similarity measures between two fingerprint images.

Another approach based on measuring the similarity between a set of rotated fingerprint images of the registered image over an angular range $-40 \leq \theta \leq 40$, and the input image, was proposed in (Ito, et al., 2005). The translation was achieved by using the position of the core point in both images. The drawback of this solution is the high expensive computations due to the need of rotating each template 80 times with different rotation angles, then the comparison of each of these rotated images with the input one is considered. Furthermore, the rotation angle of some fingerprint images exceeds this limited range of angles.

Anyway, using the registration techniques to solve the alignment and translation problems in fingerprint recognition system, may be a good solution, but it will cost a lot of computations and does not work well in all cases of fingerprint image qualities.

2.1.3 Core Point Detection

The reference point is defined as the point with maximum curvature of the concave ridges in the fingerprint image (Prabhakar, 2001). The reference point plays a very important role in many identification techniques, and in some techniques it has

to be detected accurately. At a global level, the ridge lines in a special area of fingerprint image make distinctive shapes, and notable landmark structures, such as core, delta, whorl, and loop. Locating the reference point is a critical step to solve the problem of various fingerprint image displacement (Eriksson, 2001). One of the most common and simple approach for determining the reference point is Poincaré index (Kawagoe & Tojo, 1984). The algorithm depended on the differences in ridge directions between adjacent blocks. The drawback of this solution that it failed in determining the reference point in poor quality fingerprint images with cracks, scars, dry skin, or poor ridge (Prabhakar, 2001). Another solution based on the geometry of region was used to locate the reference point (Prabhakar, 2001; Jain, Prabhakar, Hong, & Pankanti, 2000), but it also failed in poor quality fingerprint images.

Determination of singular point in (Nilsson & Bigun, 2003) was accomplished by its symmetry properties, i.e. its strong response to complex filters designed for rotational symmetry extraction. The algorithm was described briefly in Section (3.3). Algorithm in (Ohtsuka, Watanabe, Tomizawa, & Aoki, 2008) used both the global and local features of the ridge distribution to find the position of core point. The algorithm achieved better results than of Poincaré index, but it longer in computation time. The algorithm of (Tang, Wu, & Xiang, 2008) reduced the Poincaré index's computation time by applying the modified version of Poincaré index to an effective regions that may contain the singular point.

Recently, an approach based on flow curves was proposed in (Nasiri & Fathy, 2015) to detect the reference points. Both flow curves and fingerprint ridges are similar to each other, but flow curves are not affected by discontinuities which are encountered in ridge extraction. Their algorithm depended on clustering the points of high curvature, then extraction the reference point. They tested their approach on FVC2002 DB2, and FVC2004 DB1, and gained 92%, and 83% respectively. The result of reference point detection is computed by measuring the distance between the location of their approach and the manually determined location. If the distance was more than 40 pixels, then their approach failed. We suggest that their approach has to be compared with common algorithms such as Poincare, or complex filter.

2.2 Feature Extraction Techniques for Fingerprint Images Recognition System

The features of fingerprint images can be extracted from global level or local level. The global level does not has distinctive characteristics which used for identification of fingerprint images. At the local level, there are some characteristics can be used to distinguish between different fingerprint images. Minutiae is the most widely local level characteristic used in fingerprint identification. Minutiae contains ridge ending and ridge bifurcation.

It is nicely to refer here that there are some features behind the Minutiae, which can be used for matching. These different features contain: orientation-based minutiae descriptor, FingerCode, ridge feature map, orientation map, and density map. Researchers attempted to combine between these features to improve the recognition rate of fingerprint identification system. One research on comparison of combining between these features is proposed in (Chen & Zhou, 2010). They concluded that beyond four features, the improvement is limited, so they suggested to limit the number of the used features to 4.

Recently, researchers used other features techniques to overcome the limitations of minutiae based. They tended to use the frequency based algorithms at different transform to extract unique features for fingerprint images.

In this section we summarises some proposed algorithms based on various multiresolution transforms to extract features from the fingerprint images.

A comparison study of three frequency based feature extraction techniques was proposed by (Dale & Joshi, 2008). They used Discrete Cosine Transform (DCT), FFT and Discrete Wavelet Transform (DWT) to create a feature vector for matching fingerprints images by using Euclidean distance. The results showed that DCT and FFT performed better than DWT technique. However, their algorithm did not achieve a good recognition rate since they do not perform any enhancement process on their tested fingerprint dataset.

An early approach based on Wavelet decomposition was proposed by (Tico, Immonen, Ramo, Kuosmanen, & Saarinen, 2001). They did not use an enhancement process, but they depended on finding a reference point in fingerprint image, so they

found it manually. Their algorithm included locating the core point, cropping the ROI around the core point, dividing the ROI into non overlapping blocks, then applying the Wavelet decomposition on each block to extract a global feature vector of length 48 which was classified by KNN. The results showed a high recognition rate on 13 subjects selected from Bologna's fingerprint database.

The use of Curvelet transform has been proposed by many researchers as a feature extraction technique. The proposed solution in (Guesmi, Trichili, Alimi, & Solaiman, 2012) included: enhancement process, core point detection, cropping of ROI of size 175x175, resizing this ROI to be 512x512, then applying Curvelet transform for 5 scales, and encoded three statistical features (Energy, entropy, and standard division) from each. The feature vector size was 164x3 for each image. They used the similarity distance to match 30 subjects from FVC2004 database. They achieved a good results, however, using 492 features is a large number of features compared to the number of subjects they tested. Furthermore, they solved the rotation problem by rotating the ROI of template with 5 angles, then they compared the test image with all of these templates. The drawback of this solution is the multiple of 5 overhead computation will be occurred.

Similarly, another approach using the Curvelet transform was proposed in (Mandal & Jonathan Wu, 2008). They divided the ROI area into 4 parts 32x32 subimages, applied the Curvelet transform on each subimage with different scales and angles, then a standard deviation was taken for each subimage to reduce the dimensionality of Curvelet's coefficients, then they concatenated the feature vector from each one to be ready for comparison. They achieved the maximum recognition rate on 15 subjects from FVC2004 database. However, this high recognition rate was due two reasons: first they determined the core point manually so there was no core point algorithm is used, and the second is the small number of subjects, and the efficient number of samples per finger.

Another approach that using the Curvelet transform as a feature extraction was proposed in (Humaira, Bushra, Firdous, Khan, & Islam, 2013). Their algorithm included image enhancement process, core point detection, alignment process, cropping the ROI of size 50x50, applying Curvelet transform to extract the feature

vector, then using the mean and standard deviation statistics to get the final feature vector which would be matched with the KNN algorithm. They tested their solution on a small database of selected 10 subjects from FVC2002 dataset, and got a high recognition rate of about 90%. They rejected the fingerprint images which their core point is near the image borders. We think this high recognition rate is due to very small testing dataset, however their solution was a robust algorithm. Another hint for their alignment process, is that their alignment process depended on rotation the test and the rest of training images according to the reference image. The reference image was chosen as the maximum energy response by applying Gabor filter to all fingerprint subject samples. This process is known as a registration process.

A different feature extraction technique based on Contourlet transform was proposed by (Omidyeganeh, Javadtalab, Ghaemmaghami, & Shirmohammadi, 2012). The algorithm contained image enhancement, core point detection, cropping the ROI of size 192x192, dividing the ROI into two non-overlapping blocks with the core point at the centre, followed by applying the Contourlet transform on each block, then the feature vector extracted from each block based on Generalized Gaussian Density (GGD). The results were matched using KNN classifier on 25 subjects from FVC2004 dataset. The results showed an improvement in recognition rate with respect to Wavelet transform. We can observe from their paper that they did not refer to the alignment problem, which is an important process in fingerprint identification.

Another approach based on correlation matching between the input image and the test image was proposed by (Haddad, Beghdadi, Serir, & Mokraoui, 2008). The authors used the Radon transform to extract the rotation features from fingerprint images. They tested their algorithm on 10 subjects from FVC2004 dataset. One drawback of their solution is that they assumed that the fingerprint images were already aligned, so their solution did not deal with the alignment problem.

Another approach based on Wave Atom transform was proposed by (Mohammed, Jonathan Wu, & Sid-Ahmed, 2010). The algorithm resized the fingerprint image to size 64x64, the Wave Atom was applied to this resized image, then the bidirectional wo-Dimensional Principal Component Analysis (B2DPCA) was applied to reduce the feature vectors dimension which were classified using the

Extreme Learning Machine (ELM). They evaluated their algorithm on 100 subjects of the three databases FVC2000, FVC2002, and FVC2004. They got a recognition rate of 93%, 87%, and 89% respectively. The proposed algorithm did not include an enhancement or rotation processes, however it showed the powerful of B2DPCA algorithm for dimensionality reduction, and ELM as a classifier. According to our research, this is the only paper we found, which used the Wave Atom transform as a feature extraction technique for fingerprint identification.

In (Jena & Dalal, 2014) the fingerprint image was firstly converted to grey scale image, a 3 level DWT was applied to grey scale image and the feature extraction was performed using the mean and variance. Features database was created in which 24 features of a person's fingerprint were stored. Finally matching the feature vectors was performed using Euclidean distance. They selected 25 person's fingerprint images from CASIA-FingerprintV5 (200- 299). The system gave FAR as 2.3 % and FRR as 0.9%. One drawback with this approach is that they did not refer to the rotation and translation problems, although their selected database has a strong rotation level and translation within the same subjects.

Recently, an approach based on Gabor filter bank was proposed in (Chavan, Mundada, & Pal, 2015). They used the Gabor filter bank to extract fingerprint image features. Their approach included: normalization, segmentation, cropping the selected ROI, locating the reference point, then the Gabor filter is applied on the ROI to extract the feature vectors. Finally the feature vectors of query fingerprint image are compared using the Euclidian distance with database fingerprint images. They extracted some features from the Gabor filter response such as ridge frequency, width of Gaussian envelope, and filter orientation. These features are transformed into a feature map, which is circularly tessellated with different 5 bands and 8 sectors with consideration of reference point as a centre of an image. The algorithm was tested on 20 subjects from FVC2000 and 50 subjects from DBIT fingerprint database, and they achieved an average efficiency of 82.95 % and 89.68 % respectively.

2.3 Classification Techniques for Fingerprint Images Recognition System

Most of the explained approaches in Section 2.2 which are based on multiresolution transformation techniques as a feature extraction algorithms, used a

simple matching algorithm to measure the similarity between vectors, such as ED or KNN, instead of using complex classifiers, such as Neural Networks (NN), or SVM. This is because they aim to reduce the computation time of their algorithms for AFRS.

Some approaches did not use the enhancement process in their algorithms, and they dealt with small fingerprint image. However, they depended on a strong dimensional reduction techniques to reduce their feature vectors, and they depended on a strong matching algorithm to perform identification process. This kind of matching needs enough sample for matching.

One of these algorithms was the approach introduced by (Luo, Lin, Lei, & Ni, 2008). The algorithm resized the fingerprint image to 64x64, applied a two-lever Wavelet decomposition to the image to extract a feature vector, followed by using 2DPCA to reduce the dimension of the feature vector, finally the matching process was accomplished by Ellipsoidal Basis Function Neural Network (EBFNN).

The approach of (Mohammed, Jonathan Wu, & Sid-Ahmed, 2010) replaced the Wavelet decomposition with the Wave Atom decomposition, and 2DPCA with B2DPCA, and EBFNN with extreme learning machine matching algorithm.

An approach based on NN matching was proposed by (Altun & Allahverd, 2006). They used the Contourlet transform for image enhancement after some filtering process. The extracted features depended on FingerCode algorithm, in which the feature vector was determined by dividing the circle area around the core point into sectors which was divided into bands, then computing the grayscale variance of each sector. A feature vector of size 384 was input to the NN. They tested their algorithm on their own dataset, which contains 1000 images for only 10 persons, and achieved a recognition rate of 99.6%. This means that each subject contained 100 samples which is an excellent condition to the NN to learn. Furthermore, they did not refer to the rotation problem in their paper, however the rotation problem was solved in the main reference (Jain, Prabhakar, Hong, & Pankanti, 2000) in matching stage by cyclically rotating the FingerCode feature eight steps with an angle of 22.5 degree.

An approach based on fingerprint texture pattern and Hidden Markov Model (HMM) was proposed in (Guo, 2005). The feature vector was based on the orientation field of fingerprint image, and it was extracted from different regions of the image

after scanning, rotation, and core point detection. The result gave an EER of 7.1% on FVC2002 DB1. This approach skipped the process of thinning and minutiae selection, however the difficulty of FVC2002 DB1 is classified a low difficulty database in (Turroni, 2012).

Another approach based on Hilbert curve and HMM was proposed in (Azarnoush & Kiani, 2014). The algorithm contained: fingerprint enhancement, locating the core point, binarization, cropping the image around the core point, feature extraction using Hilbert curve, and finally classification with HMM. They added an extra process which rejected the defected fingerprint image. Defected images are those of non-clear core point, or the core point is near the margins. The result gave an ERR of 2.4% on FVC2002 DB1.

An approaches based on Back Propagation Neural Network (BPNN) classifier and invariant moment features was proposed in (Yang & Park, 2008). Their approach contains: image enhancement using STFT, detection of reference point, determination of ROI, partition the ROI into 4 non overlapping regions, applying moment features of size of 24 features, and finally matching using BPNN. The result gave an ERR of 3.685% on four databases of FVC2002.

The same approach was proposed in (Balti, Sayadi, & Fnaiech, 2014), but with a different feature extraction technique based on linear algebra, which known as Singular Value Decomposition (SVD). They improved the ERR from 3.685% to 3.475%.

An approach based on multilayer perceptron NN was proposed in (El-Feghi, Tahar, & Ahmadi, 2011). They used the segmentation with an elliptical shape, the pseudo-Zernike moments (PZM) technique to extract the feature vector of size 21, and finally the matching was performed using MLP. They tested their approach on a database of 40 subjects, each subject contains 10 samples. They gained a recognition rate of 100%. However, they have to test their approach on one of the common databases to make a comparison to other approaches. Anyway, choosing a database of 10 samples for each subject is a good choice to train the NN.

An approach based on SOM was proposed in (Acquah & Gyimah, 2014). They detected the core point based in (Jain, Prabhakar, Hong, & Pankanti, 2000), extracted

the feature vector from Gabor filter, and used the SOM for matching the fingerprint images. They achieved a recognition rate of 82% on FVC2004 DB3. The same approach was proposed in (Elmir, Elberrichi, & Adjoudj, 2012). The results of recognition rate were: 68.4%, 63%, 73.6%, and 78.9% on databases of FVC2004 DB1, DB2, DB3, and DB4 respectively.

Some approach combined between clustering and neural network techniques, such as a combination between SOM and Radial Basis Function Network (RBFN) (Kundu & Sarker, 2015).

SVM algorithm was first used in fingerprint classification in (Yao, Frasconi, & Pontil, 2001). An approach based on SVM for fingerprint verification was proposed in (Daramola, Sokunbi, & Adoghe, 2013). Their approach contained: image enhancement, feature extraction based on the centre of gravity, and finally matching using SVM. They tested their approach on fifty students of Covenant University Otaon, and achieved a recognition rate of 80%. However, they have to test their approach on common databases.

Another approach based on Fourier-Mellin transform as a feature extraction algorithm and SVM as a matching algorithm was proposed in (He, Ou, & Guo, 2003). They tested their approach on a small database which is built by the Biometric System Lab of size 21 subjects. They achieved a recognition rate of about 94%.

It is worth to know that most of the research which we did on using SVM and SOM classifiers in fingerprint recognition system, showed that these classifiers were used much in verification and classification, and they were used less in identification.

Chapter 3

Fingerprint Pre-processing Techniques

Chapter 3
Fingerprint Pre-processing Techniques

In this chapter, we introduce the pre-processing techniques, which are one of the most important part in any fingerprint recognition system. We divide this chapter into three parts: the first part introduces the alignment technique which is used to rotate the fingerprint image, the second part introduces the enhancement techniques, which are used to improve the clarity of poor fingerprint images, and the last part introduces the reference point detection technique, which is used to select a small region from the fingerprint image, and is considered as an input image to the feature extraction technique.

3.1 Alignment Techniques

There are three major challenges involved in the acquired fingerprint samples: translation, rotation and scaling. Fingerprint translation and rotation processes are the most important steps in any automatic fingerprint recognition system, since capturing fingerprint images does not lead to scaling problem since most fingerprint images could be scaled as per the dpi (Dot per Inch) specification of the sensors. Fingerprint translation refers to the position of a captured fingerprint with respect to the fingerprint image background, and for optimum functionality of AFRS, the fingerprint should be positioned in the central area of the fingerprint image background. Fingerprint rotation refers to the alignment of a captured fingerprint when measured against the image background, and for optimum functionality of a fingerprint recognition system, the captured image should be sat at an angle of approximately 0 degree (more or less upright) relative to the vertical axis (Msiza, Leke-Betechuoh, & Malumedzha, 2011). In order to achieve a high recognition rate, the fingerprint images have to be aligned and translated accurately.

We first used the image registration technique for image alignment problem. We use an intensity based image registration function; imregister; which is already implemented in Matlab toolbox. This function takes two images: the first is the fixed image, and the other is the image which will be rotated and transmitted to match the fixed one.

However, the image registration technique may achieve good results, it costs high computations. Furthermore, it requires to select a base image, and for each test image, the registration process is performed with all the training images. When we applied this technique in CASIA-FingerprintV5 database, we faced a problem that for every type of noises in this database, the configuration parameters needed to be optimized differently.

We implement the proposed alignment algorithm in (Msiza, Leke-Betechuoh, & Malumedzha, 2011). This approach is independent of fingerprint classes, and can be used for all fingerprint classes. The algorithm is simple and efficient, and contains the following processes:

1- **Segmentation**: this process is an important step to separate the foreground region from the background region. This is useful to avoid the subsequent extraction of fingerprint feature in the background noise (Alonso-Fernandez , et al., 2009). It generates a mask image, which contains two colors: white and black. The white area is the area of the ridge structure; the foreground region; while the black area is the area of background. See Figure 3.1. The task of segmentation is to decide which part belongs to the foreground and which part to the background. The result of the used segmentation technique which based on grey level variance in Msiza et al. is shown in Figure 3.1. We replace the segmentation technique used by Msiza et al technique with another segmentation technique based on morphological operation (Fahmy & Thabet, 2013), which does not depend on a threshold value, and has additional features over the one used in Msiza et al. These features affect and improve the performance of the alignment technique in Msiza et al. such as: first they used the erosion function which has the effect of removing isolated foregrounds, and the dilation function which has the effect of broadening or thickening narrow regions, so it removes the small holes. The mechanics of erosion and dilation are similar to convolution in filtering operations. Furthermore, it improves the foreground edges by smoothing the contour. We will see the results of using this technique over the one used by Msiza et al in Chapter 6.
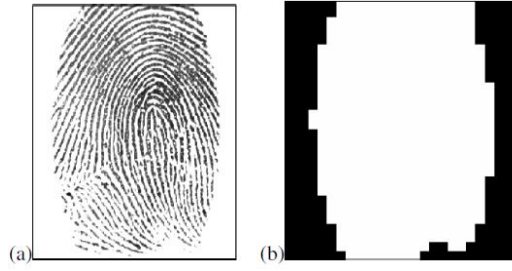
Figure (3.1): Fingerprint segmentation. Quated from (Msiza, Leke-Betechuoh, & Malumedzha, 2011)

2- **True Fingerprint Center Point (TFCP) Location**: this process aims to find an optimum center point (TFCP), which lies on the center of foreground area. This process is described in Table 3.1, which is achieved by three steps. The first step locates the center point of the fingerprint image, which is computed by dividing both the x-coordinate, and y-coordinate by 2, and hence this is the starting point that is required to the next step. The second step is to navigate the x-axis of the foreground area by first navigate to the right until reaching the foreground edge, and then to navigate to the left until reaching the foreground edge. This navigation distance is divided by 2 to obtain the center point of the foreground x-axis. The third step is to navigate the y-axis of the foreground area by starting at the center point, then we navigate upward until reaching the upper edge, then navigate downward until reaching the lower edge. This navigation distance is divided by 2, to obtain the center point of the foreground y-axis. Now we have the center point of the foreground area.

3- **Fingerprint Re-alignment:** First, we determine the re-alignment direction and, second, we determine the re-alignment angle. If a fingerprint is rotated anti-clockwise, the realignment direction is clockwise, and vice versa, as shown in Figure 3.2. This process depends on locating a point with x-coordinate refers to the TFCP point, and y-coordinate refers to the upper navigation point of y-coordinate. From this point location, a horizontal upper edge is determined. From the point which is lied on the upper edge, three distances are computed. The first one is the distance between this point and the right edge C1. The second one is the distance between this point and the left edge C2. The direction of rotation is determined according to which one

is longer than the other. If C1 > C2 then the rotation direction is anti-clockwise, and if C1< C2, then the rotation direction is clockwise. The third distance is the vertical distance between the TFCP and the upper edge C4. An offset distance C3, equals to the distance of C1 is added to right or to the left side of C2 according to the rotation direction to complete the upper line of the triangle, while C4 is the vertical line of the triangle. The angle of rotation is the angle of the triangular. This process is described in Table 3.2 and Table 3.3, and are characterized by two main procedures.
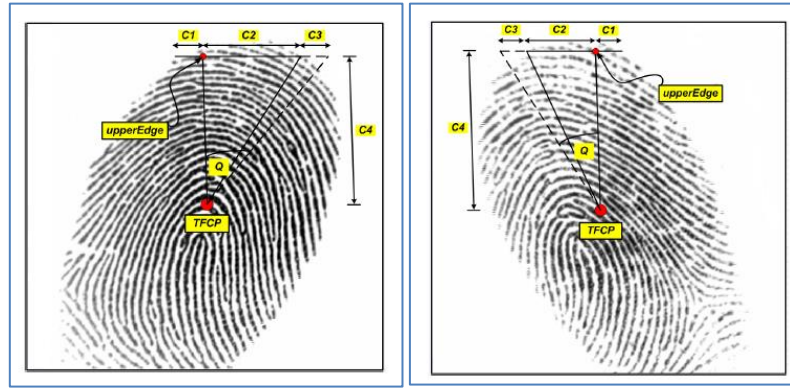
Figure (3.2): Determining the re-alignment angle. Quated from (Msiza, Leke-Betechuoh, & Malumedzha, 2011)

$Input :$ $Fingerprint\ mask\ image, M$
$Output :$ $TFCP\ coordinates, (x_f, y_f)$
$Constants: W, the\ width\ of\ M;$ $and\ H, the\ height\ of\ M$
$Variables : x_r;\ x_l;\ y_u;\ and\ y_l$

$Compute: (x_b, y_b)\ using:\ x_b = 0.5 \times W, y_b = 0.5 \times H;$
if $M(x_b, y_b) = 1$ **then**
 $Initialize: x_r = x_b;$
 while $M(x_r, y_b) = 1\ AND\ x_r \leq W\ do$
  $increment: x_r;$
 end
 $Initialize: x_l = x_b;$
 while $M(x_l, y_b) = 1\ AND\ x_l >= 0\ do$
  $decrement: x_l;$
 end
 $Initialize: y_u = y_b;$
 while $M(x_b, y_u) = 1\ AND\ y_u >= 0\ do$
  $decrement: y_u;$
 end
 $Initialize: y_l = y_b;$
 while $M(x_b, y_l) = 1\ AND\ y_l <= H\ do$
  $increment: y_l;$
 end
 $Compute: (x_f, y_f)\ using\ x_f = \dfrac{(x_r, x_l)}{2}, y_f = \dfrac{(y_u, y_l)}{2}\ ;$
end
Terminate;

Table (3.1): Pseudocode for locating the TFCP based on fingerprint mask image

$Input$: Fingerprint mask image, M; x_f; and y_u $Output$: Re − alignment direction, D $Constants$: W, the width of M $Variables$: x_u; C_1; and C_2

$Initialize$: $x_u = x_f$;
 $Start$: at the point (x_u, y_u), the $upperEdge$;
 if $M(x_u, y_u) = 1$ **then**
      while $M(x_u, y_u) = 1$ AND $x_u <= W$ **do**
        $increment$: x_u;
      end
      $Compute$: $C_1 = x_{u\,7} − x_f$;
      $Re − initialize$: $x_u = x_f$;
      while $M(x_u, y_u) = 1$ AND $x_u >= 0$ **do**
        $decrement$: x_u;
      end
      $Compute$: $C_2 = x_{f\,12} − x_u$;
      if $C_1 < C_2$ **then**
        D is $clockwise$;
      else if $C_2 < C_1$ **then**
        D is $anti − clockwise$;
      else
        D is $upright$ (no $re − alignment$ $required$);
      end
      $Re − initialize$: $x_u = x_f$;
 end
 Terminate;

Table (3.2): Pseudocode for determining the realignment direction of a rotated fingerprint

$Input$: Re − alignment direction, D; C_1; C_2; y_f; & y_u $Output$: Re − alignment angle, Q $Variables$: C_3 and C_4

$Initialize$: $Q = 0$ degrees;
 if D is not upright **then**
      $Compute$: $C_4 = y_{f\,3} − y_u$;
      if D is clockwise **then**
        Add: an $offset$, $C_3 = C_1$, to the left of C_2;
      else if D is anti − clockwise **then**
        Add: an $offset$, $C_3 = C_1$, to the right of C_2;
      end
      $Q = \arctan\big(divide(sum(C_2, C_3), C_4)\big)$ degrees;
 end
 Terminate;

Table (3.3): Pseudocode for determining the realignment angle of a rotated fingerprint

3.2 Fingerprint Enhancement Techniques

One of the most popular and an effective fingerprint enhancement algorithm is proposed in (Chikkerur, Cartwright, & Govindaraju, 2007). The enhancement algorithm is based on short time Fourier transform (STFT) analysis, and on contextual filtering in the Fourier domain whose parameters depend on the local ridge frequency and orientation. The idea of this algorithm is to create an adaptive filter whose

parameters depend on the contextual information of fingerprint image to be able to recover corrupted and occluded regions. The purpose of the filter is to fill small gaps (low pass effect) in the direction of the ridge, and to increase the discrimination (band-pass effect) between ridges and valleys in the direction orthogonal to the ridge (Jea, 2005). The contextual information includes the ridge continuity and the regularity, which is obtained by computing the intrinsic images through the STFT analysis. The intrinsic images represent the important properties of the fingerprint image as a pixel map. These include: orientation image, frequency image, and region mask or segmentation.

An orientation image O, is defined as an $N \, x \, N$ image, where $O(i,j)$ represents the local ridge orientation at pixel (i,j). The orientation image is usually specified for a block rather than for every pixel (Hong, Wang, & Jain, 1998). The local ridge frequency indicates the average inter ridge distance within a block. Region mask indicates the parts of the image where ridge structures are present. It is also known as the foreground mask, or segmentation process. These three intrinsic properties are important tasks in fingerprint recognition system, and the reliable estimation of these processes lead to a robust fingerprint recognition system.

(a) (b) (c) (d)
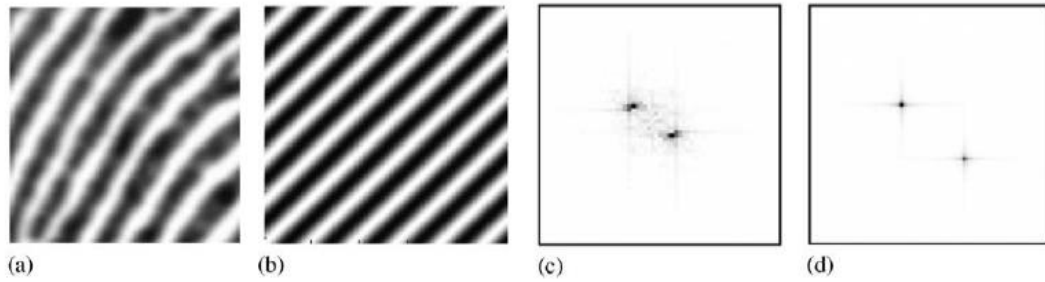
Figure (3.3): Local region in a fingerprint image and its surface wave approximation and its fourier spectrum of the real fingerprint and the surface wave. Quoted from (Chikkerur, Cartwright, & Govindaraju, 2007)

The first stage of the enhancement algorithm consists of STFT analysis, in which the intrinsic properties are computed, while the second stage performs the contextual filtering. During the STFT analysis, the image is divided into small overlapping windows. This assumption based on that any local region in the image is assumed stationary within this small window, and has a consistent orientation, and can be modelled approximately as a surface wave as shown in Figure 3.3 (a) and (b), characterized by its orientation θ and frequency f, which are obtained from its Fourier

spectrum that consists of two impulses whose distance from the origin indicates the frequency and its angular location indicates the orientation of the wave as shown in Figure 3.3 (c) and (d). However, this assumption is not true in the regions with singularities, such as core and delta. Furthermore, because of creases in fingerprint image, this approach is not very useful in all cases of fingerprint images. Instead, a probabilistic approximation of the dominant ridge orientation and frequency is proposed. In the case of corrupted regions or creases in fingerprint image with poor ridge structure, the ridge orientation can be estimated by considering the orientation of its immediate neighbourhood. Figure (3.4): illustrates how the spectral window is parameterized, and we see that the position of the window is overlapped by OVRLP pixels with the previous position. This preserves the ridge continuity and eliminates 'block' effects common with other block processing image operations. The Fourier spectrum within each window is analysed and a probabilistic approximation of the dominant ridge orientation and frequency are obtained. The algorithm is described in Table 3.4
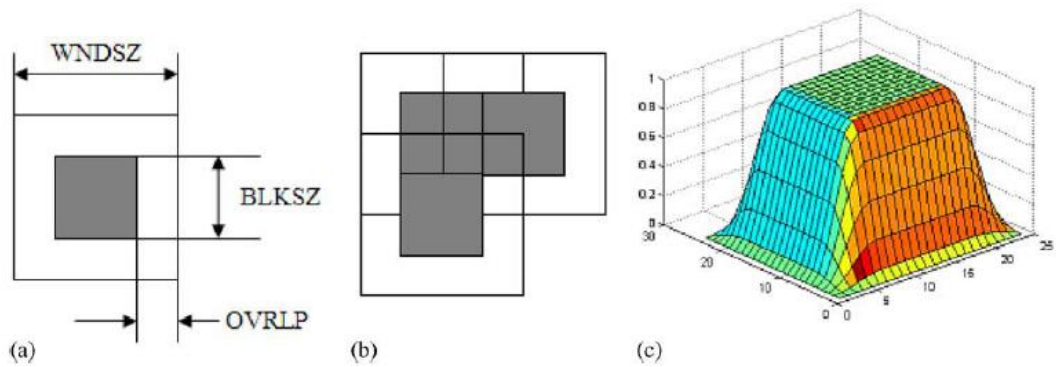
Figure (3.4): The Spectral Window parameters. Quoted from (Chikkerur, Cartwright, & Govindaraju, 2007)

An Energy map is also obtained during the STFT analysis, which is used as a region mask to separate the foreground region from the background region, where the background and the noisy regions have a little energy content in the Fourier spectrum. The Energy map is obtained by thresholding, and for automatic determination of threshold value, the authors use the Otsu's optimal thresholding (Otsu, 1979). But in case of bad quality fingerprint images as our selected CASIA-FingerprintV5 database, especially the problem of humidity in fingertip, which causes some important regions

to be dark or black. This causes the thresholding technique to consider this black regions a part of the background area, and so it will be ignored. We solve this problem by replacing the process of computing the Energy map by the segmentation technique proposed by (Fahmy & Thabet, 2013) as we did in the alignment step. This technique does not depend on the thresholding to estimate the foreground region. The results of the comparison of both techniques will be discussed in Chapter 6.

The orientation image is then used to compute the Coherence image, which is used to adapt the angular bandwidth. The resulting contextual information is used to filter each overlapping window in the Fourier domain. The filter used is separable in radial and angular domain, and is given by:

$$H(r, \varphi) = H_r(r) H_\varphi(\varphi),$$ (3.1)

$$H_r(r) = \sqrt{\left[\frac{(rr_{BW})^{2n}}{(rr_{BW})^{2n} + (r^2 - r_c{}^2)^{2n}}\right]},$$ (3.2)

$$H_\varphi(\varphi) = \begin{pmatrix} \cos^2 \frac{\pi}{2} \frac{(\varphi - \varphi_c)}{\varphi_{BW}}, & if \ |\varphi| < \ \varphi_{BW} \\ 0 & otherwise \end{pmatrix},$$ (3.3)

Where rr_{BW}, φ_{BW} are the radial bandwidth and the angular bandwidth respectively. The enhanced image is obtained by tiling the result of each analysis window.

Input : Image $I(x,y)$
Output: Enhanced Image $Í(x,y)$, Ridge Orientation Image $O(x,y)$, Ridge Frequency Image
* $F(x,y)$, Energy Image $E(x,y)$, Orientation Coherence Image $C(x,y)$, Region Mask $(x,$*
Stage 1: STFT Analysis
   1- *For each overlapping block $B(x,y)$ in the image do:*
          a. *Remove DC content of $B, B = B - avg(B)$*
          b. *Multiply by spectral window W*
          c. *Obtain the FFT of the block, $F = FFT(B)$*
          d. *Perform root filtering on F*
          e. *Perform STFT Analysis. The Analysis yield values of $E(x,y), O(x,y), F(x,y$*

      End for
   2- *Smoothen orientation image $O(x,y)$ by vector averaging to yield $Ó(x,y)$*
   3- *Perform isotropic diffusion on frequency map $F(x,y)$ to yield $Ḟ(x,y)$*
   4- *Copmute coherence image $C(x,y)$ using $Ó(x,y)$*
   5- *Compute region mask $R(x,y)$ by (Fahmy & Thabet, 2013)*

Stage 2: Enhancement
   1- *For each overlapping block $B(x,y)$ in the image do:*
          a. *Compute angular filter F_A centered around $O(x,y)$ and with bandwidth*
inversely proportional to $C(x,y)$

---

b. *Compute radial filter F_R centered around frequency $F(x,y)$*

c. *Filter the block in the FFT domain $F = F * F_A * F_R$*

d. *Compute the enhanced bock $\acute{B}(x,y) = IFFT(F)$*

End for

2- *Reconstruct the enhanced image by composing enhanced blocks $\acute{B}(x,y)$*

Table (3.4): Pseudocode for Fingerprint Image Enhancement using STFT Analysis

3.3 Core Point Detection

The reason of needing a common reference point is that the two fingerprint images are probably not perfectly aligned. One of the images might be a little displaced compared to the other one (Eriksson, 2001). So detecting the reference point solves the image transition problem.

Fingerprints are classified into six main classes (Iwasokun & Akinyokun, 2014; Prabhakar, 2001; Alonso-Fernandez , et al., 2009), named as: arch, tented arch, right loop, left loop, whorl, and twin loop, which are shown in Figure 3.5.

Figure (3.5): The six major fingerprint classes: (a) Arch, (b) Tented Arch, (c) Left Loop, (d) Right Loop, (e) Whorl, and (f) twin loop. Quoted from (Alonso-Fernandez , et al., 2009)

To be familiar with the fingerprint classification percentage: Arches and tented arches are the least common found in about 5% of all fingerprint pattern. Loops are the most common type of fingerprint patterns, and they found in about 60-65%. Whorls are found in about 30-35%. (Leo, 2004; Hamilton, 2008).

Some parts of the ridge curves resemble semicircles, whose centre is called a core. Also there are triangular patterns in the fingerprints, whose centre is called a

delta. The core and delta are defined as the singular points of a fingerprint (Ohtsuka, Watanabe, Tomizawa, & Aoki, 2008). It is known that the singular points of a fingerprint are important reference points for its classification. The core point locations in some fingerprint classes are shown in Figure 3.6.
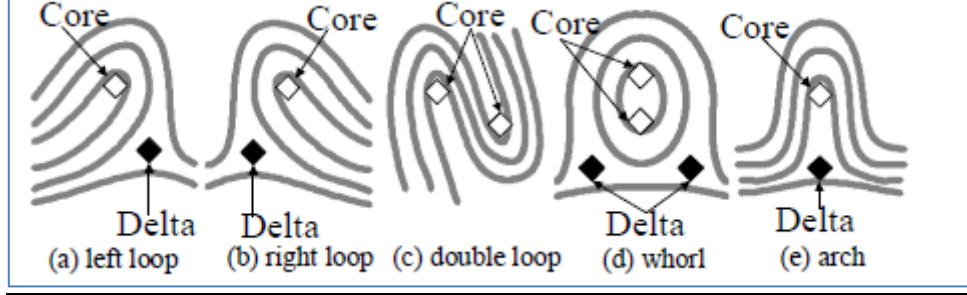
Figure (3.6): Core point locations in some fingerprint classes

We determine the singular point location by using the idea of complex filters, which their shapes are similar to the core and delta point (Nilsson & Bigun, 2003). The singular points have symmetry properties which make them easy to identify even from humans.

To find the singular point we convolve the complex filter of order one with the complex orientation images $z(x, y) = (f_x + if_y)^2$, where f_x the derivative of the original image in the x-direction and f_y is the derivative in the y-direction. Two filters are used, one for core point and the other for delta point. The first order filters are:

$$h_1(x, y) = (x + iy)g(x, y) = r \exp\{i\varphi\} g(x, y), \tag{3.4}$$

$$h_2(x, y) = (x - iy)g(x, y) = r \exp\{-i\varphi\} g(x, y) \tag{3.5}$$

Where g is a Gaussian, and $\exp\{i\varphi\}$ is the complex filters of order 1 for the detection of patterns with radial symmetries Patterns that have a local orientation description of $z = \exp\{i\varphi\} (m = 1)$ and $z = \exp\{-i\varphi\} (m = -1)$ are shown in Figure 3.7, which are similar to patterns of core and delta points. The response of complex filter is $c = \mu\exp\{i\alpha\}$, where μ is a certainty measure of symmetry, and α is the ''member'' of that symmetry family. By using the certainty measures μ_1 and μ_2 for core point and delta point symmetry, we can identify a singular point of type core if $|\mu_1| > T_1$ and of type delta if $|\mu_2| > T_2$, where T_1 and T_2 are thresholds.

The proposed solution uses the singular point as landmark point for alignment (registration) of two fingerprint images. We first need to find the singular point of both

the reference fingerprint image and the unknown one, then rotate and translate the unknown fingerprint image according to the position and orientation of the reference one.
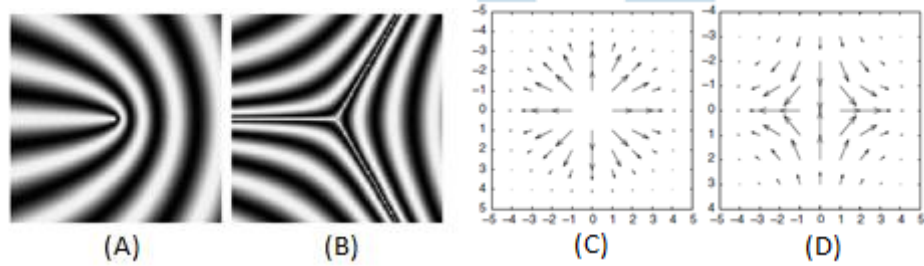
Figure (3.7): Complex Filter Patterns.

In this thesis, we focus on determining the core point only, since we need only one point for fingerprint image alignment, also, not all types of fingerprint classes have a delta point.

3.4 The Proposed Methodology of Fingerprint Pre-processing Stage

The proposed methodology of fingerprint pre-processing stage contains the following steps as shown in Figure 3.8: image acquisition, image segmentation, image rotation, image enhancement, and finally core point detection.
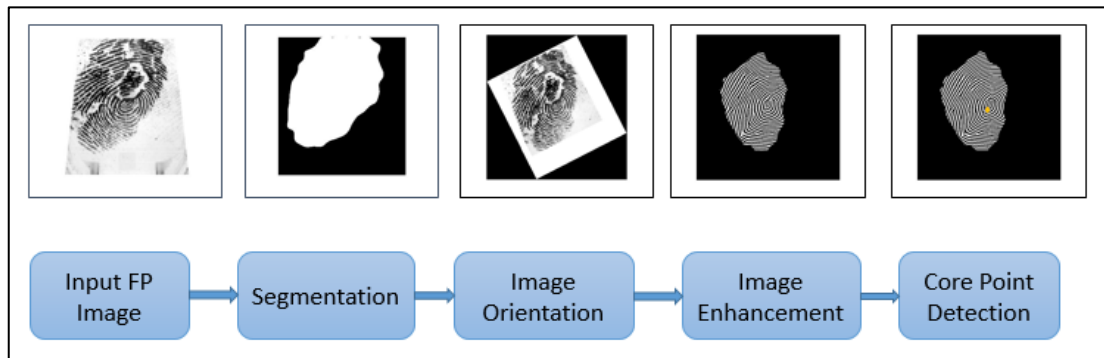
Figure (3.8): The Proposed Methodology of Pre-processing stage of AFIS

Chapter 4

Feature Extraction Techniques

Chapter 4
Feature Extraction Techniques

In this chapter, we introduce some modern feature extraction techniques. This stage is a very important process in any fingerprint recognition system, since extracting distinctive features from poor quality fingerprint image is one of the most challenging problem in fingerprint recognition. We divide this chapter into three parts: the first part gives a brief introduction about the Curvelet transform, the second part introduces the Wave Atoms transform, and the last part introduces the Shearlet transform.

Multiresolution analysis is simply analyses the signal at different frequencies with different resolutions. This idea comes from the problem of Uncertainty Principle. This principle states that one cannot know the exact time-frequency representation of a signal, i.e., one cannot know what spectral components exist at what instances of times. What one can know are the time intervals in which certain band of frequencies exist, which is a resolution problem (Polikar, 2016). Multiresolution techniques have been widely used in the field of biometric recognition.

One of the primary tasks in computer vision is to extract features from an image. The features can be points, lines, edges, and textures. A feature is characterized by position, direction, scale, and other property parameters. An important motivation for computer vision is to obtain directional representations that capture anisotropic lines and edges while providing sparse decompositions (Ma & Plonka, 2010).

The most popular multiresolution analysis tool is the Wavelet Transform. In Wavelet analysis, an image is decomposed at different scales and orientations using a Wavelet basis vector. However, the drawback of wavelet is that it performs well only at representing point singularities, and ignores the geometric properties of structure, so it does not exploit the regularity of edges, i.e. poor directionality. These limitations of Wavelet is known as isotropic basis elements. However, the anisotropic structures can only be distinguished by location and orientation/direction. These two different approximation schemes with isotropic and anisotropic basis elements are illustrated in Figure 4.1 (A) and (B) respectively.

To overcome the poor directionality, several directional representation systems had been introduced in recent years, with the aim of gaining better analysis and optimal representation of directional features of signals (Grohs, Keiper, Kutyniok, & Schaefer, 2013). These techniques; called X-let; are developed independently to extract geometric features, namely as steerable wavelets, Gabor wavelets, Wedgelet, Beamlet, Bandlet, Contourlet, Shearlet, wave atoms, platelets, and Surfacelet.
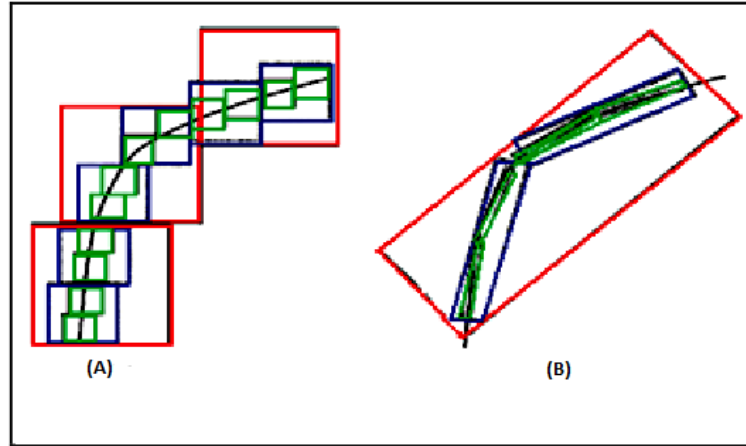
Figure (4.1): Approximation schemes with isotropic and anisotropic basis elements**.**

Each of X-let transforms has its characteristics, Ridgelet transform is an anisotropic geometric Wavelet transform, which is optimal at representing straight-line singularities, but it only applicable to objects with global straight-line singularities which is rarely observed in real application. To analyse local line or curve singularities, an image has to be partitioned, then the Ridgelet transform is applied to each subimage, which is the idea of the first generation of Curvelet. However it is limited since the geometry of Ridgelet is unclear. This leads to the second generation of Curvelet by the same authors which based on frequency partition. Steerable wavelets is translation-invariant and rotation-invariant representations of the position and the orientation of considered image structures, but its drawback is the high redundancy. Contourlet can deal effectively with piecewise smooth images with smooth contours. Curvelet constructions require a rotation operation and correspond to a partition of the 2-D frequency plane based on polar coordinates, and it has more clear features than Contourlet. Surfacelet are 3-D extensions of the 2-D Contourlet, and they can be used to efficiently capture and represent surface-like singularities in multidimensional volumetric data such as video processing and computer vision. The

Surfacelet transform is less redundant than the 3-D Curvelet transform, but its drawback is a certain loss of directional features. Curvelet transform uses angled polar wedges or angled trapezoid windows in frequency domain to resolve directional features. The performance of Curvelet is higher than Wavelet and Ridgelet, since the Curvelet transform is able to capture multidirectional features in wedges, as opposed to lines or points as in the Ridgelet or Wavelet transform. The discrete implementations of Shearlet and Curvelet transforms are very similar, and both of them are similarly well suited for approximation of smooth images with singularities along smooth curves. In contrast with the previously mentioned transforms, the Bandlet transform is based on adaptive techniques and has a good performance for images with textures beyond C2-singularities, but it has much higher computational cost for its adaptation (Ma & Plonka, 2010).

4.1 Digital Curvelet Transform

The first generation of Curvelet was proposed by E. Candes and D. Donoho in 2000 (Donoho, Candes, & L., 2000). Curvelet transform has a highly redundant dictionary which can provide sparse representation of signals that have edges along regular curve. Curvelet was redesigned later as Fast Digital Curvelet Transform (FDCT) by the same authors in 2004, which is faster, simpler to understand and use, and less redundant. The idea of Curvelet is to represent a curve as a superposition of functions of various lengths and widths obeying the scaling parabolic law: width $\cong$ (length) ², which says that at scale 2^{-j} , each curvelet element has an envelope which is aligned along a "ridge" of length $2^{-j/2}$ and width 2^{-j} as depicted in Figure 4.2.
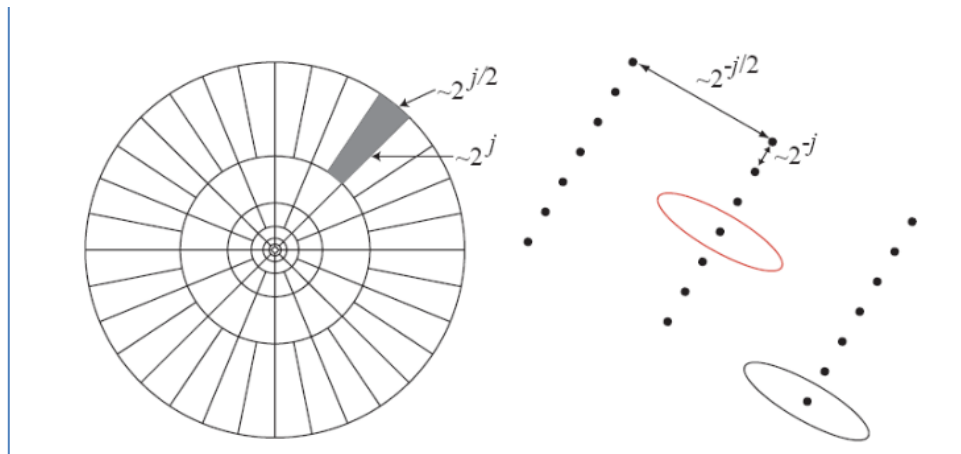
Figure (4.2): Curvelets in Fourier frequency and spatial domain.

This law is suited for approximating C^2 singularity carves (Grohs, Keiper, Kutyniok, & Schaefer, 2013). Figure 4.2 shows Curvelets in Fourier frequency domain and spatial domain. Figure 4.3 (a) shows the Curvelets frequency tilling in continues domain which is defined by using coronae and rotations, while Figure 4.3 (b) shows the Curvelet transform in the discrete domain.

In order to implement Curvelet transform (Cand`es, Demanet, Donoho, & Ying, 2005), first 2D Fast Fourier Transform (FFT) of the image is taken. Then the 2D Fourier frequency plane is divided into wedges (see the grey region for j=5 in Figure 4.2, and Figure 4.3). The length of the localizing windows is doubled at every other dyadic subband. The parabolic shape of wedges is the result of partitioning the Fourier plane into radial (concentric circles, and squares) and angular (rotations and shears) divisions. Different scales are obtained by radial division; the smallest scale defines the finest resolution while the largest scale defines the coarsest resolution. Angular division divides each scale into different orientation; the maximum number of orientations was found at the finest resolution and the lesser number of orientations was found at coarsest resolution. The concentric circles are responsible for the decomposition of an image into multiple scales (used for bandpassing the image at different scale) and the angular divisions partition the bandpassed image into different angles or orientations. Thus if we want to deal with a particular wedge we'll need to define its scale j and angle θ.
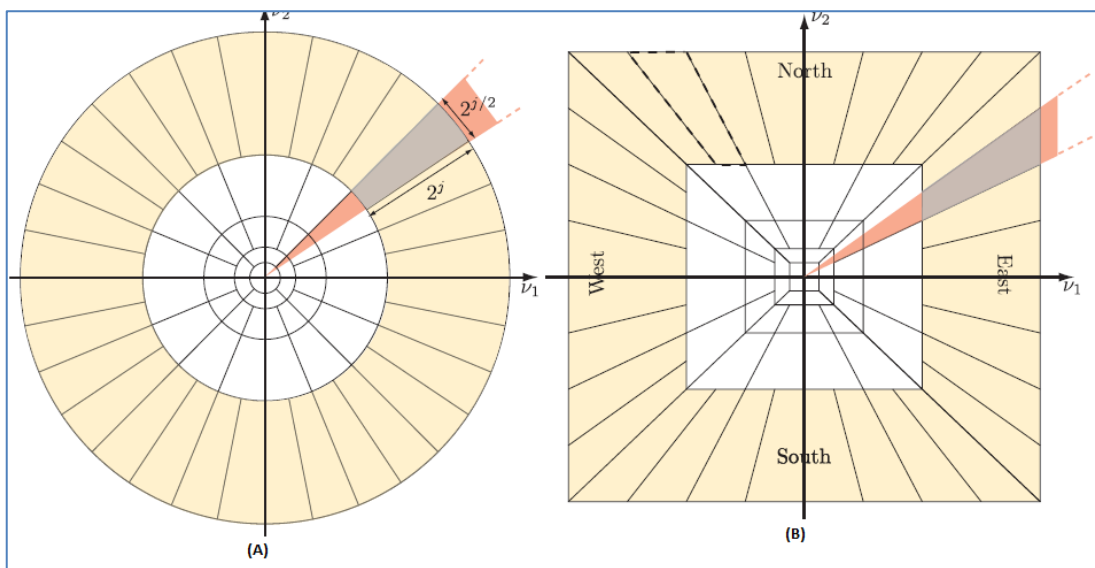
Figure (4.3): Curvelet Frequency Tilling. Quoted from **(Fadili & Starck, 2009)**

Now let's have a look at the spatial domain (Figure 4.2 right). Each of the wedges here corresponds to a particular Curvelet (shown as ellipses) at a given scale and angle. This indicates that the inverse FFT of a particular wedge if taken, will determine the Curvelet coefficients for that scale and angle. Figure 4.2 (right) represents Curvelets in spatial Cartesian grid associated with a given scale and angle. (Wu, Guha, & Jonathan, 2010)

Compared to wavelet, Curvelet provides a more sparse representation of the image, with improved directional elements and better ability to represent edges and other singularities along curves (Abduljaleel, Khaleel, & Kareem, 2013). Figure 4.1 shows edge representation by both Wavelets and Curvelet Transforms. It can be noticed, it would take many Wavelet coefficients to accurately represent such a curve while Curvelet needs small number of coefficients; Wavelet needs three, six, and twelve coefficients, while Curvelet needs one, two, and four coefficients, in the largest, middle, and smallest scale respectively

The values of Curvelet coefficients are determined by how they are aligned in the real image. The more accurately a Curvelet is aligned with a given curve in an image, the higher is its coefficient value. A very clear explanation is provided in Figure 4.4. The Curvelet named 'c' in the figure is almost perfectly aligned with the curved edge and therefore has a high coefficient value. Curvelets 'a' and 'b' will have coefficients close to zero as they are quite far from alignment. It is well known that a signal localized in frequency domain is spread out in the spatial domain or vice-versa. A notable point regarding Curvelets is that, they are better localized in both frequency and spatial domain compared to other transforms. This is because the wedge boundary is smoothly tapered to avoid abrupt discontinuity

To define Curvelets transform in continues domain, suppose we work in the space R², with spatial variable x, frequency variable ω, and polar coordinates r and θ in the frequency domain. Let W(r) and V (t) be two window functions, which we call the radial window and angular window respectively, and both are real, nonnegative, and supported on r ∈ [1/2, 2] and on t ∈ [−1, 1] respectively. These windows should obey the admissibility conditions (Cand`es, Demanet, Donoho, & Ying, 2005):

$$\sum_{j=-\infty}^{\infty} W^2(2^j r) = 1 \quad , \quad r > 0 \tag{4.1}$$

$$\sum_{j=-\infty}^{\infty} V^2(t - l) = 1 \quad , \quad t \in \mathbb{R} \tag{4.2}$$

For each j, introduce the frequency window U_j defined in the Fourier domain by:

$$U(r, \theta) = 2^{-\frac{3j}{4}} W(2^{-j} r) V\left(\frac{2^{\lfloor \frac{j}{2} \rfloor} \theta}{2\pi}\right), \quad \left\lfloor \frac{j}{2} \right\rfloor \text{ is an integer part of } \frac{j}{2} \tag{4.3}$$
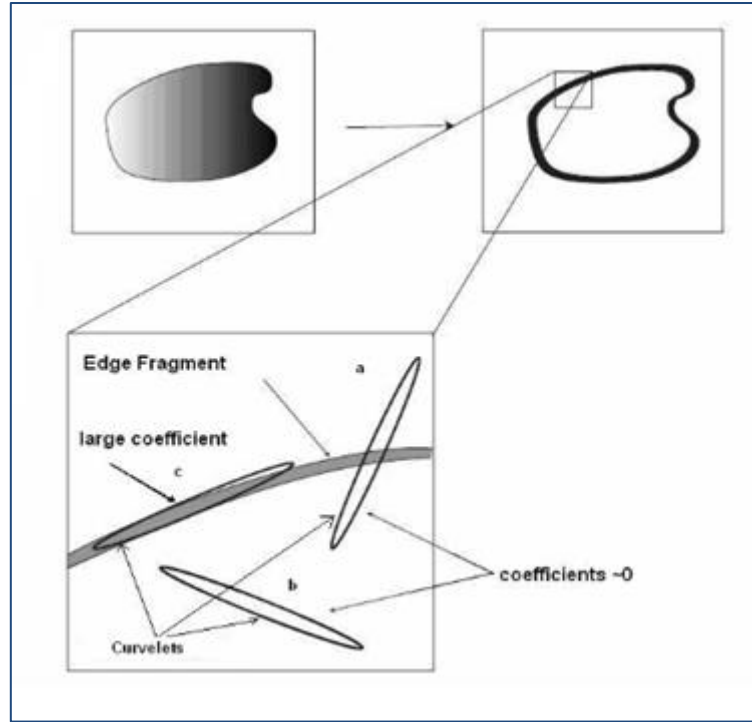
Figure(4.4): Alignment of curvelets along curved edges. Quated from (Majumdar & Ward, 2008)

Thus the support of U_j is a polar wedge defined by the support of W and V at given scale.

A waveform $\varphi_j(x)$ can be defined by letting $\varphi_j(\omega) = U_j(\omega)$. The Curvelet transform can be defined as a function of $x = (x_1, x_2)$ at scale 2^{-j}, orientation θ_t where $\theta_l = 2\pi. 2^{\lfloor \frac{j}{2} \rfloor}. l, l = 0, 1, \dots, \ 0 < \theta_l < 2\pi$ and position $x_k^{(j,l)} =$

46

$R_{\theta_l}(k_1.2^{-j}, k_2.2^{-j/2})$, where $k = (k_1, k_2)$ is the shift parameter by (Cand`es, Demanet, Donoho, & Ying, 2005):

$$\varphi_{j,l,k}(x) = \varphi_j\left(R_{\theta_l}\left(x - x_k^{(j,l)}\right)\right) \qquad (4.4)$$

A Curvelet coefficient is the inner product between an element $f \in L^2(\mathbb{R}^2)$ and a Curvelet $\varphi_{j,l,k}$:

$$c_{j,l,k} := (f, \varphi_{j,l,k}) = \int_{\mathbb{R}^2} f(x)\,\overline{\varphi_{j,l,k}(x)}\;\; dx \qquad (4.5)$$

Where $c_{j,l,k}$ is the Curvelet coefficient, and $\overline{(.)}$ donates the conjugate operator.

Based on Plancherel's Theory,

$$c_{j,l,k} := \frac{1}{2\pi^2}\int_{\mathbb{R}^2} \hat{f}(\omega)\overline{\varphi_{j,l,k}(x)}\; d\omega \qquad (4.6)$$

$$c_{j,l,k} := \frac{1}{2\pi^2}\int_{\mathbb{R}^2} \hat{f}(\omega)U_j\left(R_{\theta_t}\,\omega\right)e^{i\,(x_k^{(j,l)},\omega)}\; d\omega \qquad (4.7)$$

If the input $f[x_1, x_2]$ $(0 \le x_1, x_2 < n)$ the spatial Cartesian is an image, then the discrete form of the continuous Curvelet transform can be expressed as the following:

$$c^D{}_{j,l,k} := \sum_{0 \le x_1, x_2 < n} f[x_1, x_2]\,\overline{\varphi^D{}_{j,l,k}[x_1, x_2]}\; d\omega \qquad (4.8)$$

Where each $\varphi^D{}_{j,l,k}$ is a digital curvelet waveform (D stands for "digital")

There are two generations of Curvelet transform. The first generation uses complex series of steps, involving Ridgelet analysis of the image, and its performance is very slow. The second generation eliminates the use of Ridgelet transform as a pre-processing step in the first generation, and it is simpler, faster, and less redundant than the original one. This new generation is known as Fast Discrete Curvelet Transform (FDCT), which is implemented by two different forms: Curvelets via USFFT (Unequally Spaced Fast Fourier Transform) and Curvelets via Wrapping. The difference between them is the choice of spatial grid to translate Curvelets at each scale and angle. FDCT wrapping is the fastest Curvelet transform currently available. Because of this, Curvelet via wrapping will be used for this work.

If we have the object $g[t_1, t_2]$ and ($0 \le t_1,\ t_2 < n$) as Cartesian array and $\hat{g}[n_1, n_2]$ to denote its 2D Discrete Fourier Transform, then the architecture of Curvelets via wrapping is as follows:

1. 2D Fast Fourier Transform (FFT) is applied to $g[t_1, t_2]$ to obtain Fourier samples $\hat{g}[n_1, n_2]$.

2. For each scale j and angle l, the product $\widehat{U}_{j,l}[n_1, n_2] \cdot \hat{g}[n_1, n_2]$ is formed, where $\widehat{U}_{j,l}[n_1, n_2]$ is the discrete localizing window (Figure 4.5 (a)).

3. This product is wrapped around the origin to obtain $\hat{g}_{j,l}[n_1, n_2] = W(\widehat{U}_{j,l}\,\hat{g})[n_1, n_2]$; where the range for n_1, n_2 is now $0 \le n_1 < L_{1,j}$ and $0 \le n_2 < L_{2,j}$; $L_{1,j} \approx 2^j$ and $L_{2,j} \approx 2^{j/2}$ are constants (Figure 4.5 (b)).

4. Inverse 2D FFT is applied to each $\hat{g}_{j,l}$, hence creating the discrete Curvelet coefficients.

The discrete Curvelet transform is very efficient in representing curve-like edges. But the current Curvelet systems still have two main drawbacks: 1) they are not optimal for sparse approximation of curve features beyond C2-singularities, and 2) the discrete Curvelet transform is highly redundant. (Ma & Plonka, 2010)
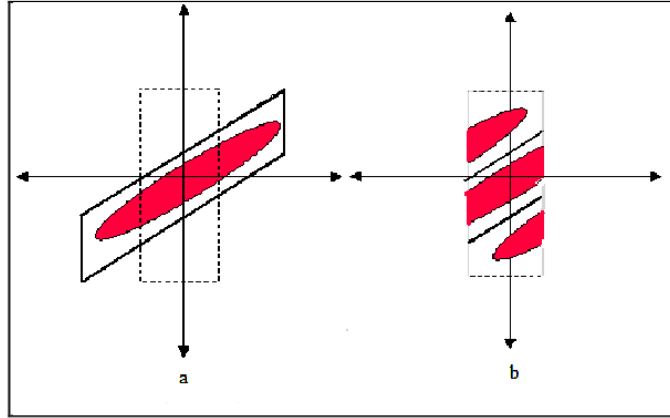
Figure (4.5): Discrete localizing window before and after Wrapping.

4.2 Wave Atoms Transform

Wave Atoms was presented by Demanety and Ying (Demanet & Ying, 2007), and it is a new type of two-dimensional multi-scale transformation, and still meets the parabolic proportional scaling relation and anisotropic characteristics of curve wave.

The name of wave atoms comes from the property that they also provide an optimally sparse representation of wave propagators, a mathematical result of independent interest, with applications to fast numerical solvers for wave equations (Demanet & Ying, 2007).

Wave atoms satisfies all multiresolution transform properties which are described as follows (Majumdar & Ward, 2008; Hejazi & Alhanjouri, 2010):

1- Multiresolution: this property state that the transform should allow images to be successively approximated, from coarse to fine resolutions. The frequency plane of Wave Atom is divided into concentric rings in order to facilitate bandpassing at multiple resolutions.

2- Localization: this means that the basis functions of the transforms should be localized in both the spatial and the frequency domains. Wave Atom is localized in both spatial domain and frequency domain.

3- Critical sampling: For some applications (e.g., compression), the transforms should form a basis, or a frame with small redundancy. Wave Atom form tight frames with redundancy two.

4- Directionality: this means that the transform should contain basis functions oriented at a variety of direction. In Wave Atom the entire frequency plane is divided into angular wedges, and this allows for analyzing the image at various orientations

5- Anisotropy: When a physical property changes with direction, that property is said anisotropy For image transforms, anisotropy means that the basis elements of the transforms should not be circular (similar in all directions) but may be elliptical (more along the major axis and less along the minor axis). Wave Atoms are elliptical in shape (the major and the minor axes related by a parabolic scaling law), thus they are anisotropic.

Wave atoms interpolate exactly between directional wavelets and Gabor, in the sense that the period of the oscillations of each wave packet (wavelength) is linked to the size of the essential support (diameter) by the parabolic scaling. Figure 4.6 shows

phase-space localization of the wave packets, on the right of Figure 4.6, the frequency plane is divided into wedges. The wedge is formed by partitioning the frequency plane into radial and angular divisions. The radial divisions (concentric circles) are for band-passing the image at different resolution/scales. The angular divisions divide each band-passed image into different angles. To consider each wedge, the band-passed image should be analysed at scale j and angle θ, and we will require that (Demanet & Ying, 2007):

- In x, the essential support of $\varphi(x_\mu)$ is of size $\sim 2^{-\alpha j}$ vs. $2^{-\beta j}$ as scale $j \geq 0$, with oscillations of wavelength $\sim 2^{-j}$ transverse to the ridge;

- In frequency ω, the essential support of $\hat{\varphi}(\omega)$ consists of two bumps, each of size $\sim 2^{\alpha j}$ vs. $2^{\beta j}$ as scale j, at opposing angles and distance $\sim 2^j$ from the origin.

Connections to other transforms are shown in Figure 4.7, which depend on choosing the parameters α and β. The parameter α is to index whether the decomposition is multiscale ($\alpha = 1$) or not ($\alpha = 0$); and β to indicate whether basis elements should be isotropic ($\beta = \alpha$) or, on anisotropic ($\beta < \alpha$). Curvelets correspond to $\alpha = 1, \beta = 1/2$, wavelets are $\alpha = \beta = 1$, ridgelets are $\alpha = 1 \ and \ \beta = 0$, and the Gabor transform is $\alpha = \beta = 0$. Wave atoms are defined as the point $\alpha = \beta = 1/2$.
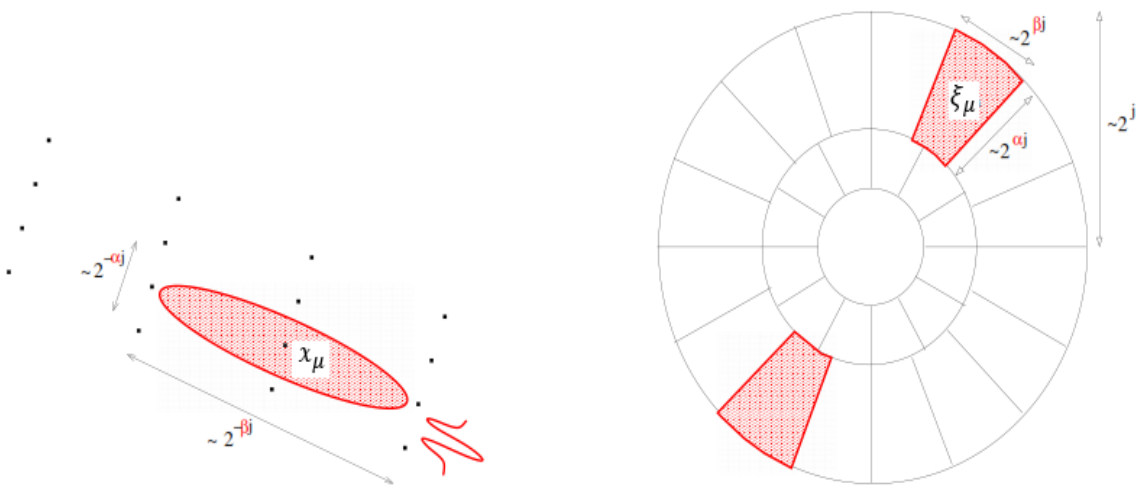
Figure (4.6): Wave Atoms Transform in spatial space and in frequency space.
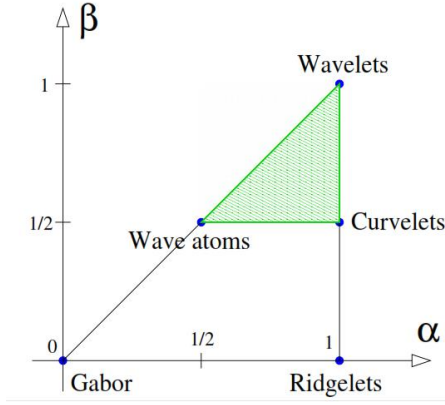
Figure (4.7): Identification of various transforms as (α, β) families of wave packets.

The theory of Wave Atoms is as follows: Suppose j, l, k are integer valued where j is the cut-off in scale, k is the cut-off in space and l labels the different wedges within each scale. Now consider a one-dimensional family of wave packets $\varphi_{l,k}^j(x)$, $j \geq 0, l \geq 0, k \in K$ centred in frequency around $\mp \omega_{j,l} = \mp \pi 2^j l$ with $c_1 2^j \leq l \leq c_2 2^j$ where $c_1 < c_2$ are positive constants, and centred in space around $x_{j,k} = 2^{-j} k$. One-dimensional version of the parabolic scaling states that the support of each bump of $\varphi_{l,k}^j(\omega)$ is of length $O(2^j)$ while $\omega_{j,l}(2^{2j})$.

Starting with Villemoes wavelets $\hat{\varphi}_l^0(\omega)$ frequency plane,

$$\hat{\varphi}_l^0(\omega) = e^{-i\omega/2}[e^{i\alpha_l} g(\epsilon_l\left(\omega - \pi\left(l + \frac{1}{2}\right)\right) + e^{-i\alpha_l} g(\epsilon_{l+1}\left(\omega + \pi\left(l + \frac{1}{2}\right)\right))$$

(4.9)

Where $\alpha_l = \frac{\pi}{2\left(l + \frac{1}{2}\right)}$, $\epsilon_l = (-1)^l$ and $\{\varphi_l(t - k)\}$ form an orthonormal basis of $L^2(\mathbb{R})$.

Dyadic dilates and translates of $\hat{\varphi}_l^0$ on the frequency axes are combined and basic functions, written as:

$$\varphi_{l,k}^j(x) = \varphi_l^j\left(x - 2^{-j}k\right) = 2^{-\frac{j}{2}}\varphi_l^0\left(2^{-j}x - k\right)$$

(4.10)

The transform $WA : L^2(\mathbb{R}) \to l^2(\mathbb{Z})$ maps a function u onto a sequence of Wave Atoms coefficients, and by Plancherel's theorem:

51

$$c_{j,l,k} = \int\limits_{-\infty}^{\infty} u(x)\, \varphi_{l,k}^{j}(x)\, dx = \frac{1}{2\pi} \int\limits_{-\infty}^{\infty} e^{-i2^{-j}k\omega}\, \overline{\hat{\varphi}^{J}_{\,l}(\omega)}\, \hat{u}(\omega)\, dw \qquad (4.11)$$

If the function u is discretized at xn = nh, h=1/K, n =1....K , then with a small truncation error (4.9) is modified as:

$$c^{D}_{\ j,l,k} = \sum_{\text{ll} = 2\pi\,(-K/2+1:1:K/2)} e^{-i2^{-j}kn}\, \overline{\hat{\varphi}^{J}_{\,l}(k)}\, \hat{u}(k) \qquad (4.12)$$

A simple wrapping trick is used for the implementation of discrete Wavelet packets and the steps involved are (Demanet & Ying, 2007):

1. Perform an FFT of size K on the samples of (n).
2. For each pair (j, l) wrap the product $\hat{\varphi}_{l}^{j}\hat{u}$ by periodically inside the interval $[2^{-j}\,\pi, 2^{j}\,\pi]$, then perform inverse FFT of size 2^{j} of the result to obtain $c^{D}_{\ j,l,k}$
3. Repeat step 2 for all pairs (jj, ll).

The positive and negative frequency components represented by:

$$\hat{\varphi}_{l,k}^{j}(\omega) = \hat{\varphi}_{l,k}^{+}(\omega) + \hat{\varphi}_{l,k}^{-}(\omega) \qquad (4.13)$$

Hilbert transform $H\,\hat{\varphi}_{l,k}^{j}(\omega)$ of eq. (4.11) represents an orthonormal basis $L^{2}(\mathbb{R})$ and is obtained through a linear combination of positive and negative frequency bumps weighted by i and –i respectively.

$$H\hat{\varphi}_{l,k}^{j}(\omega) = -i\hat{\varphi}_{l,k}^{+}(\omega) + i\hat{\varphi}_{l,k}^{-}(\omega) \qquad (4.14)$$

To extend Wave Atoms to be 2D, let $\mu =(j, \mathbf{l}, \mathbf{k})$, where $\mathbf{l} = (l1, , l2)$ and $\mathbf{k} = (k1, k2)$ so from equation 4.8.

$$\varphi_{\mu}^{+}(x_{1}, x_{2}) = \varphi_{l1}^{j}(x_{1} - 2^{-j}k_{1})\varphi_{l2}^{j}(x_{2} - 2^{-j}k_{2}) \qquad (4.15)$$

Hilbert transform was used to define the dual orthonormal basis,

$$\varphi_{\mu}^{-}(x_{1}, x_{2}) = H\varphi_{l1}^{j}(x_{1} - 2^{-j}k_{1})\, H\varphi_{l2}^{j}(x_{2} - 2^{-j}k_{2}) \qquad (4.16)$$

Now the bases function problem is that they oscillate in two directions instead of one in x space. To solve this problem we combine the primal and dual (Hilbert-transformed) basis.

$$\varphi_\mu^{(1)} = \frac{\varphi_\mu^+ + \varphi_\mu^-}{2}, \qquad \varphi_\mu^{(2)} = \frac{\varphi_\mu^+ - \varphi_\mu^-}{2} \qquad\qquad (4.17)$$

By now, basis functions have two bumps in the frequency plane and they are symmetric with respect to the origin, so we get purely directional wave atom. $\varphi_\mu^{(1)}$ and $\varphi_\mu^{(2)}$ form the wave atom frame. x_μ ξ_μ

The discretization of wave atoms closely follows the strategy of frequency sampling and wrapping used for Curvelets.

4.3 Shearlet Transform

Shearlet was introduced by Guo, Kutyniok, Labate, Lim, and Weiss in (Labate, Lim, Kutyniok, & Weiss, 2005). One of the distinctive features of Shearlet is the use of shearing to control directional selectivity, in contrast to rotation used by Curvelets. Shearlet is used for many applications such as: image compression (Thayammal & Selvathi, 2012), image denoising (Easley, Labate, & Colonna, 2009), image inpainting (King, Kutyniok, & Lim, 2013), image separation, and edge detection (Labate, Yi, Easley, & Krim, 2009).

Shearlet systems is one of the most successful systems, since they, in particular, satisfy the following list of properties commonly desired for directional representation systems (Kutyniok, Lim, & Steidl, 2014):

1. A single or a finite set of generating functions.
2. Provide an optimal sparse approximations of anisotropic features.
3. Compactly supported analyzing elements for high spatial localization.
4. Uniform treatment of the continuum and digital realm.
5. Availability of fast decomposition algorithm.

4.3.1 Continuous Shearlet Transform

The continuous Shearlet transform is a non-isotropic version of the continuous Wavelet transform with a superior directional sensitivity. Shearlet transforms can

analyse and represent data with anisotropic information at multiple scales. The continuous Shearlet transform for an image f is defined as the mapping. In dimension n=2, this is defined as the mapping,

$$f \rightarrow SH_\psi f(a, s, t) = \langle f, \psi_{a,s,t} \rangle \tag{4.18}$$

where ψ is a generating function, $a > 0$ is the scale parameter to generate elements at different scales, $s \in \mathbb{R}$ is the shearing parameter to change the orientations of the waveform, $t \in \mathbb{R}^2$ is the translation parameter to displace these elements over the 2D plane, and the analysing elements $\psi_{a,s,t}$ (shearlet basis functions) are given by:

$$\psi_{a,s,t}(x) = |\det M_{a,s}|^{-1/2} \psi \left(M_{a,s}^{-1}(x - t) \right) \tag{4.19}$$

Where $M_{a,s} = B_s A_a = \begin{pmatrix} a & \sqrt{as} \\ 0 & \sqrt{a} \end{pmatrix}$, $A_a = \begin{pmatrix} a & 0 \\ 0 & \sqrt{a} \end{pmatrix}$, $B_s = \begin{pmatrix} 1 & s \\ 0 & 1 \end{pmatrix}$, A_a is the anisotropic dilation matrix, and B_s is the shear matrix.

Each analysing element $\psi_{a,s,t}$ called shearlets has frequency support on a pair of trapezoids at several scales, symmetric with respect to the origin, and oriented along a line of slope s. The support becomes increasingly thin as a $\rightarrow$ 0 Therefore, the shearlets $\psi_{a,s,t}$ form a collection of well-localized waveforms at various scales a, orientations s and locations t (Gomathi & Kumar, 2010). Figure 4.9 illustrates the frequency support of the Shearlet.
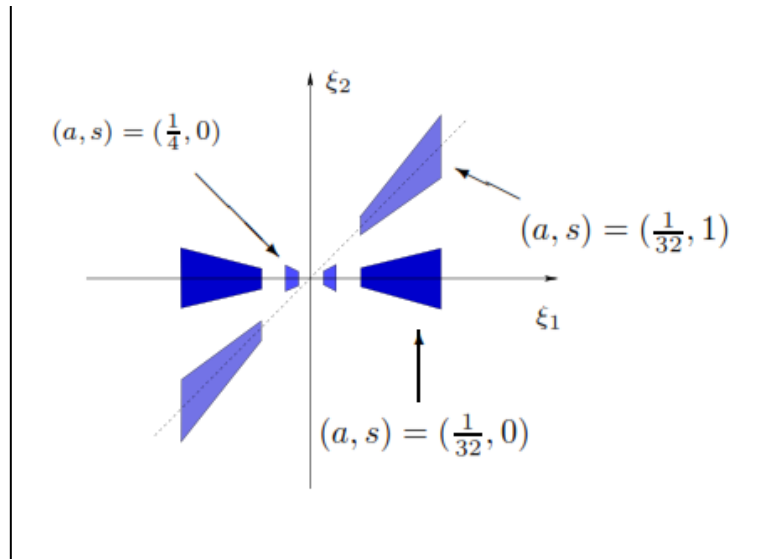
Figure(4.8): Frequency support of shearlets for various values of a and s.

The analysing functions associated to the Shearlet transform are anisotropic and are defined at different scales, locations and orientations. Thus, Shearlet have the ability to detect directional information and account for the geometry of multidimensional functions, which overcome the limitation of the Wavelet transform.

4.3.2 Discrete Shearlet Transform

By sampling the continuous Shearlet transform $SH_\psi f(a, s, t)$ on appropriate discretizations of the scaling, shear, and translation parameters (a, s, t), we can obtain a discrete transform which is associated to a Parseval (tight) frame for $L^2(R^2)$. The tiling of the frequency plane is shown in Figure 4.9.

We parametrize the anisotropic matrices A_a by dyadic numbers ($a = 2^{-j}$), and the shear matrices B_s by integers ($s = -l$). With $j, l \in Z$, we obtain the collection of matrices $M_{2^j, l}$ where:

$$M_{2^j, l} = B_0^l A_0^j = \begin{pmatrix} 2^j & l2^{j/2} \\ 0 & 2^{j/2} \end{pmatrix}, \text{ and } A_a = \begin{pmatrix} 2^j & 0 \\ 0 & 2^{j/2} \end{pmatrix}, \text{ and } B_s = \begin{pmatrix} 1 & l \\ 0 & 1 \end{pmatrix}$$

By replacing the continuous translation variable $t \in R$ by a point in the discrete lattice $\mathbb{Z}^2$, we obtain the discrete system of Shearlet $\psi_{j,l,k}$, where

$$\psi_{j,l,k} = |\det A_0|^{j/2} \psi(B_0^l A_0^j x - k) \quad , for \ j, l \in \mathbb{Z}, k \in \mathbb{Z}^2 \qquad (4.19)$$
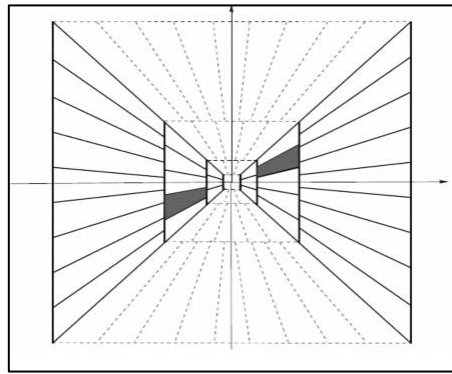
Figure(4.9): Tilling of frequency domain induced by discrete shearlets.

4.5 The Used Methodology of Fingerprint Feature Extraction Stage

The proposed methodology of feature extraction stage as shown in Figure 4.10 begins with cropping an N x M subimage with core point at the centre. The size of

subimage is taken once as 128x128, and once as 64x64. Then we divide this central subimage into a number of non- overlapping blocks of size W x W, i.e. W=64 or 32 when the size of subimage is 128x128 or 64x64 respectively. Then we take the multiresolution transforms; Wave atom, Curvelet or Shearlet; for each of the non-overlapping blocks. After that we take the standard deviation of each of the feature coefficient sets. Then the global feature vector is constructed. The standard deviation is used to reduce the dimension of the feature matrix, and it is considered as a popular feature from the first order statistical properties of the image. First order statistical features are: mean, standard deviation, skewness, and kurtosis. The second order statistical features include: energy, contrast, correlation, entropy, and homogeneity (Goshtasby, 2012). These features are exploiting the image texture, i.e. the distribution of grey level intensity over the pixels.
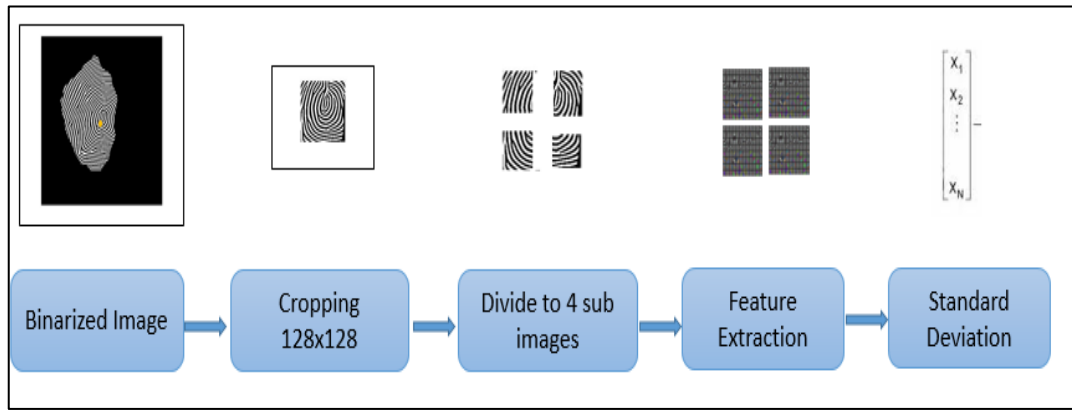
Figure(4.10): The Proposed Methodology of Feature Extraction stage of AFIS

Chapter 5

Classification Techniques

Chapter 5
Classification Techniques

Once a set of features is extracted from the fingerprint image, the final goal is to confirm the identity of a person whose fingerprint has been previously enrolled into the system. The matching mechanism is the responsible to provide a score between two fingerprints. Fingerprint matching is a crucial step in both verification and identification problems. Roughly, a fingerprint matching algorithm compares two fingerprints and returns either a degree of similarity or a hard output (matched or non-matched). Two fingerprints are called genuine if they represent the same finger, and impostor when they are different.

The reasons of making matching process of fingerprint images is an extremely difficult problem are due to the following:

1. The process of acquisitions of fingerprint images which are collected from different devices, which lead to random scale, displacement and rotation compared to the fingerprint images templates.
2. As a result of different displacement and rotation, there is an overlap area in the foreground area between the input and the fingerprint image templates.
3. The difficulty to describe the random nonlinear deformation of collected fingerprint images with a mathematic model, due to the plasticity of finger skin.
4. Poor quality of fingerprint images due to various finger pressure, sweat, dirt, grease, dryness of the skin, oily of the skin, skin disease, and humidity in the air.
5. Some enhancement and feature extraction algorithms loss true minutiae, or adding spurious one.
6. Not enough fingerprint image samples in some datasets, such as CASIA-FingerprintV5 dataset.

Fingerprint matching as a pattern recognition problem is still popular up to now, because the issue of matching low-quality and partial fingerprint image has not been solved well (Tong, Wang, Pi, & Zhang, 2006; Amira, 2011).

Fingerprint matching algorithms can be classified into various categories, such as correlation-based matching, minutiae-based matching, ridge feature-based matching, and texture-based matching, and each one of these algorithms has its own features in accuracy and speed. However, they classified into three major categories (Alonso-Fernandez , et al., 2009):

1. **Minutiae-based Matching**: is the most popular algorithm, which is used in most recognition systems. This matching type requires extraction of minutiae features from the registered fingerprint image and the input fingerprint image, and the number of corresponding minutiae pairings between the two images is used to recognize a valid fingerprint image. Minutiae features contains a list of attributes such as: minutiae position, minutiae direction, and type of minutiae (ridge ending, ridge bifurcation). To compare the minutiae sets between two fingerprints, an alignment process has to be done, which requires to compute the displacement and rotation, then the corresponding minutiae at similar position in both fingerprints are looked for. Extracting minutiae is difficult in the low and poor quality fingerprints. Generally, minutiae based methods require a significant amount of pre-processing to produce accurate results.

2. **Image-based (Pattern-based, ridge-based or non-minutiae feature based) Matching**: since minutiae based matching is unreliable in poor quality fingerprints, an alternative features are exploited such as: local orientation and frequency, ridge shape, and texture information. Texture information is more reliable in poor quality fingerprint images than minutiae (Alonso-Fernandez , et al., 2009). Another technique for an image based fingerprint matching system involves wavelets (Diefenderfer, 2006), where fingerprint patterns are matched based on Wavelet domain features. A primary advantage to this approach is that these features can be directly extracted from the fingerprint image without applying the needed pre-processing steps in minutiae based. Once the core point has been determined, a rectangular region surrounding the core is established, which is referred to as the central sub-image. This area is then divided into non overlapping square blocks

of uniform size. Then the Wavelet decomposition is computed on each block, and its Wavelet features are extracted, then the global feature is estimated, then performing the matching sequence with the template features. The lower computational requirements of this process make using Wavelet features attractive to a small-scale system.

3. **Correlation-based Matching**: Two fingerprint images are superimposed and the correlation between corresponding pixels is computed for different alignments (e.g. various displacement and rotations). The cross correlation which measures the image similarity is maximized between two images. The drawback of this type is its computation complexity, Furthermore it has limited ability to deal with variations in scale, translation, and rotation.

In this work, we use four different classifiers to perform fingerprint recognition. These classifiers are: Minimum Distance Classifier (MD), K-Nearest Neighbour (KNN), Self-Organization Map (SOM), and Support Vector Machine Classifier (SVM).

5.1 Minimum Distance Classifier

The simplest classifier is Minimum Distance Classifier. Given a set of M training samples x_i and a set of M labels y_i belong to L different classes, where $y_i \in \{1,2,\dots,L\}$, we first represent the kth class by its mean vector m_k which can be calculated by Equation 5.1

$$m_k = \frac{1}{N_k} \sum_{i=1}^{N_k} x_i{}^{(k)} \quad k = 1,2,\dots,L \ , \tag{5.1}$$

Where N_k is the number of training samples which belong to class k and $x_i{}^{(k)}$ is the feature vector for each training sample belonging to class k. For a given test sample x, it is classified to class k if its Euclidean distance to m_k is smaller than all other classes as indicated in Equation 5.2.

$$x \in k \ if \ D(x,m_k) = \ min\{D(x,m_k)i = 1,2,\dots,L\} \ , \tag{5.2}$$

5.2 K-Nearest Neighbors

The k-nearest neighbour classification is an instance-based learning algorithm that has been shown to be very effective for a variety of problem domains. It is also called a lazy learning algorithm because it makes use of the whole training set as a reference set to classify new instances. It may be a surprise to know that KNN is considered as one of the top 10 data mining algorithms (Wu & Kumar, 2008). The objective of k-nearest neighbour classification is to discover k nearest neighbours for a given instance, then assign a class label to the given instance according to the majority class of the k nearest neighbours (Taniar, 2008). The algorithm assumes that all instances correspond to points in the n-dimensional space. The key element of this scheme is the availability of a similarity measure that is capable of identifying neighbours. The nearest neighbours of an instance are defined in terms of a distance function such as the standard Euclidean distance. More precisely, let an instance x be described by the feature vector $\{a_1(x),\ a_2(x), \ldots., a_r(x)\}$, where $a_i(x)$ denotes the value of the ith attribute of instance x. Then the distance between two instances x_i and x_j is defined as $dist(x_i, x_j)$, where:

$$dist^2(x_i,\ x_j) = \sqrt{\sum_{q=1}^{r}(a_q(x_i) - a_q(x_j))^2} \qquad (5.3)$$

5.3 Self Organizing Map (SOM)

SOM (also known as Kohonen network) is introduced by Kohonen (1990, 1989). SOM is a type of unsupervised artificial neural networks, and hence, the network is presented with input data, but, as opposed to supervised learning, the network is not provided with desired outputs. The network is therefore allowed to freely organize itself according to similarities in the data, resulting in a map containing the input data. SOM reduces dimensions by producing a map of usually one or two dimensions that plots the similarities of the data by grouping similar objects together. SOM is useful for visualization and clustering, since it can be used to explore the groupings and

61

relations within high-dimensional data by projecting the data onto a two-dimensional image that clearly indicates regions of similarity (Gan, Ma, & Wu, 2007).

Before initiating the SOM algorithm, a map is randomly initialized. First, create an array of one or more dimensions, however, the most commonly used is the two-dimensional array. The most two common forms of lattice are rectangular and hexagonal. Figure 5.1 (a) represents 16 nodes of rectangular lattice, and Figure 5.1 (b) represents 16 nodes of hexagonal lattices. In the rectangular lattice, a node has four immediate neighbours with which it interacts, while in the hexagonal lattice it has sex. The hexagonal lattice type is commonly considered better for visualization than the rectangular lattice type. The lattice can also be irregular, but this is less commonly used (Wang J. , 2003).

(a)   (b)
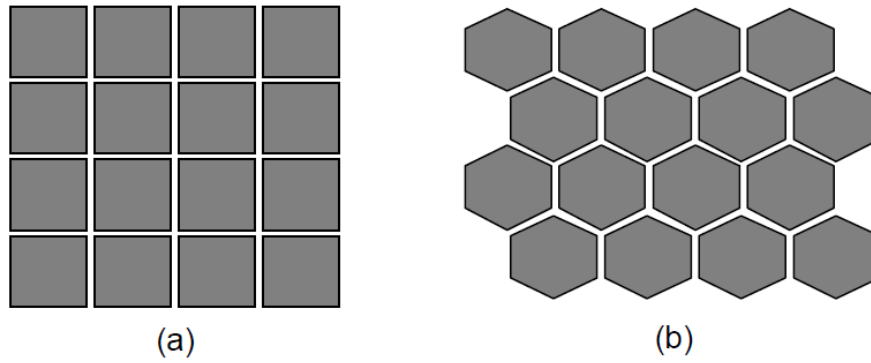
Figure (5.1): Common forms of SOM lattice.

SOM consists of two layers, namely input and Kohonen layers (Gan, Ma, & Wu, 2007), or called in other reference the competition layer (Taniar, 2008). The neurons in the Kohonen layer are arranged in a one- or two-dimensional lattice. The number of neurons in the input layer matches the number of attributes of the objects. Each neuron in the input layer is connected to all neuron in the Kohonen layer through some synaptic weights. The inputs are assumed to be normalized, i.e. $||x|| = 1$. Inputs to the Kohonen layer can be calculated as:

$$y_j = \sum_{i=1}^{d} w_{ji} x_i ,$$
(5.4)

Where w_{ji} is the weight from the input neuron i to the output neuron j. The neurons in the Kohonen layer undergo three basic stages, such as competition, cooperation, and updating. In the competition stage, the neurons in the Kohonen layer compete among themselves to be the winner. In the next stage, a neighbourhood surrounding the winning neuron is identified for cooperation among themselves. The winning neuron along with its neighbours is updated in the third stage (Taniar, 2008). The algorithm responsible for the formation of the SOM first initializes the weights in the network by assigning them small random values. Then the algorithm proceeds to the three processes, which are explained below in detail.

Competitive process: Let $x = (x_1, x_2, \ldots, x_d)^T$ be an object selected at random from the input space, where d is the dimension of the input space. Let the weight vector of neuron j in the Kohonen layer be denoted by

$$wj = (w_{j1}, w_{j2}, \ldots, w_{jm})^T, j = 1, 2, \ldots, m. \tag{5.5}$$

Where m is the total number of neurons in the Kohonen layer. The best match of the input object x with the weight vectors $w_{j1}, w_{j2}, \ldots, w_{jm}$ can be found by comparing the inner products $w_1^T x, w_2^T x, \ldots, w_m^T x$, and selecting the largest product, which is mathematically equivalent to minimizing the Euclidean distance between the vectors w_j and x. Therefore, the index $i(x)$ of the winning neuron for the input object x can be determined by

$$i(x) = \arg \min_{1 \leq j \leq m} ||x - w_j||, \tag{5.6}$$

Cooperative process: In the cooperative process, a topological neighbourhood is defined so that the winning neuron determines its topological neighbourhood of excited neurons for cooperation. They will try to update their synaptic weights through the cooperation. This will have a smoothing effect on the weight vectors in this neighbourhood. The number of nodes affected depends upon the type of lattice and the neighbourhood function.

Let $h_{j,t}$ denote the topological neighborhood centered on winning neuron t and $d_{t,j}$ denote the lateral distance between winning neuron t and excited neuron j. The

topological neighborhood function $h_{j,t}$ is assumed to follow a Gaussian distribution as given next:

$$h_{j,t} = \exp\left(-\frac{d_{t,j}^2}{2\sigma^2}\right), \tag{5.7}$$

Where σ is a parameter that measures the degree to which excited neurons in the neighborhood of the winning neuron participate in the learning process.

Updating process: The synaptic weights of the winning neuron and the excited neurons lying in its neighbourhood are updated using the rule given below:

$$w_j^{(s+1)} = w_j^{(s)} + \boldsymbol{\eta}(s)h_{j,i(x)}(s)\left(x - w_j^{(s)}\right), \tag{5.8}$$

Where $w_j^{(s)}$ is the weight vector of neuron j at time or iteration s, $w_j^{(s+1)}$ is the new weight vector at time s + 1, $\boldsymbol{\eta}(s)$ is the learning-rate parameter defined as:

$$\boldsymbol{\eta}(s) = \boldsymbol{\eta_0}\exp\left(-\frac{s}{\tau_2}\right), s = 0,1,2,\dots\dots \tag{5.9}$$

And $h_{j,i(x)}$ is the neighborhood function defined as:

$$h_{j,i(x)}(\mathbf{s}) = \exp\left(-\frac{d_{i(x),j}^2}{2\sigma^2(s)}\right), s = 0,1,2,\dots \tag{5.10}$$

With $\sigma(s)$ specified by:

$$\sigma(s) = \sigma_0\left(-\frac{s}{\tau_1}\right), \tag{5.11}$$

The constants $\boldsymbol{\eta_0}, \sigma_0, \tau_1$, and τ_2 can be configured as follows:

$$\boldsymbol{\eta_0} = 0.1, \sigma_0 = \text{the radius of the lattice}, \tau_1 = \frac{1000}{log\sigma_0}, and\ \tau_2 = 1000.$$

The training process of hexagonal SOM is shown in Figure (5.2). First, the weight vectors are mapped randomly onto a two-dimensional, hexagonal lattice as in Figure 5.2(a). The weight vectors, which illustrated by arrows in the nodes, pointing in random directions. In Figure 5.2 (a), the closest match to the input data vector x has been found in node c. The nodes within the neighbourhood $h_{c,i}$ learn from node c. The size of the neighbourhood $h_{c,i}$ is determined by the neighborhood radius. The weight vectors within the neighbourhood $h_{c,i}$ tune to, or learn from, the input data vector x.

How much the vectors learn depends upon the learning rate factor. The final and fully trained network is illustrated in Figure 5.2 (b), where a number of groups have been emerged. The weight vectors between the groups flowing smoothly into the different groups. If the neighbourhood $h_{c,i}$ is too small, then small groups of trained weight vectors will emerge with largely untrained vectors in between, i.e., the arrows will not flow uniformly into each other.
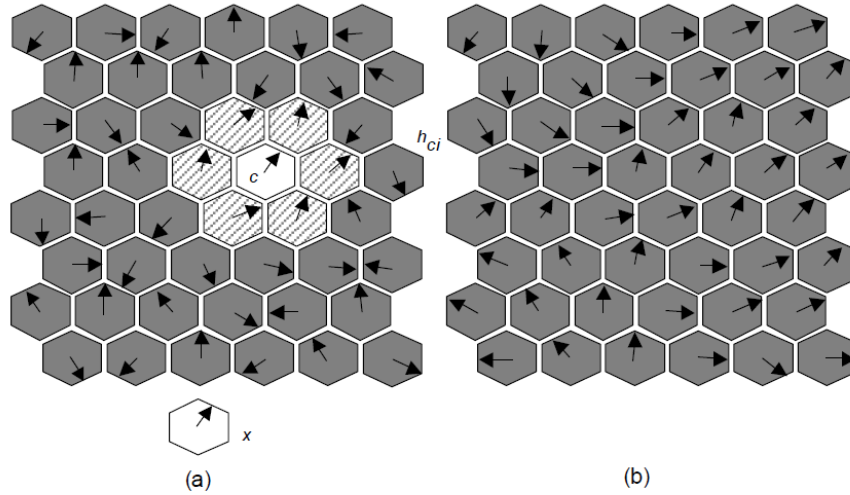
Figure (5.2): Training process of hexagonal SOM.

One advantage of the SOM algorithm is that it constantly learns and changes with changing conditions and inputs. However, the computations are high.

5.4 Support Vector Machine (SVM)

Support vector machines (SVM) was first introduced in 1995 for classification of input feature vectors (Cortes & Vapnik, 1995). The idea of SVM is to create a hyperplane in between the datasets to distinguish between two classes by linear separation. Thus SVM aims to find an optimal separating hyperplane with as large a margin as possible, and so to provide the maximum level of generalization and avoid overfitting as much as possible. Support vectors are the vectors in the training set with the minimal distance to the hyperplane where its optimum location depends only on these support vectors. This will generate two problems; finding both the optimal hyperplane, and the support vectors.

Figure 5.3 shows linearly separable binary classification problem with no possibility of miss-classification data. There are many possible linear classifiers that

can separate the data in the Figure 5.3, but there is only one that maximizes the margin (maximizes the distance between it and the nearest data point of each class). This linear classifier is termed the optimal separating hyperplane, which is defined as:

$$w.x + b = 0, \tag{5.12}$$

A separating hyperplane in canonical form must satisfy the following constraints:

$$n_i(w.x + b) \geq 1 , i = 1,2, ... N, \tag{5.13}$$
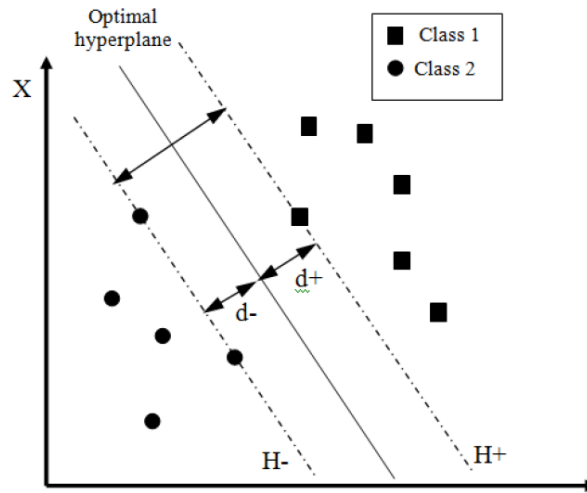
Figure (5.3): Support vector machine with linear separable data

Considering the Figure 5.3 above the margins are defined as d+ and d-. The margin will be maximized in the case d+ = d−. Furthermore, training data in the margins will lie on the hyper-planes H+ and H-. The distance between hyperplane H+ and H- is:

$$\rho = d_- = d_+ = \frac{2}{||w||} , \tag{5.14}$$

Hence, the hyperplane that separates optimally the training data is the hyperplane which maximize the margin ρ and minimizes:

$$\varphi(w) = \frac{1}{2}||w||^2, \tag{5.15}$$

Where w is the weight vector. The main problem of estimation of an optimal hyperplane, is when the training data is nonlinear separable. To overcome this

problem, two improvements for SVM have been introduced. The first one is to replace the hard margins concept with the soft margins. The idea of soft margins is to add slack variables, ξ_i into the inequalities for relaxing them slightly so that some points are allow to lie within the margin or even being misclassified completely. Thus, the maximum margin hyperplane does not necessarily separate all training instances of both classes (Taniar, 2008).

$$\varphi(w) = \frac{1}{2}||w||^2 + C\left(\sum_i L(\xi_i)\right), \tag{5.16}$$

Where C is the adjustable penalty term and L is the loss function. The most common used loss function is linear loss function, $L(\xi_i) = \xi_i$. The optimization of (5.16) with linear loss function using Lagrange multipliers approach is to maximize,

$$L_D(w, b, \alpha) = \sum_i^N \alpha_i - \frac{1}{2}\sum_{i=1}^N \sum_{i=1}^N \alpha_i \, \alpha_j y_i y_j \langle x_i, x_j \rangle, \tag{5.17}$$

Subject to $0 \leq \alpha_i \leq C$, and $\sum_{i=1}^N \alpha_i \, y_i = 0$, where α_i is the Lagrange multipliers.

This optimization problem can be solved by using standard quadratic programming technique. Once the problem is optimized, the parameters of optimal hyperplane are

$$w = \sum_{i=1}^N \alpha_i \, y_i x_i, \tag{5.18}$$

α_i is zero for every x_i except the ones that lies on the margin. The training data with non-zero α_i are called support vectors.

The second improvement is the introduction of kernel functions. The idea of kernel functions is to map the data into a higher dimensional domain, in which the data can be separated accurately. This way the data in the original space is separated in a nonlinear fashion. An important characteristic of the use of kernel functions is that the calculation of a maximum margin hyperplane in the kernel space is not much more expensive than in the original space.

Chapter 6

Results and Discussion

Chapter 6

Results and Discussion

6.1 Pre-processing Results

In this section we will show the results of applying the pre-processing techniques on CASIA-FingerprintV5 database. This stage consists of three sub-sections: the first one shows the results of alignment process, the second shows the results of the enhancement process including the original algorithm and the modified one, and the last one shows the results of core point detection process.

6.1.1 Alignment Results

When we perform the alignment process on the CASIA-FingerprintV5 database, we face some problems. One of them is the existence of some small black regions within the white regions, and this means that these black regions are considered as a part of the foreground region. This result is a by-product of segmentation process in poor quality fingerprint images. Another problem is the non-smooth contour of the image segmentation as shown in Figure 3.1. Both of these problems affect the performance of the alignment technique described in Chapter 3, since the alignment technique is based on navigation along the x-coordinate and the y-coordinate, and so while incrementing the navigation variable, it will stop the navigation when it finds a black pixel, since it finds the contour of image segmentation. This will affect the TFCP location, and the upper point location, and as a result it affects the determination of C1, C2, and C3.

We solve the problems above by using the segmentation algorithm described in (Fahmy & Thabet, 2013). Figure 6.1 shows the results of alignment, which depend on segmentation process of (Msiza, Leke-Betechuoh, & Malumedzha, 2011), where the left side is the original images. The middle side is the result of segmentation according to (Msiza, Leke-Betechuoh, & Malumedzha, 2011), and the right side is the result of rotation. Figure 6.2 shows the results of alignment which depends on segmentation process of (Fahmy & Thabet, 2013), where the results of segmentation are shown in the middle column according, and the result of rotation are shown in the last column. From both figures we can visually observe that the proposed solution is more accurate

than the other in determining the angle of rotation because of smoothing the image contour, and removing false small black blocks in the foreground region.
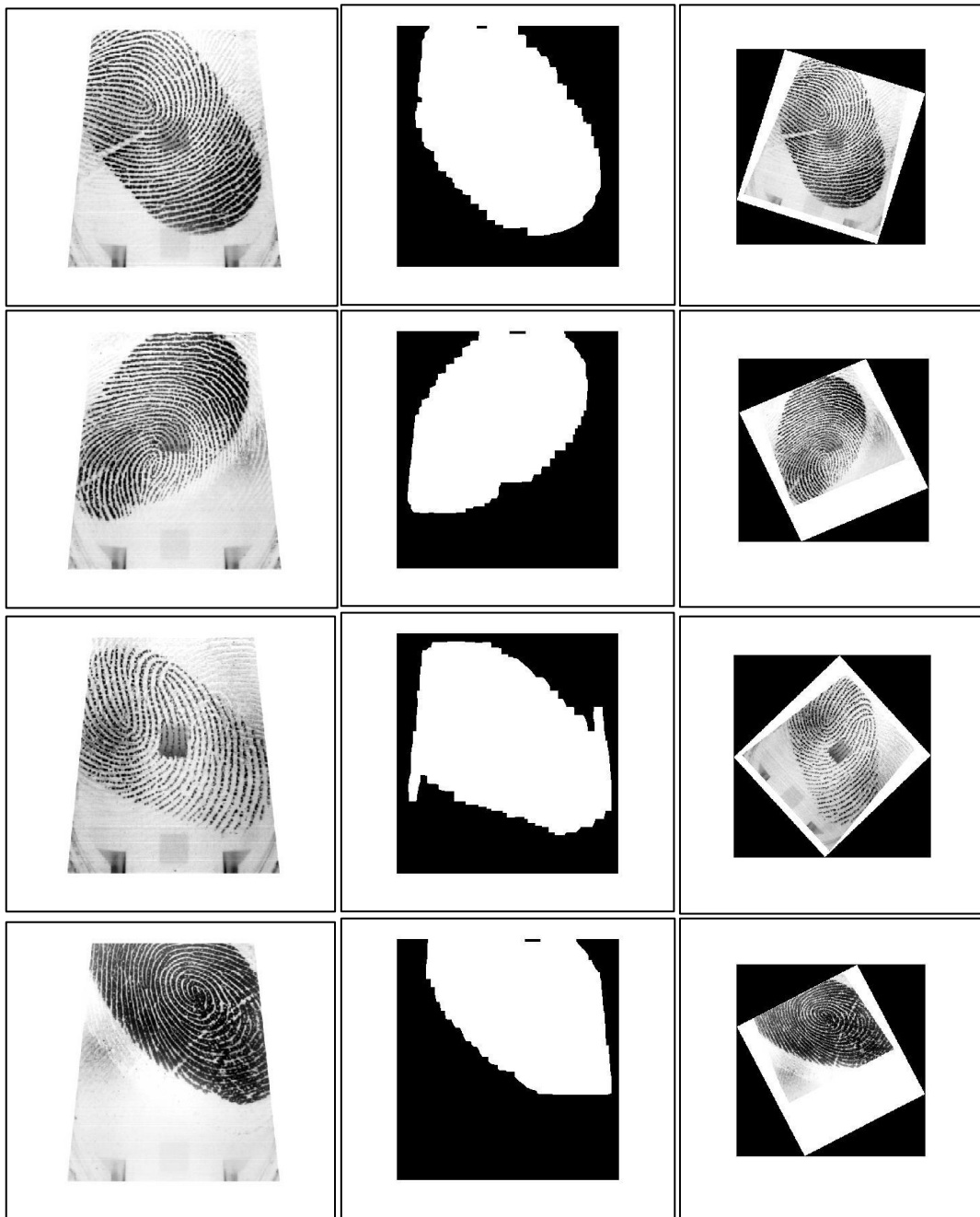
Figure (6.1): Image Rotation result according to image segmentation in the original algorithm.

Although the used algorithm of rotation is robust, it has some drawbacks. The algorithm cannot perform well in some images which need to be rotated and have cuts in the image boundaries, especially if the image is cut in more than one side, i.e. the

images which are shifted outside the scope of image boundaries, such as the images of CASIA-FingerprintV5 database.
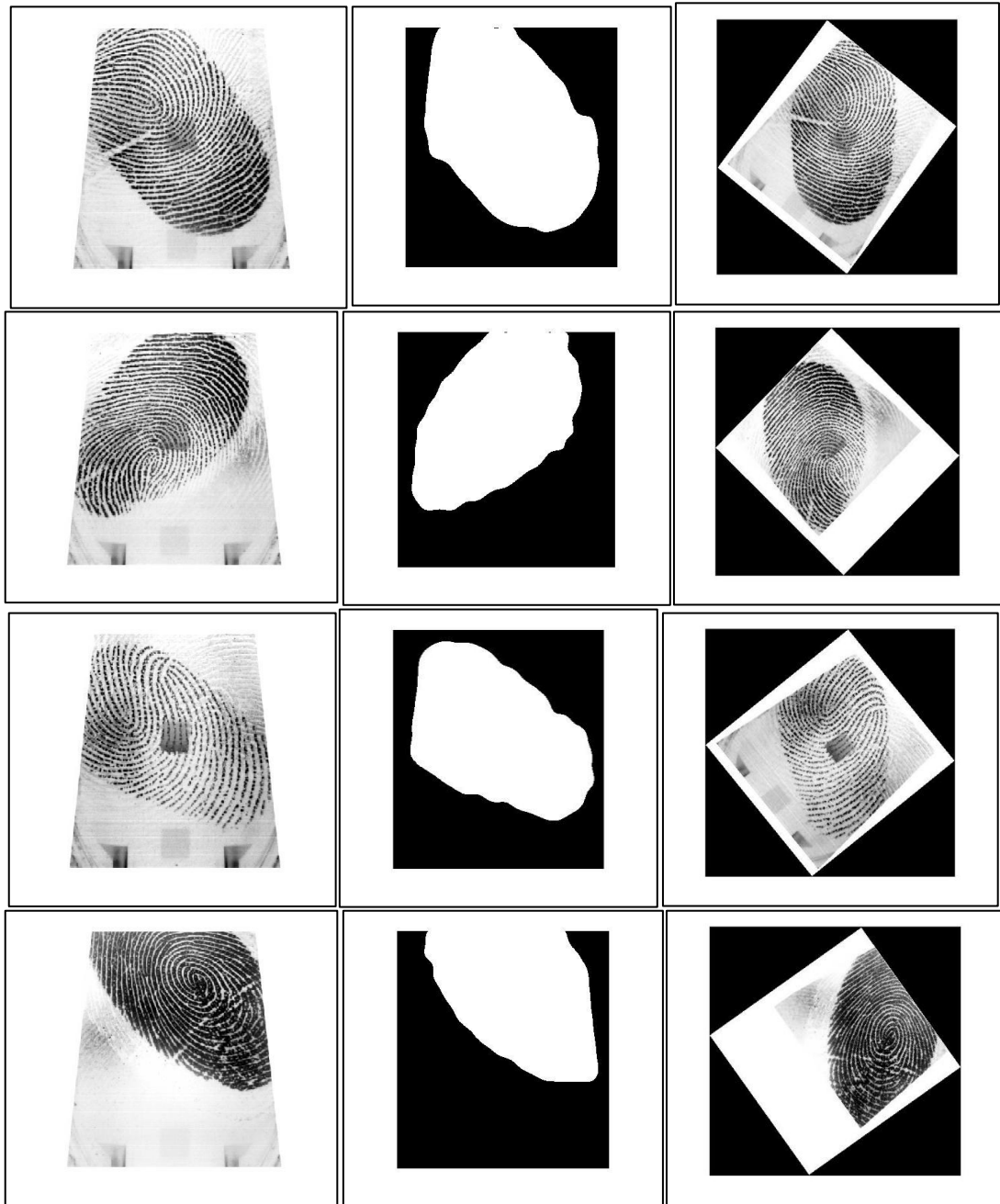
Figure (6.2): Image Rotation result according to image segmentation in the modified algorithm.

The segmentation process leaves some small black parts in the top boundary of fingerprint image, especially in fingerprint which its upper part is lost. We solve this problem by implementing a method which eliminates these parts.

Another drawback of this technique that it cannot deal with images which need a rotation angle more than 90 degree in both directions. CASIA-FingerprintV5 database contains a lot of different rotation challenges, which need to be solved efficiency. We suggest a solution as a future work, which can deal with this issue.

6.1.2 Enhancement Process Results

We use the enhancement algorithm proposed by (Chikkerur, Cartwright, & Govindaraju, 2007), in which the region mask is obtained by thresholding the energy image. When we apply the algorithm on CASIA-FingerprintV5 database, we obtain an efficient enhancement results in most types of poor quality images. The algorithm can connect the ridge discontinuity, and treats the fingertips creases and dryness. But we cannot obtain an optimum segmentation when dealing with the humidity in some images. This is because of the very bad qualities of the fingerprint images, where the humidity and dryness get together in the same fingertip, and this leads to segment some parts and to lose the others. Sometimes the opposite is true, that some fingerprint images contains some traces of the previous scanned fingertips, and this leads to segment some parts which does not belong to the targeted fingertip. This issue rarely occurs, but it is existed in the CASIA-FingerprintV5 database. Furthermore the background regions are not clean as the other databases such as FVC family. It contains some small grey blocks in different regions, which affects the segmentation process which based on single thresholding the grey level variation. Single thresholding will lose some information about the ridge regions which are hardly appeared in bad quality fingerprint images. For this reason we replace the segmentation step of Chikkerur et al. algorithm with the algorithm proposed by (Fahmy & Thabet, 2013) which we use it in the alignment step. The segmentation process of (Fahmy & Thabet, 2013) was based on computing the range image over blocks of size 16x16 then applying a local adaptive thresholding to select an appropriate threshold level for each block.

The modified enhancement technique gives a slight improvement in some poor quality images with a lot of creases and wounds as shown in Figure 6.3, where the upper row shows some bad samples with a lot of creases of CASIA-FingerprintV5 database, the middle row shows the result of the original technique, and the last row

shows the result of the modified technique. We also see that both enhancement algorithm can connect the discontinuities of the ridges, and improve the contrast between ridges and valleys, however the enhancement results of the modified algorithm give a better region mask image than the original since the segmentation technique in the modified algorithm depends on an adaptive thresholding with each block.

Another reason that degrades the quality of fingerprint images is the dryness of fingers, which leads to fragmented and low contrast ridges. Figure 6.4 shows some of these images and the result of the original and the modified algorithm, where the upper row is three samples images from CASIA- FingerprintV5, the middle row shows the result of the original technique, and the last row shows the result of the modified technique.
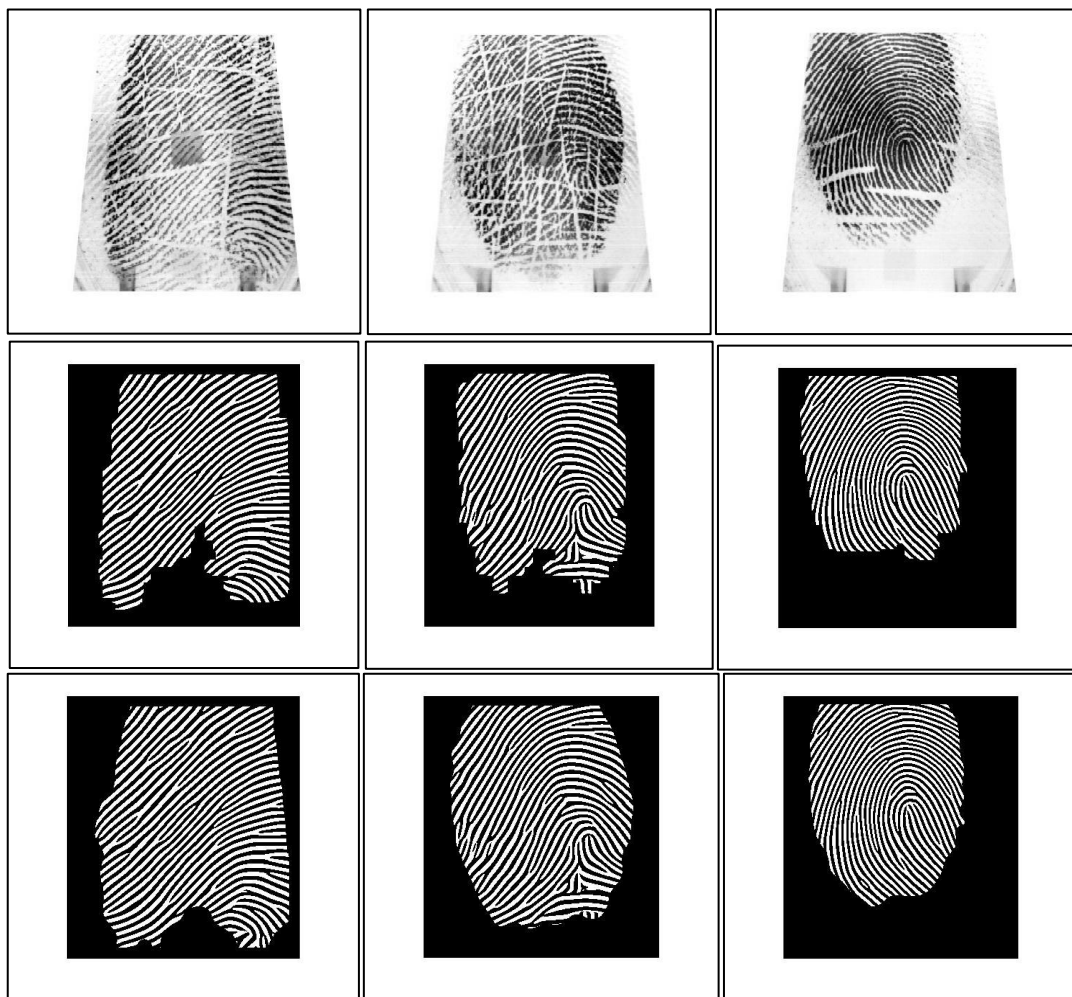
Figure (6.3): Enhancement result of both the original technique and the modified one.

The Humidity of the fingertip may degrade the quality of the fingerprint images. Some samples of these types, and the results of the original and the modified enhancement algorithm are shown in Figure 6.5, where the upper row is three samples images from CASIA- FingerprintV5, the middle row shows the result of the original technique, and the last row shows the result of the modified one.
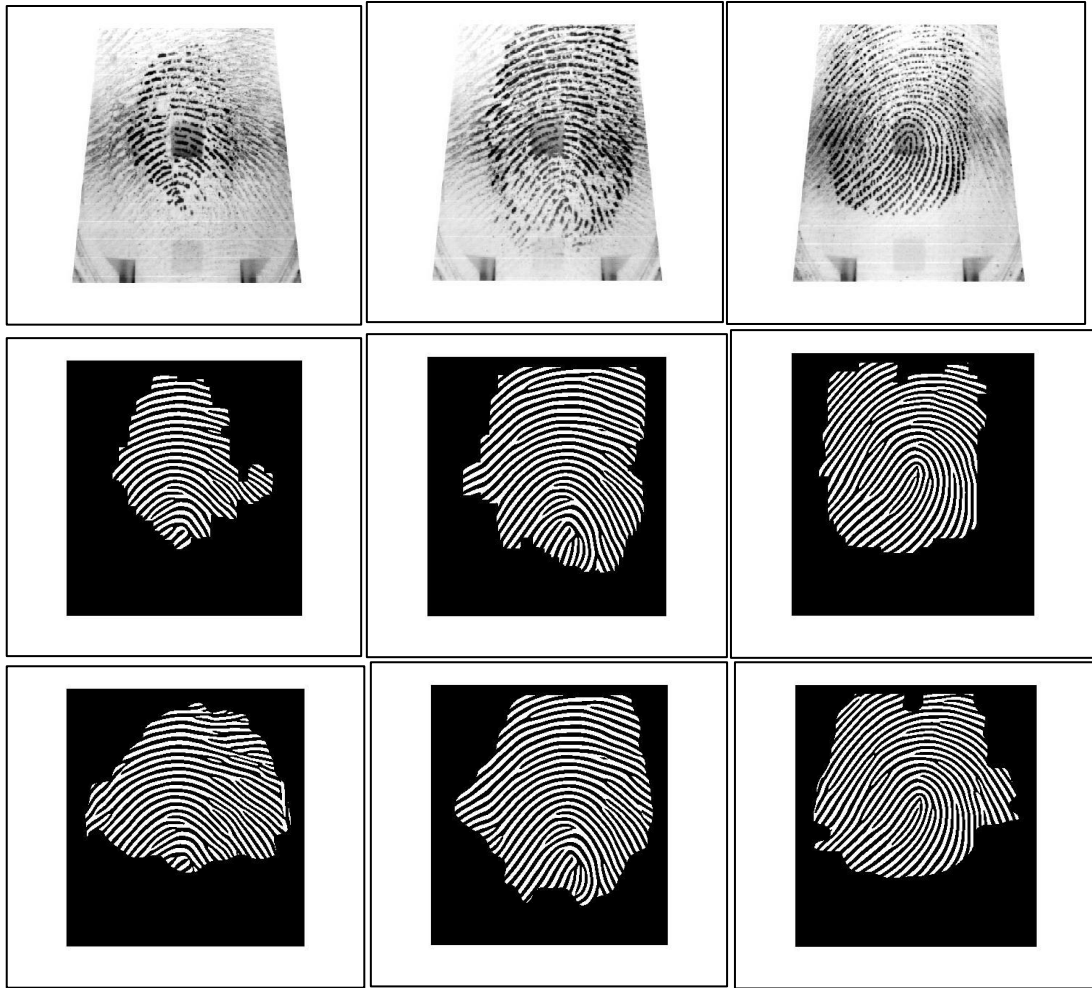
Figure (6.4): Enhancement result of some dry fingertip samples for both the original technique and the modified one.

We can observe that Chikkerur et al. algorithm cannot segment some humidity image in Figure 6.5, because they generated the region mask based on Otsu's optimal threshold after enhancement step, and this will lose this humidity region. In the other side, segmentation before enhancement will not affected by the humidity regions. We see that this problem is the most agent that affected by the segmentation process. The modified algorithm results are clearly better than the original one.

6.1.3 Core Point Result and Cropped Area

We use the complex filters algorithm (Nilsson & Bigun, 2003) to determine the singular point location. Before enhancement process the proposed algorithm can detect the core point in some fingerprint images, and fail in others. But after enhancement process, its performance is increased. The result of applying this technique on the selected database successes in most fingerprint images (98.9%), and fails only to detect the core point in 6 images, three of these images are partial fingerprint and they do not have core points, and the others are poor ridge structure images, where the algorithm determines a location around the accurate core point. Figure 6.6 shows some of these fingerprints images which have an inaccurate core point detection, where the upper images are partial fingerprint images samples which have no core point, and the lower images are false location determination of core point.
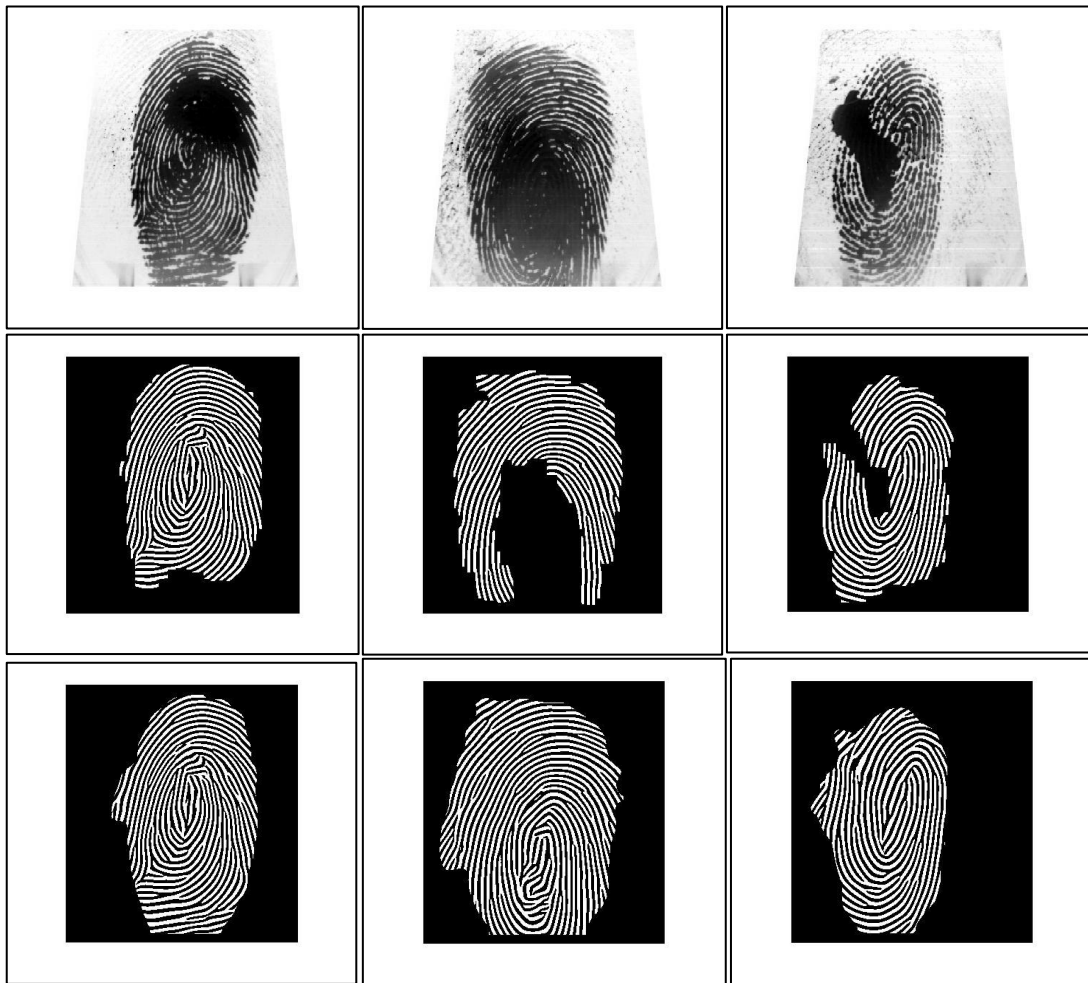
Figure (6.5): Enhancement result of the humidity in some fingerprint samples for both the original technique and the modified one.

In case of left loop and right loop fingerprint image classes, the algorithm can detect the core point accurately, as shown in Figure 6.7. However, the used core point detection algorithm performs well in most fingerprint classes, we face a problem in detection of whorl and twin loop fingerprint types. These types of fingerprints have two core points as previously shown in Figure 3.6. In some fingerprints, the algorithm detects one core point in some samples, and detects the other in the other samples of the same person as shown in Figure 6.8, where the upper images are two samples from the same person, while the lower images from another person. This will affect the cropped area which taken from the image to be entered to the feature extraction process. In our selected database, the percentage of whorl and Twin-Loop is 17%.
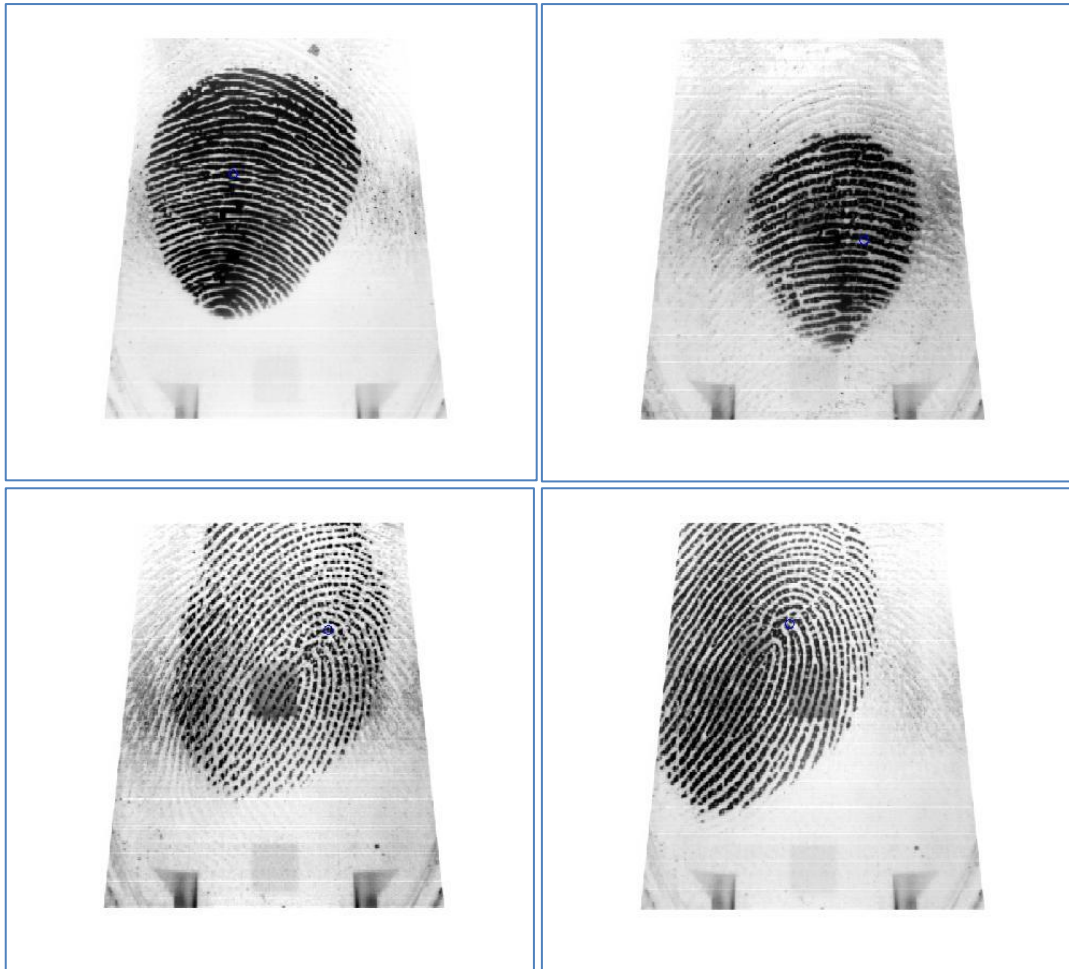
Figure (6.6): The results of detection the core point.

After detecting the core point, a region of size M x N (128x128 or 64x64) around the core point is cropped. This region is used to extract the features from it, since this region contains information which can be used to identify the fingerprints image.

Furthermore, we need to minimize the features as soon as possible, to build a fast recognition system. We face a problem in this process, that the core point locations near the image boundaries have lost much information as a result of cropping process, which considered as a black regions as shown in Figure 6.9. In our selected database, the percentage of these black regions is 22.8% from all our selected database.

Figure (6.7): The results of detection the core point in left loop and right loop fingerprint image classes.
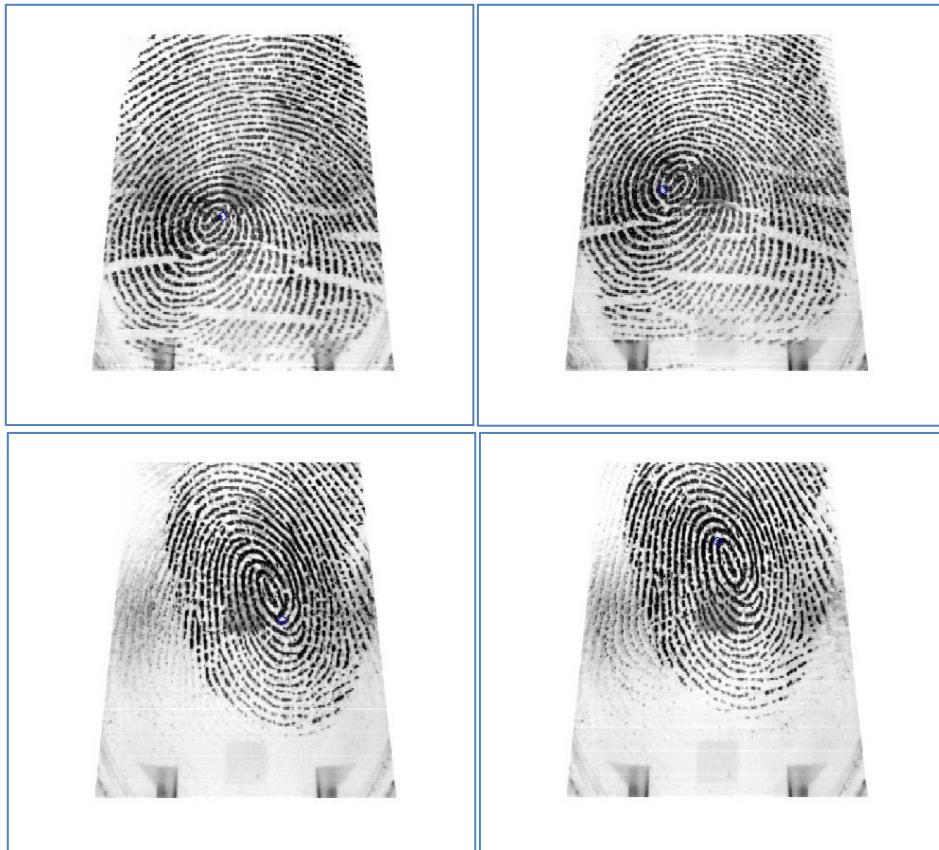
Figure (6.8): The results of detection the core point in whorl fingerprint class.
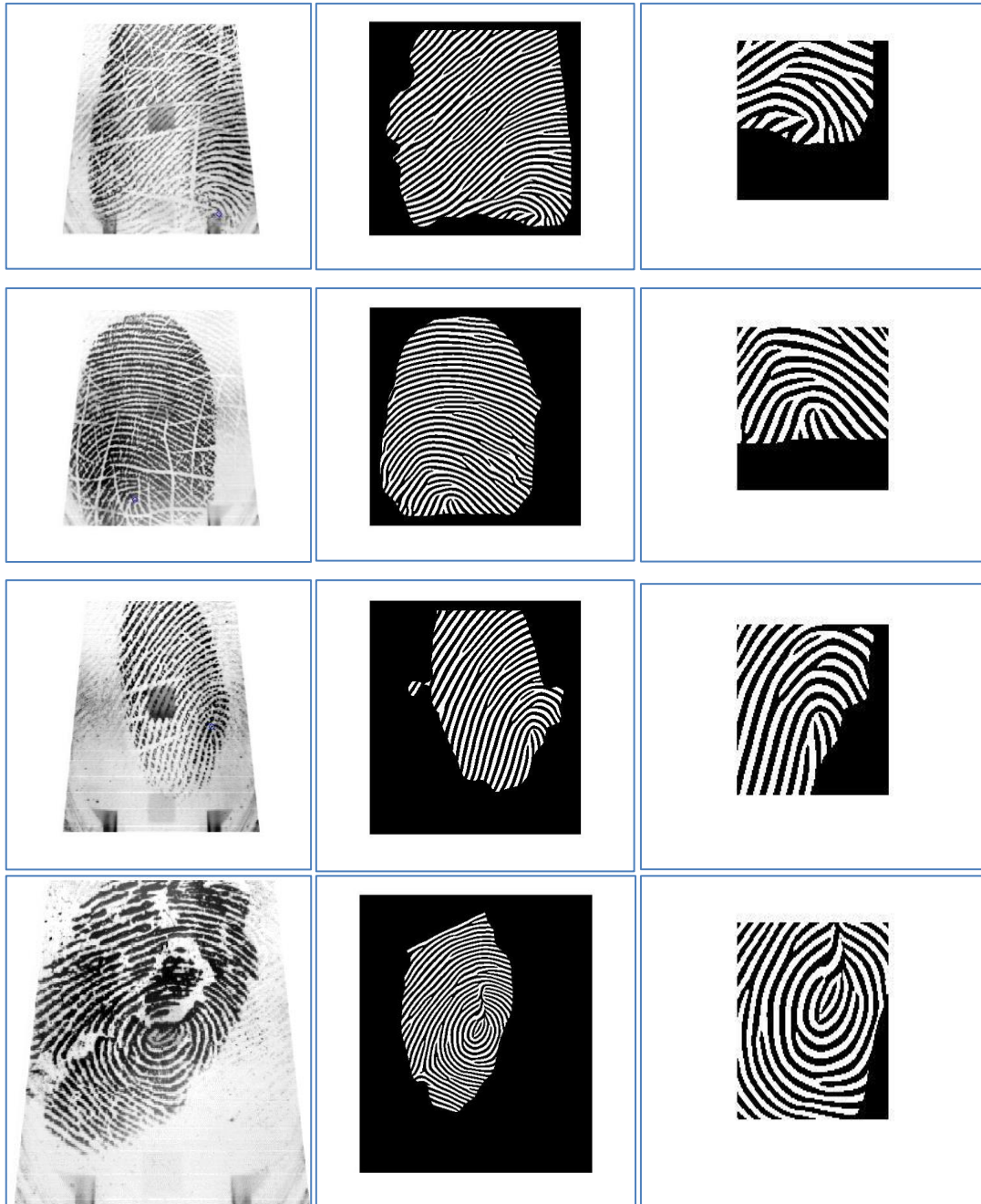
Figure (6.9): The results of cropping 128x128 region around the core point.

6.2 Feature Extraction Results

After locating the reference point or core point in the fingerprint image. We crop an N x M subimage from the fingerprint pattern with core point at the centre. This can be called 'central subimage'. The size of subimage is taken once as 64x64 and once as 128x128. We choose a subimage of size 64x64, since most fingerprint information is

concentrated in this region, and contains less noisy information. We enlarge the subimage size to 128x128, since we discover that the region of 64x64 cannot has an enough features to identify large size of fingerprint images.

We divide this central subimage into a number of non-overlapping blocks of size W x W, i.e. W=64 or 32 when the size of subimage is 128x128 or 64x64 respectively. This division will be Then we take the multiresolution transforms; Wave atom, Curvelet and Shearlet; for each of the non-overlapping blocks at Scale = S and Angle = A. After that we take the standard deviation of each of the multiresolution transforms coefficient sets to reduce the coefficient matrix dimension. Thus the obtained standard deviation for each of the four blocks of a fingerprint image constructs the global feature vector together. The obtained features vector size depends on the applied multiresolution transform. Table (6.1) shows the size of the feature vectors corresponding to the feature extraction techniques. Shearlet transform cannot handle the small region size of images, since the Shearlet toolbox gave an error when we applied it to this small size region. So we cannot get a result from image size of 64x64.

Table (6.1): Features vector corresponding to the used multiresolution transform

Feature Extraction Methods	Cropped Subimage	Feature Vector Size
Wave atom	128x128	**1x265**
	64x64	**1x128**
Curvelet	128x128	**1x536**
	64x64	**44x1**
Shearlet	128x128	**256x1**
	64x64	**NaN**

6.3 Fingerprint Database:

We select randomly 114 subjects from CASIA Fingerprint Image Database Version 5.0 (or CASIA-FingerprintV5). We eliminate the subject whose most of his fingerprint images do not have a reference point (Arch). In addition, we eliminate the subject whose fingerprint image need a rotation angle more than 90 degree. CASIA-

FingerprintV5 contains 5 samples for each subject, so we use 3 for training and 2 for testing.

6.4 Matching Techniques Results

The features vectors are classified by various matching algorithms, from simple classification to more complex ones. The recognition results of both the cropped sizes of 128x128 and 64x64 are illustrated in Table (6.2). Figure 6.10 shows the recognition results of a cropped image of size 128x128, while Figure 6.11 shows the recognition results of a cropped image of size 64x64.

Table (6.2): Fingerprint recognition results

Matching Algorithm	Feature Extraction Methods	Cropped Subimage	Recognition Rate %
Average Euclidean distance	Wave atom	128x128	84
		64x64	67
	Curvelet	128x128	87
		64x64	57
	Shearlet	128x128	76
		64x64	NaN
One to One Euclidean distance	Wave atom	128x128	99.5
		64x64	78
	Curvelet	128x128	87
		64x64	65
	Shearlet	128x128	87
		64x64	NaN
KNN	Wave atom	128x128	99.5
		64x64	78
	Curvelet	128x128	87
		64x64	65
	Shearlet	128x128	87
		64x64	NaN
SOM	Wave atom	128x128	97
		64x64	86
	Curvelet	128x128	85
		64x64	71
	Shearlet	128x128	87
		64x64	NaN
SVM	Wave atom	128x128	74
		64x64	74
	Curvelet	128x128	26
		64x64	75
	Shearlet	128x128	68
		64x64	NaN
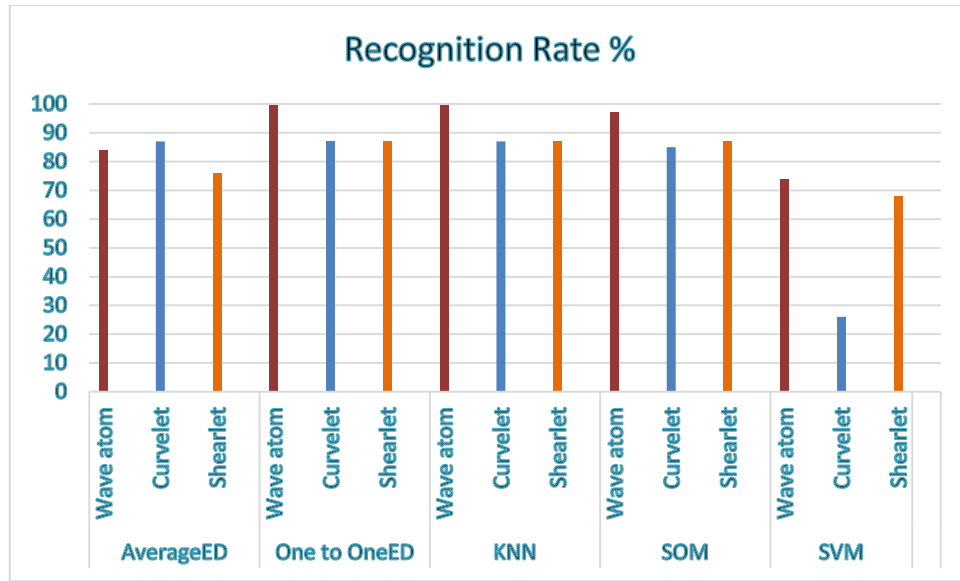
Figure (6.10): Fingerprint recognition results of cropped size of 128x128.

The first matching algorithm is the ED, which is a simple classifier, and used to measure the minimum distance between every test fingerprint images and the average distances between the remaining samples for all training subjects. For a cropped area of 128x128, we compare the feature extraction techniques using this classifier. The result of recognition rate of Curvelet transform is the highest (87%), then the Wave atom (84%), then the Shearlet transform (76%). The misclassification rate is because of the following reasons:

1- The percentage of blank areas, or the information missed as a result of cropping process is relatively high (~ 23% from the fingerprint images). These images are distributed for all fingerprint samples.

2- The number of training samples are low (3 samples), so the existence of one fingerprint image with a blank area, will affect the average feature vector, and so will affect the recognition rate.

Using the ED, we see that the Curvelet transform has the highest recognition rate, and we believe that this result is due to that the Curvelet transform is less affected by the black images of the others techniques, since the Curvelet coefficients vector (536x1) is the biggest one.
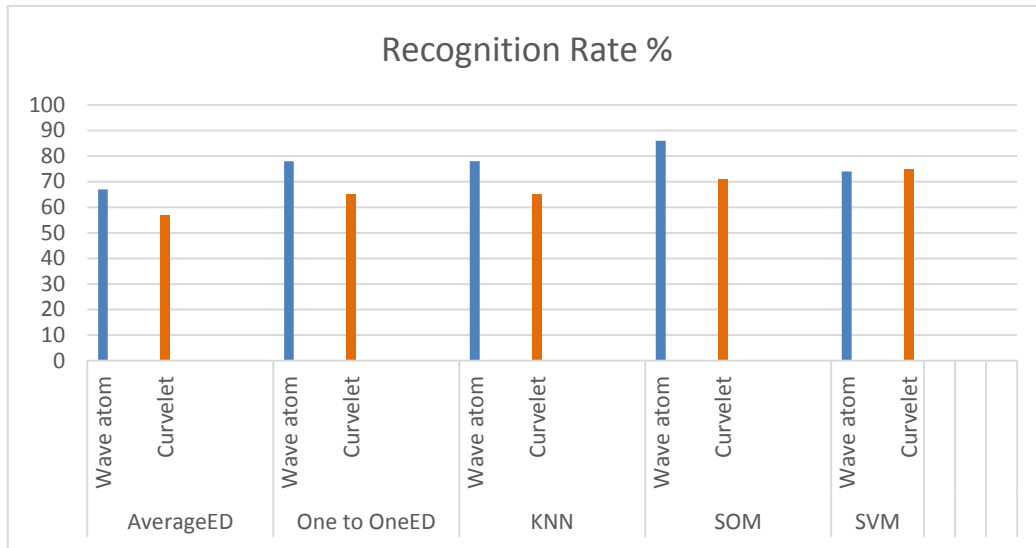
Figure (6.11): Fingerprint recognition results of cropped size of 64x64.

For a cropped area of 64x64, the recognition rate of all types of feature extraction techniques is very bad. This is because the extracted features from this small area are not enough to be identified correctly.

If we run the ED algorithm to match the similarity between vectors as one to one matching, the recognition rate will be better. This is the same idea of KNN algorithm with K=1.

The second simple matching technique is the KNN algorithm. We run the algorithm with different values of nearest neighbours K, and the highest recognition rate is when K=1. For a copped area of 128x128, the Wave atom has the highest recognition rate (99.5%), which is published in (Abudalal & Alhanjouri, 2016)(IF:3.466), while the Curvelet and Shearlet have the same recognition rate of (87%). For a cropped area of 64x64, the results are not good, however the Wave atom transform gains higher recognition rate than the Curvelet transform. The Shearlet transform does not work with this small size of area.

We conclude that for the minimum distance classifiers, the features have to be enough to be identified correctly and gain a high recognition rate

The third type of matching techniques is the Self Organizing Map (SOM). We set the parameter of dimension size equal [20 10], and the number of iterations ranges from 3000 to 9000 iterations. The results of recognition rate of SOM are good for both

types of cropped areas. For 128x128 area, the Wave atom has the highest recognition rate of (97%), followed by the Shearlet (87%), and the last one is the Curvelet (85%). For 64x64 area, the Wave atom has the highest recognition rate of (86%), while the Curvelet has (71%) which is not good enough.

We conclude that the SOM may get a better results if the features coefficients are reduced.

The fourth matching algorithm is the support vector machine (SVM). Although the Wave atom has the highest recognition rate, all results are not accepted as a good recognition rate. We also conclude that the result is improved if we reduce the feature coefficients vector.

To achieve our suggestion about improving the recognition rate, we use the Principle Component Analysis (PCA) technique to reduce the features vector. Reducing the features vector using PCA has a bad effect on the recognition rate when we use the minimum distance classifier. On the hand, it improves the recognition rate when using other classifiers. The result is tabulated at Table (6.3) and plotted in Figure 6.12.

Table (6.3): Fingerprint recognition results after using the PCA

Matching Algorithm	Feature Extraction Methods	Cropped Subimage	Recognition Rate %
SOM	Wave atom	128x128	95
		64x64	73
	Curvelet	128x128	89
		64x64	60
	Shearlet	128x128	73
		64x64	NaN
SVM	Wave atom	128x128	90
		64x64	61
	Curvelet	128x128	80
		64x64	46
	Shearlet	128x128	62
		64x64	NaN

The feature vector size of Wave Atom coefficient was 256 and gained 97% for SOM and 74% for SVM. After reducing the Wave Atom coefficient to 20 coefficients using the PCA algorithm, it gains 95% for SOM and 90% for SVM. We can conclude

that Wave Atom coefficients are heavily affected positively after reduction and matching by SVM. The features vector of Curvelet coefficient was 536 and gained 85% for SOM and 26% for SVM. After reduction by PCA, the features vector is reduced to 44 features and it gains better results. We conclude that Curvelet coefficients are heavily affected positively by reduction in both classifiers. The feature vector of Shearlet coefficient was 256 and gains 87% for SOM and 68% for SVM. After the PCA algorithm, it is reduced to 4 coefficients and gains 73% for SOM and 62% for SVM. We conclude that Shearlet coefficients are heavily affected negatively by reduction in both classifiers, since 4 features are not enough to recognise the fingerprint images.
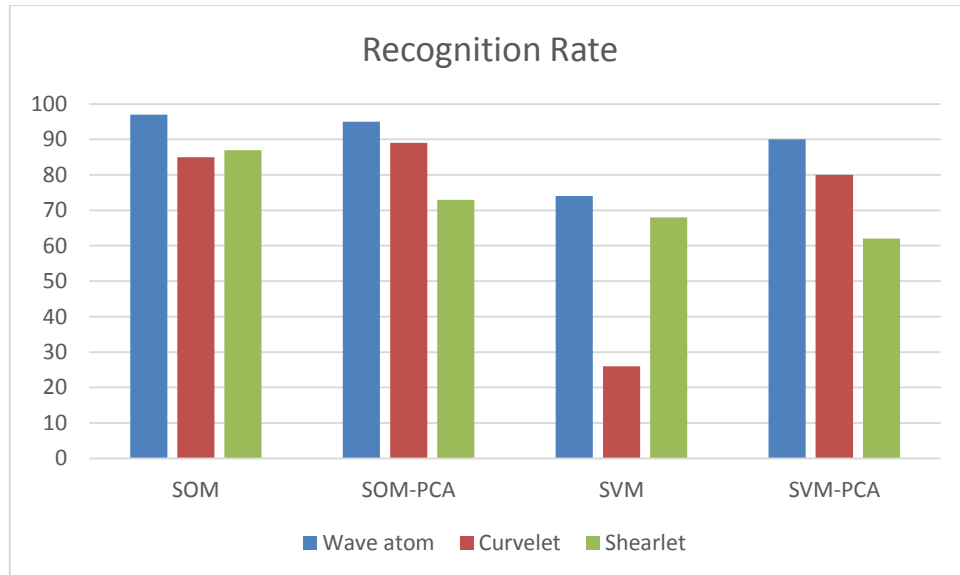
Figure (6.12): Fingerprint recognition before and after using PCA.

We can construct several models depending on the results shown above. These models are illustrated in Table (6.4)

6.5 Comparison with Other Works

In this section we compare our work with researches which used the multiresolution transforms as a feature extraction techniques, and are used the CASIA-FingerprintV5 database. Indeed, there are limited number of researchers who used the CASIA-FingerprintV5 database in their testing environment.

Table (6.4): Suggested Models for Fingerprint Recognition System

Cropped Subimages	Feature Extraction Methods	Classifier Technique	Dimension Reduction PCA	Recognition Rate %
128x128	Wave atom	KNN (K=1)	No	99.5
		SOM	No	97
		SOM	Yes	95
		SVM	Yes	90
	Curvelet	ED	No	87
		KNN (K=1)	No	87
		SOM	Yes	89
		SOM	No	85
	Shearlet	KNN (K=1)	No	87
		SOM	No	87

We want to refer here that the differences of the subimage size will not affect the comparison, since the following notes:

1- In (Omidyeganeh, Javadtalab, Ghaemmaghami, & Shirmohammadi, 2012), they used a cropped image of size of 192x192, and they compared their results with Tico et al. who used a subimage size of 64x64. Also, (Guesmi, Trichili, Alimi, & Solaiman, 2012) used a subimage size of 175x175, and they compared their results with (Yang &Park, 2008), who used a subimage size of 96x96.

2- Tico et al. reported in their paper that the reason of selection a subimage size of 64x64 was that of the noisy details located outside the fingerprint pattern were found when they tried to enlarge the cropped area.

The first research we will compare our results with is the work done in (Akbar , Ahmad , & Hayat , 2014). They compare between three feature extraction techniques, the Discrete Wavelet transform (DWT), Principal Component Analysis (PCA) and Discrete Cosine Transform (DCT), to extract their feature vector and use the KNN and SVM classifiers for matching. They test their algorithm in three different benchmarks of CASIA-FingerprintV5 database. The comparison is shown in Table (6.7). They achieve with DWT a higher accuracy than the others two techniques, so will record and compare with the highest values of their work. We have several improvement over their proposed solution, that we achieve better recognition rate with larger database size.

The second research we compare with it, was the work done in (Jena & Dalal, 2014). They used the DWT to extract their fingerprint image coefficients, and ED for matching. They selected 25 subjects from CASIA-FingerprintV5 database. They achieved FAR=2.3%, and FRR=0.9%. To compute the overall accuracy of their results, we use the EQ (6.1) (Vinothkanna & Wahi, 2014), the comparison is shown in Table (6.7). We have several improvement over their proposed solution, that we achieve better recognition rate with larger database size.

$$Accuracy = 100 - \left(\frac{\frac{FAR}{FRR}}{2} \right) \tag{6.1}$$

Table (6.5): Comparison between several works done in CASIA-FingerprintV5 database and ours

	The work done by (Akbar , Ahmad , & Hayat , 2014)			The work done by (Jena & Dalal, 2014)	Our proposed solution
	DB1	**DB2**	**DB3**		
Core point detection algorithm	Not used	Not used	Not used	Not used	Automatic
Alignment algorithm	Not used	Not used	Not used	Not used	Use an efficient alignment algorithm
Fingerprint Database	CASIA fingerprint V5	CASIA fingerprint V5	CASIA fingerprint V5	CASIA fingerprint V5	CASIA fingerprint V5
No of the fingerprint subjects	8	20	40	25	114
Feature Extraction	DWT	DWT	DWT	3 level DWT	Wave Atom
Classification	KNN	KNN	KNN	ED	KNN
Recognition Rate	90%	81%	84%	98.7%	99.5%

If we can compare our results with those who used different fingerprint databases, such as FVC families, we have a serious improvement over their work. Turroni stated that the difficulty of FVC2002 is low, while the difficulty of FVC2004

is medium   (Turroni, 2012). Some researchers have described the CASIA-FingerprintV5 as a very challenges database (Li, Busch , & Yang, 2014)

There were a series of researches which used the multiresolution techniques in fingerprint identification. These researches which started by using Wavelet transform (Tico, Immonen, Ramo, Kuosmanen, & Saarinen, 2001), followed by Contourlet transform (Omidyeganeh, Javadtalab, Ghaemmaghami, & Shirmohammadi, 2012), and Curvelet transform (Mandal & Jonathan Wu, 2008; Guesmi, Trichili, Alimi, & Solaiman, 2012; Humaira, Bushra, Firdous, Khan, & Islam, 2013). We have several improvements over their works in terms of number of testing fingerprint database, and the recognition rate.

Chapter 7
Conclusion and Future Work

Chapter 7
Conclusions and Future Work

7.1 Conclusions

During the study and the development of this thesis, various problems have been identified, which results yield contribution to the automatic fingerprint recognition system. The following conclusions are listed below:

To achieve high recognition rate in poor quality fingerprint images, the fingerprint image has to be enhanced with a reliable enhancement techniques. Fingerprint enhancement technique based on STFT analysis is a reliable and an efficient technique which applied on CASIA-FingerprintV5 database.

Accurate segmentation to distinguish between the foreground and background is an important step for the efficiency and the accuracy of subsequent enhancement and feature extraction stages. Segmentation based on one threshold value for all the fingerprint image may lose some important information at least visible and intensity regions, while segmentation based on the range image feature over blocks and local adaptive thresholding, performs better than the original since it selects an appropriate threshold level for each block. Furthermore, applying segmentation after enhancement may lose the humidity regions in fingerprint image since there are no regular signal in these regions, and hence the Fourier transform of these regions is constant and these parts will not be processed through a complete enhancement process. Segmentation based on morphological operations, closing and opening operations, before enhancement can segment these humidity regions.

An accurate displacement and rotation of fingerprint images are critical issues that affect the performance of feature extraction techniques, and decrease the recognition rate. Our used methodology is translation invariant, since we use the core point as a reference point. Detection the core point algorithm based on complex filters performs good after enhancement steps, but it fails to detect the exact location of the core point in whorl and twin loop fingerprint classes, because these classes of fingerprints have two core points. So it detects one of the core point in one sample,

and detects the other in the other sample. The percentage of whorl and twin loop fingerprint classes in our selected database is 17%.

Although the fingerprint alignment algorithm of Msiza et al. is independent and performs well in our experiments, it has some drawbacks. It performs well in the images of almost complete mask, i.e. without cuts in the image boundaries, especially if the image is cut in more than one side, such as the images of CASIA-FingerprintV5 database. Another factor of limitations, that the algorithm assumes that most fingerprint rotation angle ranges between (0-90 degree), but we found that, in CASIA-FingerprintV5 images, the rotation angle ranges between (0-360 degree). We suggest a good solution to overcome this limitation, but because the limitation in thesis schedule, we cannot implement the suggested solution, which is explained in the future work section. The segmentation process may leave some small black parts at the upper boundary of fingerprint image, especially when the fingerprint displacement is out of the top image border. We solve this problem by implementing a method to eliminate these parts.

In poor quality fingerprint images, the extracted features from a fingerprint subimage of size 64x64 are not enough to recognize the persons. When we increase the size of subimage to 128x128, the performance of recognition is increased, in spite of losing some parts of the images which contain important information about the ridge structure due to the nearest of the core point location to the image boundaries.

Curvelet and Shearlet represent and target the edge features, while Wave Atom represents the image texture (Yao Z. , 2007). This may explain the convergence of results which are obtained from Curvelet and Shearlet. Targeting the image texture in fingerprint image is more efficient than the image edge. Among all multiresolution feature extraction techniques, Wave Atoms transform is the highest recognition rate of 99.5% which is published in (Abudalal & Alhanjouri, 2016).

Most researches which used the multiresolution techniques in fingerprint identification, tested their proposed solution in small database which ranged from (10-50 subjects), since increasing the number of subjects will decrease the recognition rate. We test our methodology on a large number of subjects (114 subjects). We introduce

an automatic fingerprint recognition system on a very challenges fingerprint database, CASIA-FingerprintV5, and achieve a high recognition rate.

We choose to test our methodology in a noisy database. CASIA-FingerprintV5 database is a very challenges database, and it needs a lot of processes to solve the problems of high displacement, wide range of angle rotation, and bad quality fingerprint images.

7.2 Future Work

The following points are some suggestions for future study:

1. The alignment algorithm which is used in this thesis, has limited to a rotation angle between (0-90 degrees). The CASIA-FingerprintV5 has various rotation angle between (0-360 degrees). We can use the following solution to consider the whole angle:

   a. For a rotation angle between (90, -90): this angles can be discovered by investigating the distance of both the horizontal axis, and the vertical axis, and if the horizontal axis distance is more than the vertical axis, then the image is rotated with an angle of 90 or -90. To decide what angle has to be taken, we can look at the core point orientation: if it refers to the right, then the image has to be rotated by 90 degree, else it has to be rotated by -90 degree.

   b. For a rotation angle between (0, -180): this angles can be discovered by investigating the distance of both the horizontal axis, and the vertical axis, and if the horizontal axis distance is shorter than the vertical axis, then the image is rotated with an angle of 0 or 180. To decide what angle has to be taken, we can look at the core point orientation: if it refers to the upper, then the image has to be rotated by 180 degree, else it does not need a rotation.

2. The proposed fingerprint recognition system needs to be secured against several attacks, which can compromise the system, and steel the template. This field has received more and more attention in the last years. We found that the most last researches in IEEE is about securing the biometrics templates.

3- Core point detection technique needs to be improved to face the problem of whorl and twin loop fingerprint types.

4- We use the standard deviation to reduce the dimension of feature matrix, but there are other statistical properties of the image texture: first order and second order statistical features such as: mean, skewness, kurtosis, energy, contrast, correlation, entropy, and homogeneity. We will try to replace the standard deviation with one or a combination of them.

5- We will apply our proposed methodology in latent fingerprint, and deal with various problems in this field.

References

References

Abduljaleel, I., Khaleel, A., Kareem, S. (2013). Comparing study using DWT / CT transforms in image denoising process. *Basrah Journal of Science (A), 3*(1), 111-120.

Abudalal, W., & Alhanjouri, M. (2016). Poor Quality Fingerprint Recognition Based on Wave Atom Transform. *International Journal of Scientific Engineering and Applied Science (IJSEAS), 2*(8), 234-254.

Acquah, H., & Gyimah, M. (2014). Classification and Recognition of Fingerprints using Self Organizing Maps(SOM). *IJCSI International Journal of Computer Science Issues, 11*(1), 153-160.

Akbar , S., Ahmad , A., & Hayat , M. (2014). Identification of Fingerprint Using Discrete Wavelet Transform in Conjunction with Support Vector Machine. *International Journal of Computer Science Issues (IJCSI), 11*(5), 189-200.

Albahdal, T. (2014, April 7-9). *Problems and Promises of Using the Cloud and Biometrics*. Paper presented at IEEE 11th International Conference on Information Technology: New Generations (pp. 293-300), Las Vegas, NV.

Alonso-Fernandez , F., Bigun, J., Fierrez, J., Fronthaler, H., Kollreider, K., & Ortega-Garcia, J. (2009). Fingerprint Recognition. In Petrovska-Delacrétaz**,** Dijana**,** Chollet**,** Gérard**,** Dorizzi**,** and Bernadette (Eds.), *Guide to Biometric Reference Systems and Performance Evaluation* (pp.51-90). London: Springer-Verlag.

Altun, A., & Allahverd, N. (2006). *Recognition of Fingerprints Enhanced by Contourlet Transform with Artificial Neural Networks*. Paper presented at IEEE *28th* International Conference on Information Technology: Interfaces*,* Cavtat/Dubrovnik.

Saleh, A. (2011). *Enhanced Secure Algorithm for Fingerprint Recognition*. (Unpublished PHD Thesis). Ain Shams University, Egypt.

Azarnoush, A., & Kiani, K. (2014*). Improving the Performance of an HMM-based Fingerprint Recognition System*. Paper presented at IEEE 2014 World Symposium on Computer Applications & Research (WSCAR), Sousse.

Babatunde, I., Kayode, B., Charles, A, & Olatubosun, O. (2012). Fingerprint Image Enhancement: Segmentation to Thinning. *International Journal of Advanced Computer Science and Applications (IJACSA), 3*(1), 15-25.

Baghelani, M., Eshkaftaki, J., & Ebrahimi, A. (2010, October). *A Novel Mapping for Fingerprint Image Enhancement*. Paper presented at 6th Iranian Conference on Machine Vision and Image Processing (MVIP), Iranian. Isfahan.

Balti, A., Sayadi, M., & Fnaiech, F. (2014). *Fingerprint characterization using SVD features*. Paper presented at IEEE 1st International Conference on Image Processing, Applications and Systems (IPAS), Sfax.

Bouaziz, A. , Draa, A., & Chikhi, S. (2015, April). *Bat Algorithm for Fingerprint Image Enhancement*. Paper presented at IEEE 12th International Symposium on Programming and Systems (ISPS). Algiers.

Boutella, L., & Serir, A. (2013). Fingerprint Orientation Map Based on Wave Atoms Transform. *Journal of Image and Graphics, 1*(3), 129-134.

Cand`es, E., Demanet, L., Donoho, D., & Ying, L. (2005). *Fast Discrete Curvelet Transforms*. Applied and Computational Mathematics. Retrieved March 10, 2015, from: http://www.curvelet.org/

Chakraborty, S., & Rao, K. (2012, May). *Fingerprint Enhancement by Directional Filtering*. Paper presented at IEEE 9th International Conference on Electrical Engineering/Electronics, Computer, Telecommunications and Information Technology (ECTI-CON), Phetchaburi.

Chaudhari, S., & Patil, A. (2013). A Study and Review on Fingerprint Image Enhancement and Minutiae Extraction. *IOSR Journal of Computer Engineering (IOSR-JCE), 9*(6), 53-56.

Chavan, S., Mundada, P., & Pal, D. (2015, Febreuary 4-6). *Fingerprint Authentication using Gabor Filter based Matching Algorithm*. Paper presented at IEEE International Conference on Technologies for Sustainable Development (ICTSD-2015). Mumbai, India.

Chen, F., & Zhou, J. (2010, Augest 22-22). *A Comparative Study of Combining Multiple Features for Fingerprint Recognition*. Paper presented at IEEE International Workshop on Emerging Techniques and Challenges for Hand-Based Biometrics (ETCHB). Istanbul.

Chikkerur, S., Cartwright, A., Govindaraju, V. (2007). Fingerprint Image Enhancement Using STFT Analysis. *The Journal of Pattern Recognition, Elsevier., 40*(1), 198-211.

Chikkerur, Wu, S., Govindaraju, V. (2004). A systematic approach for feature extraction in fingerprint images. In D. Zhang and A. Jain (Eds.), *Biometric Authentication.* (pp. 344-350). Berlin: Springer.

Cortes, & Vapnik. (1995). Support-vector networks. *Machine Learning, 20*(3), 273-297.

Dale, M., & Joshi, M. (2008, November 19-21). *Fingerprint Matching Using Transform Features*. Paper presented at IEEE 10 International Conference TENCON. Hyderabad

Daramola, A., Sokunbi, T., Adoghe, A. (2013). Fingerprint Verification System Using Support Vector Machine. *International Journal on Computer Science and Engineering (IJCSE), 5*(3), 678-684.

Demanet, L., & Ying, L. (2007). Wave atoms and sparsity of oscillatory patterns. *Elsevier*, 368-387.

Diefenderfer, G. (2006). *Fingerprint Recognition* (Unpublished Master Thesis). Graduate School, California.

Candes, E., & Donoho, L. (2000). *Curvelets: A surprisingly effective nonadaptive representation.* Stanford University. Retrieved from http://statweb.stanford.edu/~candes/papers/Curvelet-SMStyle.pdf

Dyre, S. & Sumathi, C. (2014, Descember 18-20). *Hybrid approach to Enhancing Fingerprint Images using filters in the frequency domain*. Paper presented at IEEE International Conference on Computational Intelligence and Computing Research (ICCIC), Coimbatore.

Easley, G., Labate, D., & Colonna, F. (2009). Shearlet Based Total Variation for Denoising. *IEEE Transactions on Image Processing, 18*(2), 260 - 268.

El-Feghi, I., Tahar, A., Ahmadi, M. (2011). *Efficient Features Extraction for Fingerprint Classification with Multi Layer Perceptron Neural Network*. Paper presented at IEEE 8th International Multi-Conference on Systems, Signals and Devices (SSD). Sousse.

Elmir, Y., Elberrichi, Z., Adjoudj. R. (2012). *Support Vector Machine Based Fingerprint Identification*. Paper presented at IEEE International Conference on *CTIC*. Algeria.

Eriksson, M. (2001). *Biometrics Fingerprint based identity verification* (Unpublished Master Thisis). UMEÅ University, Sweden.

Fadili, J., & Starck, L. (2009). Curvelets and Ridgelets. *Encyclopedia of Complexity and Systems Science,* 1718-1738. Springer New York.

Fahmy, M., & Thabet, M. (2013). *A Fingerprint Segmentation Technique Based on Morphological Processing*. Paper presented at IEEE International Symposium on Signal Processing and Information Technology, Athens.

Gan, G., Ma, C., & Wu, J. (Eds.). (2007). *Data Clustering Theory, Algorithms,and Applications.* Alexandria, Virginia: American Statistical Association and the Society for Industrial and Applied.

Gomathi, & Kumar. (2010, December 28-29). *An Efficient GEM Model for Image Inpainting Using a New Directional Sparse Representation: Discrete Shearlet Transform*. Paper presented at IEEE 2010 International Conference on Computational Intelligence and Computing Research (ICCIC*)*, Coimbatore.

Goshtasby, A. (2012). *Image Registration: Principles, Tools and Methods.* USA: Springer.

Greenberg, S., Aladjem, M., Kogan, D., Dimitrov, I. (2000). *Fingerprint Image Enhancement Using Filtering Techniques*. Paper presented at IEEE 15th International Conference on Pattern Recognition, Barcelona.

Grohs, P., Keiper, S., Kutyniok, G., Schaefer, M. (2013). Parabolic Molecules: Curvelets, Shearlets,and Beyond. In G., Fasshauer, L., Schumaker (Eds.), *Approximation Theory XIV: San Antonio 2013*, (pp. 141-172). Switzerland: Springer International Publishing.

Guesmi, H., Trichili, H., Alimi, A., & Solaiman, B. (2012, September 6-7). *Curvelet Transform-Based Features Extraction For Fingerprint Identification*. Paper presented at IEEE International Conference of the Biometrics Special Interest Group (BIOSIG). Darmstadt .

Guo, H. (2005, August 18-21). *A Hidden Markov Model Fingerprint Matching Approach*. Paper presented at IEEE International Conference on Machine Learning and Cybernetics.Guangzhou, China.

Haddad, Z., Beghdadi, A., Serir, A., & Mokraoui, A. (2008, November 23-26). *Fingerprint Identification Using Radon Transform*. Paper presented at IEEE First Workshops on Image Processing Theory, Tools and Applications. Sousse.

Hamad, H. M., & Abudalal, W. (2016). The Two Secured Factors of Authentication. *IUG Journal of Natural and Engineering Studies (Islamic University of Gaza), 24*(1), 1-14.

Hamilton, J. (2008). *Fingerprint Analysis: Hints from Prints.* United States: ABDO publishing company.

He, Y., Ou, Z., & Guo, H. (2003, November 2-5). *A Method of Fingerprint Identification Based on Space Invariant Transforms and Support Vector Machines*. Paper presented at IEEE International Conference on Machine Learning and Cybernetics.

Hejazi, H., & Alhanjouri, M. (2010). *Face Recognition Using Curevelet And Waveatom Transform* (Unpublished Master Thesis). IUG, Gaza, Palestine.

Hong, L., Wang, Y., & Jain, K. (1998). Fingerprint Image Enhancement: Algorithm and Performance Evaluation. *IEEE Trans. Pattern Analysis Machine, 20*(8), 777–789.

Hsieh, T., Lai, E., Wang, C. (2003). An effective algorithm for fingerprint image enhancement based on wavelet transform. *Elsevier, 36*(2), 303 – 312.

Hu, Y., Jing, X., Zhan, B., Zhu, X. (2010, March 27-29). *Low Quality Fingerprint Image Enhancement Based on Gabor Filter*. Paper presented at IEEE 2nd International Conference on Advanced Computer Control (ICACC). Shenyang.

Humaira, N., Bushra, N., Firdous, Z., Khan, M., & Islam, M. (2013, May 17-18). *Curvelet Feature Based Fingerprint Recognition Using Fourier Enhancement*. Paper presented at IEEE International Conference on Informatics, Electronics & Vision (ICIEV). Dhaka.

Ito, K., Morita, A., Aoki, T., Higuchi, T., Nakajima, H., & Kobayashi, K. (2005, September 11-14). *A Fingerprint Recognition Algorithm Using Phase-Based Image Matching for Low-Quality Fingerprints*. Paper presented at IEEE International Conference on Image Processing.

Iwasokun, G., & Akinyokun, O. (2014). Fingerprint Singular Point Detection Based on Modified Poincare Index Method. *International Journal of Signal Processing, Image Processing and Pattern Recognition, 7*(5), 259-272.

Jain, A., Prabhakar, S., Hong, L., & Pankanti, S. (2000). Filterbank-Based Fingerprint Matching. *IEEE Transactions on Image Processing, 9*(5), 846-860.

Jalutharia, N. (2010). *Fingeprint Recognitin and Analysis* (Unpublished Master Thesis) Thapar University, Patiala, India.

Jea, T.-Y. (2005). *Minutiae-Based Partial Fingerprint Recognition* (Unpublished PHD Thesis). State University of New York at Buffalo, New York.

Jena, M., & Dalal, S. (2014). DWT Based Fingerprint Recognition Approach. *International Journal of Engineering Research & Technology (IJERT), 3*(5), 1800-1803.

Jia, C., Cao, K. (2012, June 24-27). *The research on the preprocessing algorithm for fingerprint image*. Paper presented at IEEE Symposium on Electrical & Electronics Engineering (EEESYM). Kuala Lumpur .

Kabir, W., Ahmad, O., & Swamy. (2013, Augest 4-7). *Enhancement of Low-Quality Fingerprint Images by a Three-Stage Filtering Scheme*. Paper presented at IEEE *56th* International Midwest Symposium on Circuits and Systems (MWSCAS), Columbus, OH.

Kankrale N., & Jawale, M. (2013). Fuzzy Logic Concatenation in Fingerprint and Iris Multimodal Biometric Identification System. *International Journal of Advanced Research in Computer Science and Software Engineering*, *3*(10), 120-126.

Kankrale, N., & Sapkal, D. (2012). *Template Level Concatenation of Iris and Fingerprint in Multimodal Biometric Identification Systems*. Paper presented at International Conference on Recent Trends in Engineering & Technology (IJECSCSE),

Kawagoe, M., & Tojo, A. (1984). Fingerprint pattern classification. *Elsevier, 17*(3), 295-303.

Kesava, R. (2010). Cloud Software As A Service. *Journal of Global Research in Computer Science,* 1(2), 16-22.

Khan, M., & Zakirullah, A. (2010, October 24-28). *Fourier Cleaning of Fingerprint Images*. Paper presented at IEEE 10th International Conference on Signal Processing Proceedings. Beijing.

Khan, M., Khan, A., & Muhammad, N. (2010, June 14-16). *Fingerprint Image Enhancement Using Principal Component Analysis (PCA) Filters*. Paper presented at IEEE International Conference on Information and Emerging Technologies (ICIET). Karachi

King, E., Kutyniok, G., Lim, W. (2013). Image Inpainting: Theoretical Analysis and Comparison of Algorithms. *SPIE Optical Engineering+ Applications* (pp. 885802-885802). International Society for Optics and Photonics.

Kumar, N. & Verma, P. (2012). Fingerprint Image Enhancement and Minutia Matching. *International Journal of Engineering Sciences & Emerging Technologies (IJESET), 2*(2), 37-42.

Kundu, S., & Sarker, G. (2015). A Modified SOM-Based RBFN for Rotation Invariant Clear and Occluded Fingerprint Recognition. *Springer*, 11-20.

Kutyniok, G., Lim, W., & Steidl, G. (2014). Shearlets: Theory and Applications. *GAMM-Mitteilungen, 37*(2), 259 – 280.

Labate, D., Yi, S., Easley, G., & Krim, H. (2009). A Shearlet Approach To Edge Analysis and Detection. *IEEE Trans. Image Process, 18*(5), 929-941.

Labate, D., Lim, W., Kutyniok, G., & Weiss, G. (2005). *Sparse Multidimensional Representation using Shearlets.* Paper presented at International Society for Optics and Photonics in Optics & Photonics.

Lam, H., Hou, Z., Yau, W., Chen, T., Li, J., Sim, K. (2009). Reference Point Detection for Arch Type Fingerprints. *Lecture Notes in Computer Science, 5558*, 666-674.

Leo, W. (2004). *Fingerprint Identification.* San Clemente: LawTech Publishing Group.

Lewis, I. (2014). Ever had your fingerprints taken? Meeting the challenges of 21st Century access control. *Elsevier, Biometric Technology Today, 2014*(5), 9-11.

Li, G., Busch, C., & Yang, B. (2014, May 26-30). *A novel approach used for measuring fingerprint orientation of arch fingerprint*. Paper presented at IEEE 37th International Convention on Information and Communication Technology, Electronics and Microelectronics (MIPRO), Opatija.

Liu, L., Jiang, T., Yang, J., & Zhu, C. (2006). Fingerprint Registration by Maximization of Mutual Information. *IEEE Transactions on Image Processing, 15*(5), 1100-1111.

Luo, J., Lin, S., Lei, M., & Ni, J. (2008, October). *Application of Dimensionality Reduction Analysis to Fingerprint Recognition.* Paper presented at IEEE '08. International Symposium on Computational Intelligence and Design (ISCID), Wuhan

Ma, J., & Plonka, G. (2010). The Curvelet Transform A review of recent applications. *IEEE Signal Processing Mahazine*, 118-133.

Majumdar, A., & Ward, R. (2008). Multiresolution Methods in Face Recognition. *Recent Advances in Face Recognition*, INTECH Open Access Publisher.

Malwade, A., Raut, R., Thakare, V. (2015). A Survey on Enhancement Technique to Improve Accuracy in Fingerprint Matching. *International Journal of Advanced Research in Computer Science and Software Engineering, 5*(4), 28-32.

Mandal, T., & Wu, Q. (2008). *A Small Scale Fingerprint Matching Scheme Using Digital Curvelet Transform*. Paper presented at IEEE International Conference on Systems, Man and Cybernetics. Singapore.

Mohammed, A., Wu, Q., & Sid-Ahmed, M. (2010). Application of Wave Atoms Decomposition and Extreme Learning Machine for Fingerprint Classification. *Springer, 6112*, 246-255.

Msiza, I., Leke-Betechuoh, B., & Malumedzha, T. (2011, December 6-8). *Fingerprint Re-alignment: A Solution Based on the True Fingerprint Center Point*. Paper presented at IEEE International Conference on Machine Learning and Computing (ICMLC 2011). Singapore.

Namburu, P. (2007). *A study on fingerprint image enhancement and minutiae extraction techniques* (Unpublished PHD Dissertation). National Institute of Technology, Rourkela.

Nasiri, A., & Fathy, M. (2015). *An effective algorithm for fingerprint reference point detection based on filed flow curves*. Paper presented at IEEE International Symposium on Artificial Intelligence and Signal Processing. Mashhad.

Nilsson, K., & Bigun, J. (2003). Localization of corresponding points in fingerprints by complex filtering. *Pattern Recognition Letters*, *24*(13), 2135-2144.

Ohtsuka, T., Watanabe, D., Tomizawa, D., & Aoki, H. (2008). *Reliable Detection of Core and Delta in Fingerprints by using Singular Candidate Method*. Paper presented at IEEE '08 Computer Society Conference on Computer Vision and Pattern Recognition Workshops CVPRW. Anchorage, AK .

Omidyeganeh, M., Javadtalab, A., Ghaemmaghami, S., & Shirmohammadi, S. (2012, May 13-16). *Contourlet Based Distance Measurement to Improve Fingerprint Identification Accuracy*. Paper presented at IEEE International in Instrumentation and Measurement Technology Conference (I2MTC), Graz.

Otsu, N. (1979). A Threshold Selection Method from Gray Level Histograms. *IEEE Trans. Systems, 9*(1), 62–66.

Pober, M. (2010). *Comparing performance of different fingerprint matchers by using StirMark distorted images* (Unpublished Master Thesis). University at Salzburg, Austria.

Polikar, R. (2016, January 17). *The Wavelet Tutorial*. Retrieved Retrieved November 12, 2015, from: http://users.rowan.edu/~polikar/WAVELETS/WTpart1.html

Prabhakar, S. (2001). *Fingerprint Classification and Matching Using a Filterbank* (Unpublished PHD Thesis). Michigan State University, USA.

Rajinikannan, M., Kumar, D., Muthuraj, R. (2010). Estimating the Impact of Fingerprint Image Enhancement Algorithms for Better Minutia Detection. *International Journal of Computer Applications, 2*(1), 36-42.

Rawat, A. (2009). *A Hierarchical Fingerprint Matching Sytem* (Unpublished Mater Thesis), Indian Institute of Technology Kanpur, India.

Saeed, A., Tariq, A., & Jawaid, U. (2011, July 23-24). *Automated System For Fingerprint Image Enhancement Using Improved Segmentation and Gabor Wavelets*. Paper presented at IEEE International Conference on Information and Communication Technologies (ICICT). Karachi.

Severance, C. (2015). Anil Jain: 25 Years of Biometric Recognition. *IEEE COMPUTER SOCIETY, 48*(8), 8-10.

Stephen, M., Reddy, P., & Vasavi, V. (2013). Fingerprint Image Enhancement through Particle Swarm Optimization. *International Journal of Computer Applications, 66*(21), 34-40.

Goodrich, M., & Tamassia, R. (2010, October 25). *Introduction to Computer Security*. Addison-Wesley Publishing Company.

Tang, T., Wu, X., Xiang, M. (2008). *An Improved Fingerprint Singular Point Detection Algorithm Based on Continuous Orientation Field*. Paper presented at IEEE '08. International Symposium on Computer Science and Computational Technology (ISCSCT) Shanghai.

Tang, H., Zhu, Z., Gao, Z., & Li, Y. (2014, November). *A Secure Biometric-Based Authentication Scheme Using Smart Card*. Paper presented at IEEE International Conference on Cyberspace Technology (CCT 2013), Beijing, China.

Taniar, D. (2008). *Data Mining and Knowledge Discovery Technologies.* New York: IGI PublIshIng.

Test Biometrics Ideal. (2010). Retrieved November 12, 2015, from http://biometrics.idealtest.org

Thayammal, S., & Selvathi, D. (2012). *Image Compression using Multidirectional Anisotropic Transform: Shearlet Transform. Devices.* Paper presented at IEEE 2012 International Conference on Circuits and Systems (ICDCS). Coimbatore

Tico, M., Immonen, E., Ramo, P., Kuosmanen, P., & Saarinen, J. (2001, May 6-9). *Fingerprint Recognition Using Wavelet Features*. Paper presented at IEEE International Symposium on Circuits and Systems, Sydney, NSW

Tong, *Y., Wang, H., Pi, D., Zhang, Q. (2006). Fast Algorithm of Hough Transform-Based Approaches for Fingerprint Matching.* Paper presented at IEEE 6th World Congress on Intelligent Control and Automation, Dalian.

Turroni, F. (2012). *Fingerprint Recognition:Enhancement, Feature Extraction and Automatic Evaluation of Algorithms* (Unpublished PHD Thises), University of Bologna.

Vinothkanna, R., & Wahi, A. (2014). Fuzzy Vault Fusion Based Multimodal Biometric Human Recognition System With Fingerprint and Ear. *Journal of Theoretical and Applied Information Technology, 59*(2), 304-317.

Wang, J.,& Sun, X.. (2010, July 7-9). *Fingerprint Image Enhancement using a fast Gabor filter*. Paper presented at IEEE 8th World Congress on Intelligent Control and Automation (WCICA). Jinan.

Wang, J. (2003). *Data Mining: Opportunities and Challenges.* United States of America: Idea Group Publishing (an imprint of Idea Group Inc.).

Wang, W., Li, J., Huang, F., & Feng, H. (2008). Design and implementation of Log-Gabor filter in fingerprint image enhancement. *Elsevier, 29*, 301–308.

Wang, Zhag, Liu, & Yu. (2011,). *Fingerprint Image Enhancement Based On Morphological Filter*. Paper presented at IEEE International Conference on Computational and Information Sciences. Chengdu, China.

Wegstein. (1982). An Automated Fingerprint Identification System. *U.S.Government Publication, U.S. Department of Commerce National Bureau of Standards,.*

Wu, Guha, T., & Jonathan, Q. M. (2010). Curvelet Based Feature Extraction. In *Face Recognition* (pp. 35-46). InTech. Retrieved November 12, 2015, from: http://www.intechopen.com/books/facerecognition/curvelet-based-feature-extraction

Wu, X., & Kumar, V. (2008). Top 10 algorithms in data mining. *Springer*, 1-37.

Wu. (2007). *Advanced feature extraction algorithms for automatic fingerprint recognition systems* (Unpublished PHD Thesis). University at Buffalo, NY.

Yang, C., & Park, D. (2008). Fingerprint Verification Based on Invariant Moment Features and Nonlinear BPNN. *International Journal of Control, Automation, and Systems, 6*(6), 800-808.

Yang, C., & Park, D. (2008). A fingerprint verification algorithm using tessellated invariant moment features. Neurocomputing, Elsevier, 71, 1939– 1946.

Yang, J., Liu, L., Jiang, T., & Fan, Y., (2003). A modified Gabor filter design method for fingerprint image enhancement. *Pattern Recognition Letters, Elsevier, 24*, 1805–1817.

Yao, Y., Frasconi, P., & Pontil, M. (2001). Fingerprint Classification with Combinations of Support Vector Machines. *Pattern Recognition Letters*, *24*(12 Springer), 253–258.

Yao, Z. (2007). *Directional Edge and Texture Representations for Image Processing* (Unpublished PHD Thesis) University of Warwick, United Kingdom.

Yusharyahya, K., Nugroho, A., Purnama, J., & Galsinium, M. (2014, August 20-21). *A Comparison of Fingerprint Enhancement Algorithms for Poor Quality Fingerprint Images*. Paper presented at IEEE International Conference of Advanced Informatics: Concept, Theory and Application (ICAICTA)